



ASSEMBLY TECHNIQUES AND TECHNOLOGIES

e-ISSN-2450-8217

ZESPÓŁ REDAKCYJNY:**Redaktor Naczelny** – dr hab. inż. Katarzyna Antosz, prof. PRZ**Z-ca Redaktora Naczelnego** – dr inż. Martyna Jachimowicz

tel. 663 311 966

Redaktorzy współpracujący:

Prof. Erika Ottaviano, University of Cassino and Southern Lazio, Italy

Prof. José Mendes Machado, University of Minho, Portugal

Prof. Vitalii Ivanov, Sumy State University, Ukraine

Redaktorzy tematyczni:

Dr inż. Rafał Kluz (technologia, automatyzacja)

Dr inż. Lidia Galda (tribologia)

Dr inż. Mirosław Chłosta (inżynieria, produkcja)

Dr inż. Andrzej Kubit (struktury i systemy montażu)

Mgr inż. Kazimierz Rychlik (eksploatacja, niezawodność)

RADA PROGRAMOWO-NAUKOWA:

Prof. Dario Antonelli (Politecnico di Torino, Włochy), prof. Bronius Baksys

(Kaunas University of Technology, Litwa), prof. Marek Balaziński (Ecole

Polytechnique Montreal, Kanada), prof. Adam BARYLSKI (Politechnika

Gdańska), mgr inż. Magdalena Borek-Daruk (SIGMA-NOT), prof. Józef

Gawlik (Politechnika Krakowska) – z-ca przewodniczącego, prof. Jan Go-

dzimirski (WAT), prof. Mikulas Hajduk (Technicka Univerzita v Kosciach,

Słowacja), prof. Michael Kheifetz (Połocki Gosudarstwiennyj Uniwersytet,

Białoruś), doc. dr inż. Radek Knofl ick (FME Brno, Czechy), prof. Mark

Kristal (Volgograd State Technical University, Rosja), prof. Józef Kuczma-

szewski (Politechnika Lubelska), prof. Piotr Łebkowski (AGH), prof. An-

tonio Maff ei (KTH Royal Institute of Technology, Szwecja), prof. Ignace

Martens (Katholieke Universiteit Leuven, Belgia), prof. Jacek Mucha (Po-

litechnika Rzeszowska), prof. Vitaliy Pasichnyk (Nacjonalnyj Techniczeskij

Uniwersitet Ukrainy „Kijewskij Politechniczeskij Instytut”, Ukraina), prof. R.

M. Chandima Ratnayake (University of Stavanger, Norwegia), prof. Emil

Spisak (Technika Univerzita v Kosciach, Słowacja), prof. Dorota Stad-

nicka (Politechnika Rzeszowska), prof. Jerzy Stamirowski (Politechnika

Świętokrzyska), prof. Michaił W. Wartanow (Moskowskij Gosudarstwiennyj

Maszynostroitelnyj Uniwersytet, Rosja), prof. Władimir P. Woronienko

(Moskowskij Gosudarstwiennyj Technologiczeskij Uniwersytet, Rosja),

prof. Jan Żurek (Politechnika Poznańska) – przewodniczący

ADRES REDAKCJI:

Kwartalnik „Technologia i Automatyzaacja Montaży”

ul. Ratuszowa 11, pok. 740, 03-450 Warszawa

Tel. 22 853 81 13

e-mail: tiam@sigma-not.pl

www.tiam.pl

PRENUMERATA:

Zakład Poligrafii i Kolportażu Wydawnictwa SIGMA-NOT Sp. z o.o.

ul. Ks. J. Popieluszki 19/21, 01-595 Warszawa

tel. 22 840 30 86

tel./fax: 22 827 43 65, 619 22 41 w. 215

e-mail: prenumerata@sigma-not.pl

portal: www.sigma-not.pl

REKLAMA:

Redakcja: tel. 22 853 81 13

e-mail: tiam@sigma-not.pl

Dział Reklamy i Marketingu

tel./fax: 22 827 43 65

e-mail: reklama@sigma-not.pl

SKŁAD I ŁAMANIE:

Wydawnictwo SIGMA-NOT

ul. Ratuszowa 11, 03-450 Warszawa

e-mail: sekretariat@sigma-not.pl

WYDAWCA:

Sieć Badawcza Łukasiewicz

Instytut Mechanizacji Budownictwa i Górnictwa Skalnego

ul. Racjonalizacji 6/8, 02-673 Warszawa



Wydawnictwo SIGMA-NOT

ul. Ratuszowa 11, 03-450 Warszawa

PATRONAT:

Stowarzyszenie Inżynierów Mechaników i Techników Polskich

Za treść ogłoszeń i artykułów promocyjnych redakcja nie odpowiada

Wersja pierwotna: elektroniczna

WSKAZÓWKI DOTYCZĄCE PRZYGOTOWANIA ARTYKUŁÓW

- Artykuły przeznaczone do opublikowania w kwartalniku „Technologia i Automatyzaacja Montaży” powinny mieć oryginalny i naukowo-techniczny charakter i być zgodne z problematyką czasopisma. Redakcja przyjmuje artykuły w jęz. polskim, jęz. angielskim i jęz. rosyjskim.
- Artykuł o maksymalnej objętości 5 stron A4 wraz z ilustracjami powinien być napisany czcionką Times Roman lub Arial 12 pkt, z interlinią 12 pkt. Formatowany tekst nie powinien mieć podziału na kolumny.
- Tytuł artykułu należy podać w jęz. polskim i jęz. angielskim. Tytuł nieprzekraczający 10 słów powinien odzwierciedlać istotne elementy treści artykułu.
- Struktura artykułów naukowo-technicznych prezentujących prace autora(ów) powinna być następująca: wstęp (wprowadzenie); metodyka (badań, analiz, pracy z podaniem ewentualnie materiałów, założeń itp.); wyniki (badań, analiz); omówienie wyników; wnioski; spis literatury.
- Podpisy pod ilustracjami oraz tytuły tablic należy podać w jęz. artykułu i jęz. angielskim.
- Ilustracje należy dołączyć również jako osobne pliki w formacie: .jpg, .tiff, z rozdzielczością co najmniej 300 dpi. Wszystkie zamieszczane ilustracje powinny być własnością autora(ów) lub należy podać źródło pochodzenia rysunków.
- Wzory matematyczne pisane w edytorze równań Microsoft Equation i powinny być oznaczane kolejnym numerem w nawiasie okrągłym. Wszystkie symbole powinny być objaśnione. Należy stosować jednostki układu SI.
- Spis literatury należy podać w kolejności cytowania w tekście, a odnośniki w tekście winny być ponumerowane cyframi arabskimi i umieszczone w nawiasach kwadratowych. W przypadku korzystania z Internetu należy podać adres strony i datę odczytu. Liczbę autocytowań należy ograniczyć do niezbędnych.
- Do artykułu należy dołączyć streszczenie w jęz. artykułu i jęz. angielskim, zawierające minimum 200–250 słów.
- Pod streszczeniem należy podać 3–6 słów kluczowych w jęz. artykułu i jęz. angielskim, zwracając uwagę, by nie były one powtórzeniem tytułu pracy.
- Po spisie literatury zaleca się podanie źródła finansowania pracy.
- Na końcu artykułu należy podać: imiona i nazwiska autorów, tytuły naukowe lub zawodowe, telefon, faks, e-mail, miejsce zatrudnienia wraz z adresem do korespondencji.

PROCEDURA RECENZOWANIA

Procedura recenzowania artykułów w czasopiśmie jest zgodna z zaleceniami Ministerstwa Nauki i Szkolnictwa Wyższego zawartymi w opracowaniu „Dobre praktyki w procedurach recenzyjnych w nauce”, Warszawa 2011.

Wszystkie artykuły naukowo-techniczne publikowane w kwartalniku „Technologia i Automatyzaacja Montaży” są recenzowane.

Nadesłane artykuły są poddawane redakcyjnej ocenie formalnej i otrzymują numer redakcyjny, identyfikujący je na dalszych etapach procesu wydawniczego, a redakcja wysyła do autorów informację o przyjęciu artykułu i wysłaniu go do recenzentów. Do oceny każdej publikacji powołuje się co najmniej dwóch niezależnych recenzentów. Redakcja dobiera recenzentów rzetelnych i kompetentnych w danej dziedzinie. Nadesłane artykuły nie są nigdy wysyłane do recenzentów z tej samej placówki, z której pochodzi autor. Prace recenzentów są poufne i anonimowe. Recenzja musi mieć formę pisemną i kończyć się jednoznacznym wnioskiem o dopuszczeniu artykułu do publikacji w czasopiśmie lub jego odrzuceniu. W przypadku pracy w języku obcym, co najmniej jeden z recenzentów jest afiliowany w instytucji zagranicznej innej niż narodowość autora pracy. Autorzy są informowani o wynikach recenzji oraz otrzymują je do wglądu. W sytuacjach spornych redakcja powołuje dodatkowych recenzentów.

Lista recenzentów publikowana jest w ostatnim zeszycie każdego rocznika.

**Kwartalnik „Technologia i Automatyzaacja Montaży”
ukazuje się formie elektronicznej w otwartym dostępie
(Open Access) i jest dostępny na Portalu Informacji
Technicznej Wydawnictwa SIGMA-NOT
www.sigma-not.pl**

3

BARYLSKI A.:

Analysis of the construction, assembly and usage of specialized fixtures illustrated with an example of machining a lever

Analiza konstrukcji, montażu i użytkowania uchwytów specjalnych na przykładzie obróbki dźwigni

8

OGRODNICZEK J., RUDAWSKA A., MÜLLER M., STANĚKOVÁ D.:

Comparative analysis of compressive strength of regenerative masses made from epoxy adhesive compounds

Analiza porównawcza wytrzymałości na ściskanie mas regeneracyjnych wykonanych z klejów epoksydowych

13

DEHTIAROV I., ANTOSZ K., AVRAMENKO S., HERASKO K., IVANOV V.:

Modeling of high-speed flywheel designs for technological equipment

Modelowanie projektów szybkobieżnych kół zamachowych dla urządzeń technologicznych

20

CIEŚLAK R., SOBCZAK P., MAKOWSKI K.:

Tests of the time consumption of the operations performed at the workstation for assembling and dismantling engines

Badania czasochłonności czynności wykonywanych na stanowisku pracy przy montażu i demontażu silników

27

CHLOST M.:

Cut layer in a machining of the cylindrical gears by the method of 5-axis roll away of the end mill cutter on the outline of the tooth

Warstwa skrawana w obróbce walcowych kół zębatych metodą 5-osiowego odtaczania frezu palcowego po zarysie zęba

36

ZIELECKI W., BAŁ Ł., GUŹLA E.:

The influence of the directivity of the geometric structure on the load capacity of single-lap adhesive joints

Wpływ kierunkowości struktury geometrycznej powierzchni na nośność połączeń klejowych

44

PATER J., BASARA D., STADNICKA D.:

Influence of temperature based process parameter compensation on process efficiency and productivity

Wpływ kompensacji parametrów procesu w oparciu o temperaturę na wydajność i produktywność procesu





TECHNOLOGIA I AUTOMATYZACJA MONTAŻU

e-kwartalnik naukowo-techniczny

w otwartym dostępie na:
www.tiam.com.pl
www.sigma-not.pl

**Autorów zapraszamy do publikacji
na łamach kwartalnika – 20 pkt. MEiN**
kontakt: tiam@sigma-not.pl
tel. 22 853 81 13



WYDAWNICTWO SIGMA-NOT 

ANALYSIS OF THE CONSTRUCTION, ASSEMBLY AND USAGE OF SPECIALIZED FIXTURES ILLUSTRATED WITH AN EXAMPLE OF MACHINING A LEVER

Analiza konstrukcji, montażu i użytkowania uchwytów specjalnych na przykładzie obróbki dźwigni

Adam BARYLSKI

ORCID 0000-0003-1672-8445

DOI: 10.15199/160.2021.2.1

Abstract: The paper presents a method of quantitative assessment of manufacturability of the construction of specialized fixtures used in machining. The assumed, simplified assessment criteria include both the complexity of the construction with respect to time-consumption of manufacturing the components and their assembly, as well as the features of the usage of fixtures. The paper contains a study case connected with variably designed functional hardware for machining a cast-iron lever.

Keywords: mechanical engineering, machining fixtures, manufacturability of construction, assessment

Streszczenie: W artykule przedstawiono sposób ilościowej oceny technologiczności konstrukcji obróbkowych uchwytów specjalnych. Przyjęte uproszczone kryteria oceny uwzględniają zarówno złożoność konstrukcji w aspekcie czasochłonności wykonania elementów składowych i ich montażu, jak i cechy użytkowania uchwytów. W pracy zamieszczono studium przypadku związanego z zaprojektowanym wariantowo oprzyrządowaniem przedmiotowym do obróbki dźwigni żeliwnej.

Słowa kluczowe: inżynieria mechaniczna, uchwyty obróbkowe, technologiczność konstrukcji, ocena

Introduction

Manufacturability of construction comprises an important criterion of assessing any product. It can be defined as a feature of construction solution that ensures achieving a set of imposed requirements for a specific batch, technological, organizational and manpower conditions in a company, with minimizing the production costs [7,9,13,15,17]. Design process involves the application of the general rules of typification, unification and normalization of components. Possible reduction of mass, selection of a semi-finished product, essential requirements for machining and assembly, as well as utility features [4,6,16,18,19] are also taken into consideration.

In relation to a specialized machining hardware, it is important to provide its basic functions, hence, correct setting and gripping of the element, decreasing the usage of construction materials and ensuring the required degree of precision of a manufactured fixture [12]. During the design, one should also consider the technical possibilities of a tool shop, as well as the ease of service and possible repairs of a fixture. The same functional range of a piece of hardware can be achieved by various construction solutions and, consequently, technological solutions, in terms of their labour intensity, material consumption, i.e. cost consumption. Beneficial conditions of producing fixtures can be ensured by an appropriate composition of the design team – including highly trained, qualified and experienced personnel [2,3].

In the process of engineering education of students, within the scope of team design of machining hardware, there is a need for a simplified assessment of the prepared construction variants and selection of the best solution.

The problem has been illustrated with an example of 5 variably-designed fixtures for machining a lever [14].

Design construction of fixtures

Machined element consists in a lever made of cast iron EN-GJL-150 (Fig.1). Machining involves face surfaces (3 mm offset on each side), two openings with 16H8 mm diameters and a central opening with 30H8 mm diameter (roughly made during casting). Milling of the face surfaces and final machining of the openings are conducted on the VF-2YT machining centre produced by Haas, equipped with the worktable whose dimensions are 914x356 mm (T-slots width: 16 mm).

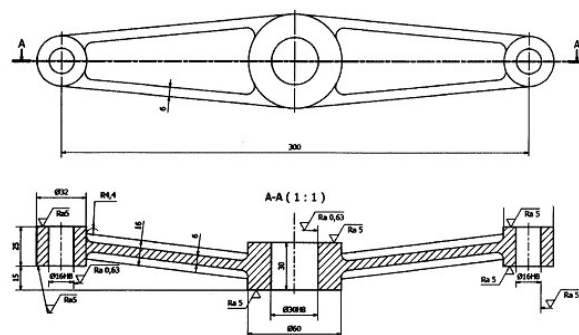


Fig.1. Design of the machined element

• Fixture U1

In the first design variant of the fixture two levers (in two holders) are machined at the same time – Fig. 2.

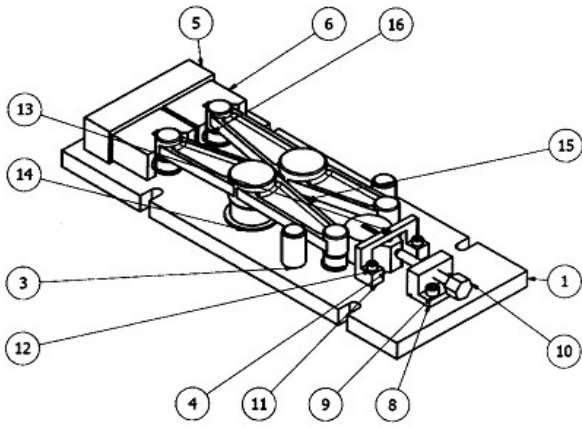


Fig. 2. Construction design of fixture U1

Each machined element is set by a fixed V-block (6), support bushings (14), (15) and (16) and a stop pin (3). Fixed V-blocks are attached with bolts (2) to the intermediate block (5) joined with the fixture base (1) with bolts (7) that are not visible in the drawing. The levers are affixed by means of a slider (4) moving in a clamping ring (11) joined with the base (1) by means of bolts (12) and through a notch in the slider (4) with a special screw (13) – by turning the screw (10) in the block (8) attached to the base (1) with bolts (9). An advantage of this solution consists in the possibility of machining two levers at the same time and quick fixing, while its flaw rests in relatively high number of specialized components in the construction.

• **Fixture U2**

In this design solution (Fig. 3) the machined lever is supported with two bushings (10) and with a center bushing (3) which sets the element in linear plane X-Y, while the occurring play ensures the freedom of fixing towards Z axis, including the precision of the semi-product. Another degree of freedom is removed by the stop pin (4). Location of the element (10) is regulated by a spring (9) covered with a cover (5) which is attached with bolts (6) to the fixture body (1). The blockade of the bushing

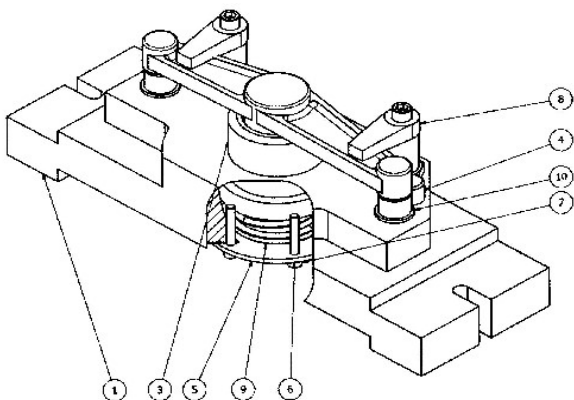


Fig. 3. Design of fixture U2

(10) is ensured by a lateral screw (2) – invisible in this drawing. Two clamps (8) are used to fix the machined element. The advantage of this concept lies in relatively low number of components, while its disadvantage is the weight of the body, caused by spring-loaded adjustment of the central support (3) and more difficult removal of the shavings from its vicinity.

• **Fixture U3**

In this concept (Fig. 4) the lever is affixed using a pair of lateral clamps (6). Setting elements in this design are: a support (5) attached to the block (4) and two supports (2) placed in the wall (1) fixed with bolts (7) and, also, support bushings (10) set in the base (3). The block (4) is attached to the base (3) with two bolts (8) that are not shown in the drawing; similarly to the clamp (6) that is attached with bolts (9) that are not shown in the drawing. The advantages of this fixture consist in quick fixing of the lever without the need of using extra tools and relatively low number of components.

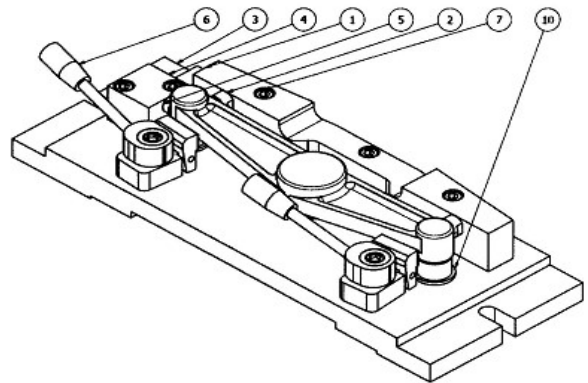


Fig. 4. Design of fixture U3

• **Fixture U4**

In this case (Fig. 5) a pair of horizontal clamps (7) fixing the machined lever from the top and attached with bolts (10) that are not visible in the drawing. A support beam (6) attached to the base (2) with bolts (13) was

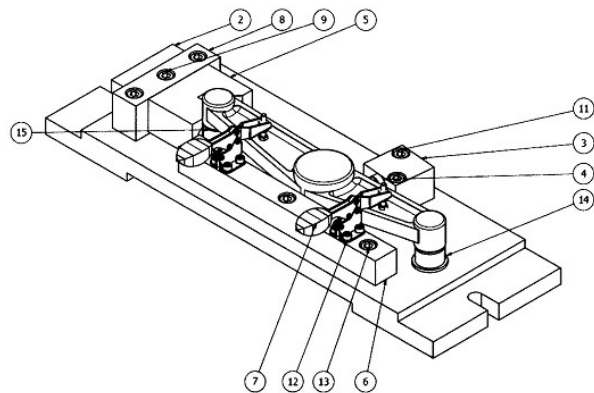


Fig. 5. Design of fixture U4

applied in this solution. Machined element is set by means of a fixed V-block attached to the block (8) with bolts (1) that are not visible in this drawing. Block (8) is attached to the base (2) with bolts (9), while block (3) is attached with bolts (11). Block (3) features a stop pin (4). Machined element is supported with flanged bushings (14) and (15). The advantage of this solution is quick fixing of the machined element, while its disadvantage lies in a high number of specialized and normalized elements, hence a high number of machined surfaces.

• Fixture U5

This version of the equipment (Fig. 6) features a pair of V-blocks – fixed one (2) attached to the block (3) with bolts (12) that are not visible in the picture, and a sliding one – joined with the slider (4). The slider runs through clamping rings (5) and is moved by a screw (6) attached with the aid of a cotter pin (7). The screw is driven into an angular support (9) attached to the base of the grip (1) with bolts (10). The machined lever rests upon two flat supports (13) connected with the base (1). The advantage of this grip consists in its low weight and easy operation, while its flaw rests in a relatively high number of precise special elements.

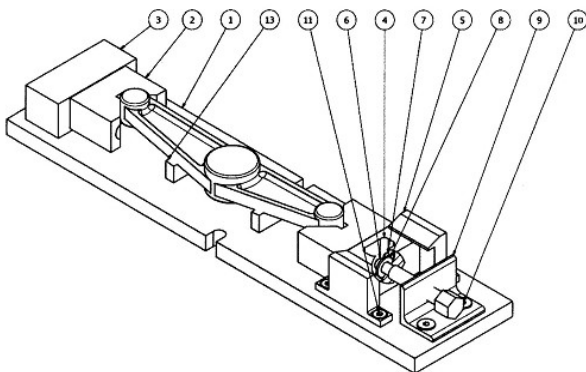


Fig. 5. Design of fixture U4

Assessment of the manufacturability of the proposed designs of fixtures

In the assessment of the manufacturability of a design, three groups of analysed features connected with the manufacturing of the fixture – group X_1 (assumed importance factor $w_k = 0.35$), usage and operation – X_2 ($w_k = 0.45$) as well as transport and regeneration – X_3 ($w_k = 0.2$).

Final assessment O_{Tk} is determined as:

$$O_{Tk} = \sum w_k \cdot O_{Tx} \quad (1)$$

where O_{Tx} is the value of the factor in each of the three analysed groups and is:

$$O_{Tx} = \sum w_c \cdot O_x \quad (2)$$

where w_c denotes the assumed importance factor for a specific feature, while O_x is the numerical value of the feature. The higher the O_{Tk} value is, the more manufacturable is the design.

Features regarding the manufacturing of a fixture

These features influence the machining and assembly costs as well as the material consumption of the fixture (Tab. 1). In the case of assessing the costs of manufacturing of special elements, a simplification that they are proportional to the number of machined surfaces of a fixture was introduced. During the calculation it was assumed that threaded openings are treated as two surfaces (boring of an opening and threading), the calculations excluded the bottom sections of deepened openings and it was assumed that grooves are singular surfaces. Machined surfaces also include welds.

Table. 1. Indicators of the manufacturability of a design - X_1 group of features

Specification	Determination method	Importance factor w_c
Number of components	$O_{Ex} = C_{Emax}/C_{Ex}$	1
Share of normalized components	$O_{nx} = C_{nrx}/C_{Ex}$	1.2
Cost of normalized components	$O_{nkx} = K_{nmax}/K_{nrx}$	1.5
Cost of manufacturing specialized components	$O_{swx} = N_{max}/N_x$	1.5

O_{Ex} – indicator of the number of components in a fixture,
 C_{Emax} – maximum number of elements among analysed fixtures,

C_{Ex} – number of components in the analysed fixture,

O_{nx} – indicator of the share of normalized components,

C_{nrx} – number of normalized components in the analysed fixture,

O_{nkx} – indicator of the cost-consumption for the normalized components,

K_{nmax} – maximum total amount of costs of normalized components among analysed fixtures,

K_{nrx} – cost of the normalized elements of the analysed fixture,

O_{swx} – indicator of the cost-consumption of manufacturing specialized elements,

N_{max} – maximum number of the machined surfaces among analysed fixtures,

N_x – number of the machined surfaces in the analysed fixture.

Table 2. Values of the indicators of the assessment of manufacturability of the fixtures

Specification	U1	U2	U3	U4	U5
O_E	1.120	1.330	1.867	1.000	1.217
O_n	0.624	0.856	0.800	0.943	0.626
O_{nk}	2.815	4.582	1.969	2.637	1.599
O_{sw}	2.757	2.508	1.962	1.500	1.561
Summary O_{Tx1}	7.316	9.277	6.598	6.080	5.003

Tab. 2 contains the collected results of the assessment of manufacturability of the five analysed fixtures, determined on the basis of the dependencies listed in Tab. 1 and multiplied by the assumed importance factor w_c .

Features regarding the operation and usage of a fixture

Features associated with the usage of the fixture regard the reduction of the fixing time (including, among others, handling the fixing assemblies, removing and mounting the machined element, as well as removing the chippings with compressed air), necessity of using additional tools and the number of elements mounted at the same time (Tab. 3).

Table 3. Indicators of manufacturability of a design - X_2 feature group

Specification	Determination method	Importance factor w_c
Time of mounting the machined element	$O_{mx} = t_{mmax}/t_{mx}$	2
Number of additional tools required to operate the fixture	$O_{dx} = 1 - 0.25n_{dx}$	1
Number of elements mounted in the fixture at the same time	$O_{lx} = 1 - 0.25n_{lx}$	1

O_{mx} – indicator of mounting the machined element in the analysed fixture,

t_{mmax} – maximum time of mounting the machined element among analysed fixtures,

t_{mx} – time of mounting the element in the analysed fixture,

O_{dx} – indicator of the number of additional tools required to mount the element in the fixture,

n_{dx} – number of additional tools used to mount the machine element,

O_{lx} – indicator of the number of elements mounted at the same time in the analysed fixture,

n_{lx} – number of elements mounted at the same time in the analysed fixture.

Determined collected results of the assessments of features in group X_2 are listed in table 4 (considering the assumed importance factor w_c).

Table 4. Values of the indicators of the assessment of operation and usage of the fixtures

Specification	U1	U2	U3	U4	U5
O_{mx}	4.518	2.000	4.518	4.518	2.838
O_{dx}	0.75	0.75	1	1	0.75
O_{lx}	1.25	1	1	1	1
Summary O_{Tx2}	6.518	3.750	6.518	5.518	4.588

Features regarding transport and regeneration of a fixture

The method of the assessment of features associated with transport and regeneration of fixtures is defined in Tab. 5.

Table 5. Indicators of the manufacturability of a design – X_3 feature group

Specification	Determination method	Importance factor w_c
Weight of the fixture	$O_{Mx} = M_{max}/M_x$	1.25
Overall dimensions of the fixture	$O_{Gx} = G_{max}/G_x$	1.1
Number of movable pairs of friction surfaces in the fixture	$O_{px} = 2 - C_{px}/C_{pmax}$	1.2

O_{Mx} – indicator of the weight of the analysed fixture, M_{max} – weight of the lightest fixture among the analysed ones,

M_x – weight of the analysed fixture,

O_{Gx} – indicator of the overall dimensions of the analysed fixtures,

G_{max} – maximum overall dimension of the fixture among the analysed designs,

G_x – maximum overall dimension of the analysed fixture,

O_{px} – indicator of the number of pairs of friction surfaces in analysed grips,

C_{px} – number of pairs of friction surfaces in the analysed fixture,

C_{pmax} – maximum number of pairs of friction surfaces among analysed fixtures.

Determined assessment of features in X_3 group are listed in Table 3 – considering the value of the assumed importance factor.

Table 6. Values of the indicators of the assessment of transport and regeneration of fixtures

Specification	U1	U2	U3	U4	U5
O_{mx}	1.343	1.250	2.455	2.368	2.646
O_{dx}	1.155	1.308	1.359	1.260	1.100
O_{lx}	1.440	1.920	2.400	2.400	1.200
Summary O_{Tx3}	3.938	4.478	6.214	6.027	4.946

Final assessment of the manufacturability of the fixture designs

Considering the dependency listed above (1) after including the assumed importance factor w_k , summary values of the indicator of manufacturability O_{Tk} were determined for the designs of fixtures U1 – U5 (Tab. 7).

Table 7. Summary values of the indicators of manufacturability of designs for the analysed specialized grips for machining a lever

Specification	U1	U2	U3	U4	U5
O_{Tk}	6.281	5.830	6.485	6.267	4.805

Summary

Manufacturability of a construction can be assessed descriptively, however, it requires detailed, specialized knowledge. A common criteria of assessment can be total cost, time for preparing the production and manufacturing time (machining or assembly), or a stipulated complex criteria. Time and cost criteria are difficult to apply when a specialized hardware is produced in limited numbers.

In the case of quantitative assessment of the manufacturability of a design, there is a possibility of adopting complex, hence multifaceted, criteria, as well as a possibility of selecting the method of a common scale (monetary or point), method of a function of weighted sum or product, quantitative determination of the level of modernity, value analysis, comparative method and others, using, among others, fuzzy logic [1, 5, 8, 10, 11].

The method proposed in the paper can be useful in the work of less-experienced constructors, so the ones who begin their professional career, or in the very process of educating mechanics and process engineers.

The assumed, simplified assessment criteria include both the complexity of the construction with respect to time-consumption of manufacturing the components and their assembly, as well as the features of the usage of fixtures.

The results of the conducted analysis of the specialized fixtures indicate that the design marked as U3 was given the highest mark. This mark results from the short time of mounting the machined element, easy operation of the fixture, as well as its relatively small dimensions and weight. The advantages of this fixture consist in quick fixing of the lever without the need of using extra tools and relatively low number of components.

References

[1] Antic R., Cvetkovic S., Pejovic B., Cvetkovic M. 2013. "Definition of manufacturability – product of mathematical expressions and fuzzy logic for his early design". *International Journal of Engineering and Technology* 2(3): 239-246.
[2] Barylski A. 2012. „Analiza jakości konstrukcji uchwytów”. *Zarządzanie i Finanse* 3: 345-353.

[3] Barylski A. 2017. „Ocena technologiczności konstrukcji uchwytów obróbkowych w aspekcie ich montażu i cech użytkowych”. *Przegląd Mechaniczny* 3: 31-37.
[4] Bralla J.G. 1999. *Design for Manufacturability*. New York: McGraw-Hill.
[5] Bramal D.G., Mckay K.R., Rogers B.C., Chapman P., Cheung W. N., Maropoulos P.G. 2003. "Manufacturability analysis of early product design". *International Journal of Computer Integrated Manufacturing* 7-9: 501-508.
[6] Boothroyd D., Dewhurst P., Knight W. 2002. *Product Design for Manufacture and Assembly*. New York: Marcel Dekker.
[7] Elgh F. 2004. "A generic framework for automated cost evaluation of product variants and fabrication plants". *Proceedings of the 2004 ASME Design Engineering Technical Conferences and Computers and Information in Engineering Conference*. Salt Lake City, UT, 28 September - 2 October.
[8] Elgh F. 2006. *Automated cost estimation of product variants – a tool for enhanced producibility*. Gothenburg: Chalmers University of Technology.
[9] Elgh F., Cederfeldt M. 2006. "A design automation system supporting design for cost – underlying method, system applicability and user experiences". *Proceedings of CE 2005: ISPE International Conference on Concurrent Engineering*. Fort Worth, TX, 27-29 July.
[10] Elgh F., Cederfeldt M. 2007. "Concurrent cost estimation as tool for enhanced producibility – system development and applicability for producibility studies". *International Journal of Production Economics* 109: 12-26.
[11] Elgh F., Cederfeldt M. 2008. "Cost-based producibility assessment: analysis and synthesis approaches through design automation". *Journal of Engineering Design* 2: 113-130.
[12] Feld M. 2002. *Uchwyty obróbkowe*. Warszawa: WNT.
[13] Gawlik E., Gill S. 2011. „Koncepcja systemu oceny technologiczności konstrukcji części maszyn i zespołów maszynowych”. *Zeszyty Naukowe Politechniki Rzeszowskiej* 83(279). *Mechanika* 1: 239-249.
[14] Insadowski S. 2019. *Analiza technologiczności konstrukcji zaprojektowanych uchwytów specjalnych*. Praca dyplomowa, prowadzący pr. A. Barylski, Politechnika Gdańska, Wydział Mechaniczny.
[15] Matusiak-Szaraniec A. 2007. „Analiza konstrukcyjna i technologiczna korpusów maszyn i urządzeń technicznych”. *Archiwum Technologii Maszyn i Automatykacji* 2 (27): 121-129.
[16] Poli C. 2001. *Design for Manufacturing: A Structured Approach*. Woburn: Butterworth-Heinemann.
[17] Turo D. 2005. "Methods for the determination and improvement of the manufacturability – product" connecting with integrated computer information system. *4 Scientific conference "Quality 2005"*. Fojnice, B &H: 123-129.
[17] Żurek J. 1989. *Problematyka technologiczności konstrukcji w budowie maszyn. Synteza teorii i praktyki przemysłowej*. Rozprawy nr 219. Poznań: Politechnika Poznańska.
[18] Żurek J., Briese W. 1999. „Algorytmizacja oceny technologiczności konstrukcji części i zespołów maszyn montowanych automatycznie”. *Technologia i Automatykacja Montażu* 4: 27-30.

Prof. dr hab. inż. Adam Barylski
Politechnika Gdańska,
Wydział Inżynierii Mechanicznej i Okrętownictwa,
Instytut Technologii Maszyn i Materiałów
ul. G. Narutowicza 11/12, 80-233 Gdańsk
e-mail: abarylsk@pg.edu.pl

COMPARATIVE ANALYSIS OF COMPRESSIVE STRENGTH OF REGENERATIVE MASSES MADE FROM EPOXY ADHESIVE COMPOUNDS SURFACES ROUGHNESS OF FLAT CERAMIC ELEMENTS AFTER LAPPING

Analiza porównawcza wytrzymałości na ściskanie mas regeneracyjnych wykonanych z epoksydowych związków adhezyjnych

Jacek OGRODNICZEK

ORCID: 0000-0002-6484-2245

Anna RUDAWSKA

ORCID: 0000-0003-3592-8047

Miroslav MÜLLER

ORCID: 0000-0002-3460-4254

Dana STANĚKOVÁ

ORCID: 0000-0003-0713-8750

DOI: 10.15199/160.2021.2.2

Abstract: The aim of this paper is to analyse statistically the compressive strength of two epoxy regenerative masses with different properties, which were subjected to the same three seasoning conditions. The first epoxy adhesive compound contained Epidian 5 epoxy resin mixed in mass ratio 100:80 with PAC curing agent, while the second epoxy adhesive compound consisted of Epidian 5 epoxy resin mixed in mass ratio 100:10 with Z-1 curing agent. The epoxy adhesive compounds were subjected to three seasoning variants. The first seasoning variant was carried out under normal conditions, at a temperature of $29^{\circ}\text{C} \pm 1^{\circ}\text{C}$ and at humidity of $20\% \pm 1\%$, for 1 week. The other variants of seasoning were performed in a climate chamber at a temperature of 80°C and humidity of 95%. The seasoning period in the climate chamber was continued for 4 or 6 weeks, depending on the variant. The obtained compressive strength results of both epoxy adhesive compounds were analysed statistically. The mean compressive strength values of the tested compounds differed significantly for particular variants. In order to obtain a precise statistical analysis, the ANOVA was used, which allowed to compare the results with regard to the seasoning variants for a given epoxy adhesive compound. The analysis showed a lack of similarity between variants of seasonings of epoxy adhesive compound consisting of Epidian 5 epoxy resin and PAC curing agent. In the case of compound made up of Epidian 5 epoxy resin and Z-1 curing agent, the ANOVA showed a very high similarity of compressive strength with respect to the compared seasoning variants.

Keywords:

Streszczenie: Celem niniejszej pracy jest analiza statystyczna wytrzymałości na ściskanie dwóch epoksydowych mas regeneracyjnych o różnych właściwościach, które poddano sezonowaniu w tych samych warunkach. Pierwsza epoksydowa masa klejowa składała się z żywicy epoksydowej Epidian 5 zmieszanej w stosunku masowym 100:80 z utwardzaczem PAC, natomiast druga masa składała się z żywicy epoksydowej Epidian 5 zmieszanej w stosunku masowym 100:10 z utwardzaczem Z-1. Epoksydowe masy klejowe poddano sezonowaniu. Pierwszy wariant sezonowania prowadzono w warunkach normalnych, w temperaturze $29^{\circ}\text{C} \pm 1^{\circ}\text{C}$ i przy wilgotności $20\% \pm 1\%$, przez 1 tydzień. Pozostałe warianty sezonowania przeprowadzono w komorze klimatycznej w temperaturze 80°C i wilgotności 95%. Czas sezonowania w komorze klimatycznej kontynuowano w zależności od wariantu przez 4 lub 6 tygodni. Uzyskane wyniki wytrzymałości na ściskanie obu epoksydowych mas klejących poddano analizie statystycznej. Średnie wartości wytrzymałości na ściskanie badanych mieszanek różniły się istotnie dla poszczególnych wariantów. W celu uzyskania precyzyjnej analizy statystycznej zastosowano metodę ANOVA, która pozwoliła na porównanie wyników w zakresie wariantów sezonowania dla danej epoksydowej masy klejowej. Analiza wykazała brak podobieństwa pomiędzy wariantami sezonowania epoksydowej masy klejącej składającej się z żywicy epoksydowej Epidian 5 oraz utwardzacza PAC. W przypadku mieszanki złożonej z żywicy epoksydowej Epidian 5 i utwardzacza Z-1 analiza ANOVA wykazała bardzo duże podobieństwo wytrzymałości na ściskanie w odniesieniu do porównywanych wariantów sezonowania.

Słowa kluczowe:

Introduction

The long-term operation of machines used in the technical field is associated with a wear and tear process of parts used in a given machine, this results in disruptions of the proper operation of the machine. Parts such as gears, crankshafts or housings are often exposed to various types of material damage. Examples of such damage are cracks, scratches or losses of material.

There are several types of wear and tear processes, they include [4]:

- mechanical-chemical wear,
- abrasive wear,

- corrosive-mechanical wear,
- erosive wear,
- adhesive wear,
- fatigue wear.

Typically, defective parts are replaced with new ones. A part can be purchased or manufactured by designing an appropriate technological process. However, this involves costs and machine downtime. A defective part can also be reconditioned. This process reduces operating costs and shortens downtime of the machine containing the faulty part [15].

The reconditioning process is a universal method and is widely used in technology. Its purpose is to restore the

functional properties of a given part of a technological machine. However, in this process it is very important to determine the degree of wear and tear of a given part. The damage may be too serious to undergo the reconditioning process. This applies mainly to cracks and material loss. Therefore, before proceeding with regeneration of a part, it is necessary to check whether it is possible to restore the original properties of the damaged part as a result of the process.

In the regeneration process, various methods are used to ensure the reconstruction and restoration of the component to a renewed operation. The methods used in the generation process include [13]:

- welding,
- surfacing,
- spraying,
- application of regenerative coatings,
- application of regeneration masses.

Parts which undergo wear and tear process are usually reconditioned by welding, surfacing or spraying. During the regeneration process using the above methods, a material with similar structure is used. When applying regenerative coatings, the phenomenon of electrolysis is used, which changes the chemical structure of the surface layer of the material of the damaged part, the process is due to the diffusion of the elements which are regenerating and strengthening the structure of the material. The most commonly used regenerative coatings include iron coatings, chromium coatings and iron-nickel coatings [2, 3].

Currently, regenerative masses based on polymeric materials are more widely used in the process of regeneration of parts. The popularity of regenerative masses is caused by their good mechanical properties. Moreover, they are easy to use which means that operations of the technological process, such as preparation or application of polymer regeneration masses, do not require special equipment as it happens in, for example, welding. Other advantages of this method are significantly lower repair costs and shorter period of machine downtime.

Usually regenerative masses consist of 2 components, an adhesive substance and a curing agent. To create an adhesive compound, both components need to be mixed in the appropriate mass ratio, recommended by the manufacturer. Improper mixing of these ingredients can reduce the strength of the compound. Curing and seasoning processes which can be carried out in different climatic conditions are also important for strength of the regenerative masses. In some cases, the impact of higher temperature on cured regenerative masses may accelerate the aging process, which leads to a significant reduction in the strength of the regenerative mass [11].

This paper, focuses on strength studies of epoxy adhesive compounds, which can be used as regenerative masses. Compressive strength tests have been performed on the epoxy adhesive compounds tested. The type of strength test was chosen because of the forces that mainly affect the regenerated areas in a worn-out part.

The ANOVA comparing both adhesive compounds with respect to compressive strength was also performed. For the comparison the STATISTICA program was used.

Research methodology

– description of the research preparation

Two epoxy adhesive compounds were used in the study as regenerative masses. The contents of these compounds is shown in Tab. 1. The epoxy adhesive compounds were based on Epidian 5 epoxy resin. This resin is characterised by low shrinkage during the curing process and is resistant to chemical agents, such as greases and oils. It also has excellent adhesion to most materials such as glass, metals and wood, making it suitable for a range of industrial applications [7].

Table 1. List of adhesive compounds

Compound No.	Contents		Stoichiometric ratio	Designation
	Resin	Curing agent		
1.	Epidian 5	PAC	100:80	E5/PAC/100:80
2.	Epidian 5	Z-1	100:10	E5/Z-1/100:10

The first adhesive compound was made of Epidian 5 epoxy resin mixed with PAC curing agent (E5/PAC/100:80). The structure of this compound was a homogeneous thick liquid which was dark yellow in colour. After being mixed with the epoxy resin, PAC curing agent required approximately 180 minutes to start the curing process. It is classified as a slow reacting curing agent. After 72 hours from the beginning of the curing process, the epoxy adhesive compound was pre-cured with PAC curing agent [16]. The curing process of the epoxy adhesive compound containing PAC curing agent was performed under conditions where the air humidity did not exceed 70% [17].

The second adhesive compound contained Epidian 5 epoxy resin mixed with Z-1 curing agent (E5/Z-1/100:10). The structure of this compound was a homogeneous liquid with a light yellow colour. When using Z-1 curing agent, the curing process started as soon as the curing agent was added to the epoxy resin. The time needed to pre-cure the epoxy adhesive compound with the applied Z-1 curing agent was 48 hours [9]. Z-1 curing agent is a chemical compound based on triethylenetetramine [17]. The excess of this curing agent in the epoxy adhesive compound causes a decrease of the physical properties of the created compound [8].

In case of both curing agents used in epoxy adhesive compounds, the period of full curing was 7 days. Comparing the properties of epoxy adhesive compounds,

the ones containing PAC curing agent were characterized by higher elasticity, but had lower resistance to elevated temperature than epoxy adhesive compounds for which Z-1 curing agent was used [1, 10]. In the study, the epoxy adhesive compounds were prepared immediately before filling the moulds.

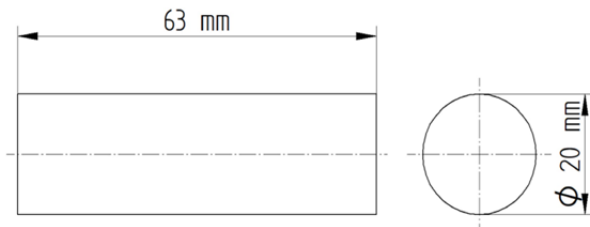


Fig. 1. Sample dimensions of epoxy adhesive compound

Samples of epoxy adhesive compounds were cylindrical in shape, their dimensions are shown in Fig. 1. Thirteen samples were made for each epoxy adhesive compound studied. During the preparation of the samples of the epoxy adhesive compounds the following conditions existed in the room : temperature $29^{\circ}\text{C} \pm 1^{\circ}\text{C}$, humidity $20\% \pm 1\%$.

During the curing process, the temperature and air humidity in the room were monitored. After 7 days, the cured samples of both epoxy adhesive compounds were subjected to 3 variants of seasoning.

The first seasoning variant involved seasoning of the samples for 7 days in room conditions at an ambient temperature of $29^{\circ}\text{C} \pm 1^{\circ}\text{C}$ and humidity of $20\% \pm 1\%$. For the second and third variants of sample seasoning, the Espec SH 661 climate chamber was used, which allowed for adjusting seasoning conditions, such as temperature and humidity. For both variants seasoned in the climatic chamber, identical seasoning conditions were applied. In the climatic chamber, the following conditions were created : temperature 80°C , humidity 95%. The temperature 80°C is the border temperature of resistance of this epoxy resin [18]. The difference between the seasoning variants was the period of curing the samples in the climatic chamber. Table 2 summarises the adhesive compounds, the number of prepared samples and the seasoning parameters.

After seasoning the samples according to individual variants, the samples were subjected to compressive strength tests according to PN-EN ISO 604:2006 [5] with the following parameters: initial force equal to 10 N, test speed 10 mm/min. The strength tests were performed using Zwick/Roel Z150 testing machine. The tested specimens were fixed in a compressive test device, which consists of two parallel flat plates, between which the samples were fixed. Fig. 2 shows the way of fixing the specimens in the compressive test device.

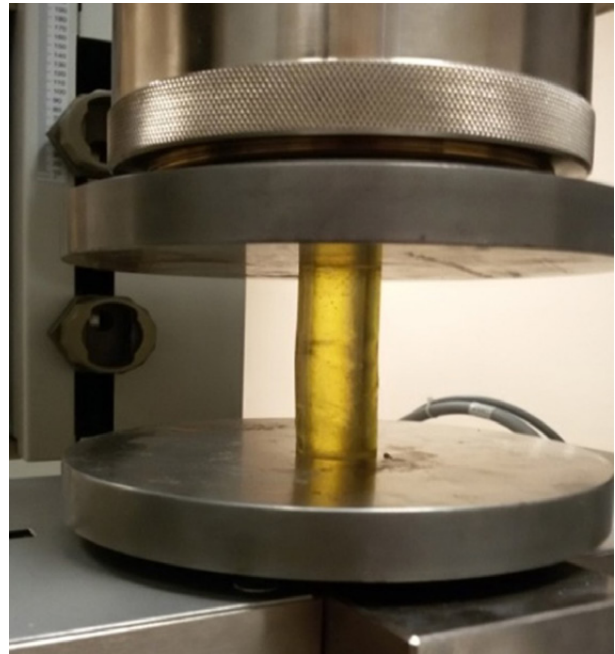


Fig. 2. System of the forced feed of abrasive compound

During the compression test, some slight buckling of the samples was observed. The obtained compressive strength results were then subjected to statistical analysis to compare the strength of the two adhesive compounds with regard to different seasoning options.

The statistical analysis used in this paper was ANOVA. This analysis allows for comparison of multiple mean results of tests coming from different groups, in this case seasoning variants [16,17]. The analysis of variance was applied only within a given adhesive compound,

Table 2: Summary of sample seasoning options

		Sampling seasoning variants		
		Variant 1	Variant 2	Variant 3
Number of cylindrical forms	E5/PAC/100:80	5	5	3
	E5/Z-1/100:10	5	5	3
Type of curing		Without climatic chamber	Climatic chamber	Climatic chamber
Seasoning period [week]		1	4	6
Temperature [$^{\circ}\text{C}$]		29°C	80°C	80°C
Humidity		20%	95%	95%

comparing the obtained compressive strength results with regard to the applied seasoning variant.

Results of studies

Table 3 shows the compressive strength results of epoxy adhesive compounds. The obtained results were subjected to a descriptive statistical analysis.

Analysing the obtained values by comparing the descriptive statistics in Tab. 3, it is possible to conclude that the mean compressive strength values in the different variants between the two adhesive compounds differ significantly. For the first variant this difference is 34%, for the second variant 57% and for the third variant 63%. These differences show a significant discrepancy between the compressive strength of the analysed adhesive compounds. Similar differences are also visible in the case of the median, which is the middle value of the set. Due to significant differences of average strength results of both adhesive compounds with regard to one seasoning variant, no further statistical tests were performed to check the convergence of mean results of adhesive compounds with respect to the seasoning variant.

On the basis of the data from descriptive statistics, it is also possible to compare

the results of compressive strength of a given adhesive compound with respect to the seasoning variant. The average values of compressive strength of Epidian 5 epoxy resin with PAC curing agent clearly decrease with a longer time of curing the compound. The difference between the average strength results of variant 1 and variant 3 is 42%. In the case of compound with Z-1 curing agent, the mean result of compressive strength of the seasoning variants is similar.

The ANOVA was used for further comparative analysis of the obtained compressive strength values of the tested specimens. Equality of the obtained mean strength results was assumed as hypothesis H₀. The test probability level was $\alpha=0.05$. One-way ANOVA was chosen as the type of analysis of variance.

Fig. 3 shows a comparative graph of the ANOVA of 3 seasoning variants of the E5/PAC/100:80 adhesive compound. The confidence interval of this test was $p=0.0003$. This means that the H₀ hypothesis should be rejected and the alternative hypothesis accepted [12, 14]. On the basis of the result of this statistical analysis, a significant difference can be seen between the results of the seasoning variants of the adhesive compound of Epidian 5 epoxy resin with PAC curing agent.

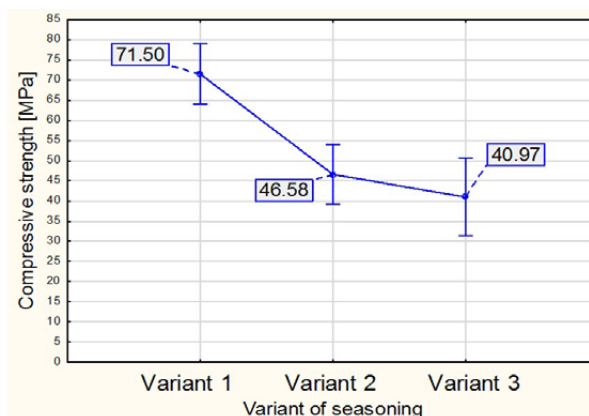


Fig. 3. The ANOVA of 3 seasoning variants of the E5/PAC/100:80

Fig. 4 presents the comparative ANOVA of 3 seasoning variants of E5/Z-1/100:10 adhesive compound. The presented graph shows the similarity of the average compressive strength results of this adhesive compound with regard to the seasoning variants. The confidence level of the test obtained by performing the analysis of variance was $p=0.999$. This means that the condition $\alpha < p$ was met. The confidence level of the test is close to 100%, which indicates a very high probability that the compressive strength of the adhesive compound of Epidian 5 epoxy resin with Z-1 curing agent for 3 different seasoning conditions is the same [11].

Table 3. Parameters of descriptive statistics for compounds compressive strength

Compound	Seasoning Variant	Number of samples	Mean [MPa]	Median [MPa]	Variance [MPa]	Standard deviation [MPa]	Skewness
E5/PAC	Variant 1	5	71.50	71.45	8.52	2.92	-1.03
	Variant 2	5	46.58	46.10	60.57	7.78	1.36
	Variant 3	3	40.97	35.40	140.96	11.87	1.65
E5/Z-1	Variant 1	5	107.54	106.00	181.06	13.46	0.32
	Variant 2	5	107.40	107.00	2.80	1.67	-0.51
	Variant 3	3	111.00	111.00	4.00	2.00	0

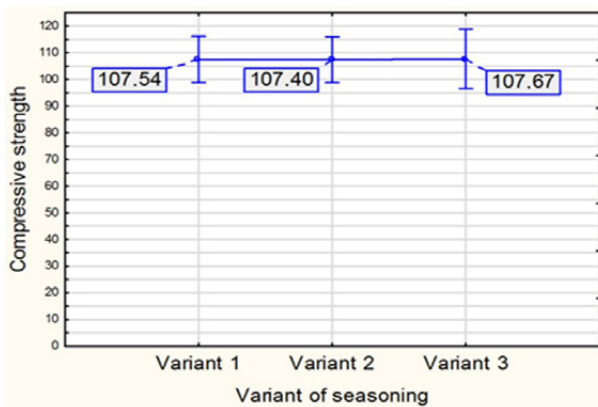


Fig. 4. The ANOVA of 3 seasoning variants of the E5/Z-1/100:10

Conclusion

After the test and statistical analysis, the following conclusions can be drawn:

- The type of curing agent and its amount in the adhesive compound, with different seasoning variants, clearly affects the value of compressive strength. In the case of the comparison of E5/Z-1/100:10 and E5/PAC/100:80 epoxy adhesive compounds with regard to the first variant, the difference was 34%, with regard to the second variant – 57%, and with regard to the third variant – 63%.
- Similar values of compressive strength of epoxy adhesive compounds in relation to different seasoning variants were obtained for E5/Z-1/100:10 compound. This means that the conditions of high temperature and humidity acting on the cured E5/Z-1/100-10 compound do not result in strength decrease. This compound can be used as a regeneration mass in machine parts.
- The change of temperature and humidity with regard to the conditions that prevailed during seasoning, negatively influenced E5/PAC/100:80 epoxy adhesive compound. Increasing the seasoning period in the climatic chamber by 2 weeks also contributed to a decrease in the compressive strength of the epoxy adhesive compound containing PAC curing agent. By increasing the seasoning period by 2 weeks, under the same conditions, a decrease of 19.08% in the compressive strength of variant 3 was observed in relation to variant 2 seasoning of the samples. This means that E5/PAC/100:80 epoxy adhesive compound is not a suitable regenerative compound to restore the usefulness of a broken machine part. This result also supports the finding that PAC curing agent is less heat resistant than Z-1 curing agent [8].

References

- [1] Czub P., Bończa-Tomaszewski Z., Penczek P., Pielichowski J. 2002. *Chemia i technologia żywic epoksydowych*. Warszawa: Wydawnictwo WNT.

- [2] Konarowska D. 2004. *Powłoki ochronne*. Radom: Wydawnictwo Politechniki Radomskiej.
- [3] Mistur L. 1971. *Spawanie gazowe i elektryczne*. Warszawa: Państwowe Wydawnictwa Szkolnictwa Zawodowego.
- [4] Mychajło P., Kindrachuk M. 2017. *Tribologia*. Lublin: Wydawnictwo Politechniki Lubelskiej.
- [5] PN-EN ISO 604:2006 – *Tworzywa sztuczne – Oznaczanie właściwości przy ściskaniu*.
- [6] Rabiej M. 2018. *Analizy statystyczne z programami Statistica i Excel*. Gliwice: Wydawnictwo Helion.
- [7] Rudawska A. 2020. "The Impact of the Acidic Environment on the Mechanical Properties of Epoxy Compounds in Different Conditions". *Polymers* 12(12): 1–19.
- [8] Rudawska A., Celejewski F., Miturska I., Kowalska B. 2018. „Wpływ warunków utwardzania i sezonowania na wytrzymałość połączeń klejowych doczołowych”. *Technologia i Automatyzacja Montażu* 4: 48–52.
- [9] Rudawska A., Głogowska K. 2014. „Analiza porównawcza wytrzymałości połączeń klejowych wykonanych przy użyciu klejów epoksydowych”. *Przetwórstwo Tworzyw* 4: 320–325.
- [10] Rudawska A., Semeniuk M. 2014. „Wpływ rodzaju żywicy epoksydowej i utwardzacza na wytrzymałość połączeń klejowych blach stalowych”. *Technologia i Automatyzacja Montażu* 4: 65–68.
- [11] Rudawska A., Wierzbowski A., Müller M., Petru J., Náprstková N. 2017. "The properties of regenerative polymer mass". *Advances in Science and Technology Research Journal* 11(3): 130–138.
- [12] Seltman H. 2018. *Experimental Design and Analysis*. Pittsburgh: Wydawnictwo Carnegie Mellon University.
- [13] Tyra A., Świerczyński S., Poreda A. 1989. *Regeneracja części maszyn i urządzeń*. Radom: Wydawnictwo MC-NEMT.
- [14] Wasilewska E. 2015. *Statystyka matematyczna w praktyce*. Warszawa: Wydawnictwo Difin S.A.
- [15] Wojdak J., Sędlak P., Wanke P., Stawicki T. 2009. „Analiza rozwoju metod regeneracji części maszyn w aspekcie przemian gospodarczych”. *Inżynieria Rolnicza* 1: 347–353.
- [16] <https://www.zywicesarzynna.pl/epidian-5-utwardacz-pac/> (21.04.2021).
- [17] <https://www.zywicesarzynna.pl/epidian-5-utwardacz-z1/> (21.04.2021).
- [18] <https://www.zywicesarzynna.pl/produkty/epidian-5/> (21.04.2021).

mgr inż. Jacek Ogrodniczek
doktorant Wydziału Mechanicznego Politechniki Lubelskiej
e-mail: jacek.ogrodniczek@pollub.edu.pl

dr hab. inż. Anna Rudawska, prof. PL
Katedra Podstaw Inżynierii Produkcji Wydziału Mechanicznego Politechniki Lubelskiej
ul. Nadbystrzycka 36, 20-618 Lublin
e-mail: a.rudawska@pollub.pl

Miroslav Müller,
Czech University of Life Science Prague,
Faculty of Engineering
165 21, Prague, Czech Republic
e-mail: muller@tf.czu.cz

Dana Stančeková,
University of Žilina, Faculty of Mechanical Engineering
Univerzitná 1, 010 26, Žilina, Slovak Republic
e-mail: dana.stancekova@fstroj.uniza.sk

Modelowanie konstrukcji szybkobieżnych kół zamachowych w urządzeniach technologicznych

Ivan DEHTIAROV
Katarzyna ANTOSZ
Serhiy AVRAMENKO
Kostyantyn HERASKO
Vitalii IVANOV

ORCID 0000-0001-8535-987X

ORCID 0000-0001-6048-5220

ORCID 0000-0003-0595-2660

DOI: 10.15199/160.2021.2.3

Abstract: The article analyzes the design of mechanical energy drives and their use areas. Based on the analysis, the kinetic energy drive designs based on the composite material's flywheel, capable of working with a high frequency of rotation. The most optimal flywheels in terms of accumulation of kinetic energy and at the same time the maximum strength of the design are proposed, and their numerical simulation is carried out. The modal analysis results established the values and forms of the eigenfrequencies of oscillations of rotors with flywheels of various structures, which allows controlling the process of overlocking, knowing the limit values of the maximum permissible frequency of rotation of the flywheels. Numerical modeling established that the flywheel's shape and its mass significantly affect the rotor speed limit with the flywheel. At the same time, the flywheel with the lowest mass but the highest frequency of rotation has the maximum specific energy intensity per unit of mass, which determines it as the most effective option in terms of the cost of material and the use of this design in devices for energy accumulation during the operation of technological equipment. The calculation results also show that the lamb flywheel has the most incredible absolute energy intensity. Simultaneously, the costs of the composite material above 68% are compared with the flywheel, which has the maximum specific value of the energy intensity per 1 kg of its mass.

Keywords: energy efficiency, moment inertia, eigenfrequencies, rotor, carbon fiber

Streszczenie: W artykule przeanalizowano konstrukcję napędów mechanicznych oraz obszary ich zastosowania. Na podstawie przeprowadzonej analizy opracowano projekt napędu kinetycznego opartego na sprzęgle z materiału kompozytowego, przeznaczonego do pracy z wysoką częstotliwością obrotową. Zaproponowano najbardziej optymalne koła zamachowe pod względem akumulacji energii kinetycznej i jednocześnie maksymalnej wytrzymałości konstrukcji oraz przeprowadzono ich symulację numeryczną. Na podstawie wyników analizy modalnej ustalono wartości i postaci częstotliwości własnych oscylacji wirników ze sprzęglami o różnych konstrukcjach, co pozwala na sterowanie procesem, znając graniczne wartości maksymalnej dopuszczalnej częstotliwości obrotów. Na podstawie modelowania numerycznego ustalono, że kształt sprzęgła oraz jego masa mają istotny wpływ na ograniczenie prędkości obrotowej. Jednocześnie sprzęgło o najmniejszej masie, ale największej częstotliwości obrotów ma maksymalną jednostkową energochłonność, co świadczy o tym, że jest to najbardziej efektywny wariant pod względem kosztów materiałowych i zastosowania tej konstrukcji w urządzeniach do gromadzenia energii podczas pracy urządzeń technologicznych. Porównano koszt dla sprzęgła o zawartości materiału kompozytowego powyżej 68% z kosztem sprzęgła, które ma maksymalną wartość jednostkową energochłonności na 1 kg masy.

Słowa kluczowe: sprawność energetyczna, moment bezwładności, częstotliwość własna, wirnik, włókno węglowe

Introduction

In connection with the active development of the world's technical progress in the XXI century, energy re-source consumption increased significantly [23]. Since the planet's fossil resources have a limited reserve, humanity is already whiter than 20 years increases the volume of energy production by developing new and improving existing methods based on the use of renewable energy sources. The energy of wind, sun, water, geothermal energy, and biofuels, whose share in total since 1999, has increased ten times [24]. The European Union countries plan to increase renewable energy sources from 20% in 2020 to 32% by 2030 [25, 26]. By

2050, an increase in energy consumption is predicted by more than two times compared with 2020 [23]. To preserve the world ecosystem, there is no other option except renewable sources. In the future, it is expected that the entire energy market will be captured by them [15]. Also, renewable sources are necessary for the regions where it is difficult and expensive to mount the power grid, while much energy is lost when transmitting it over long distances. However, one of the main aspects remains its accumulation and returns at a particular time. Currently, lithium-ion batteries and hydro accumulators used in reservoirs [27, 28] are the most common accumulation methods. Nevertheless, lithium-ion batteries are very dependent on the temperature regime and relatively short

service life and disposal problems. The main disadvantage of hydro accumulators is their cost and non-clean. Therefore, recently develops on the improvement of mechanical drives of flying type energy and their mass introduction in all areas of human life, where fast returns and high KPD are needed [29].

Literature Review

The latest research confirms the relevance of the development and research in mechanical energy drives with flywheels. Namely, D. Erdemir in [5] on the example of the practical use of flywheels in rapidly charging electric buses with a drive from renewable energy sources proved that power reduction could be reached electric batteries from 60% to 72% due to energy accumulation in flywheels.

In [21], we are modeling a flywheel with variable inertia in the design of a diesel generator using a flywheel rotation, depending on the generator shaft's rotation frequency, making it possible to increase the efficiency and reduce the shock loads of the mechanism. In studies [2, 6, 7, 9, 11, 16], a comprehensive review of the energy accumulation system's technology with the flywheel is shown. Practical ways of developing this technology in the future are presented in the scheme of wind power and solar energy to prevent sharp voltage drops in power systems using optimization methods, simulation and simulation methods, and active control systems.

K. Pullen in [12] and A. Arabkooohsar in [1] presented a whole scheme of a mechanical energy storage device based on flywheel motor-generator, efficiency which reaches 85-90%. The diagram [12] is currently used on the Formula 1 cars for substantially giving the acceleration at the critical moment and the graph [1] in NASA satellites.

M. Spiryagin and P. Wolfs In [18], the modeling of the Flywheel-diesel engine's hybrid system for heavy-duty locomotives was performed, the results of which are confirmed by experimental studies. Also in the paper presents the developed integrated intelligent control system for traction. What made it possible to get fuel economy. Work [14] S. Rastegarzadeh is devoted to creating a new modular design of the rotor with a flywheel consisting of a set of rings to optimize power consumption in the subway trains made it possible to reduce energy consumption by 35%. The development and testing of the two-pole mass device with the inertia variable's flywheel are represented by S. Yang in [19], which shows the flywheel's design with four sliders. It allows changing the equivalent mass as the speed of rotation of the flywheel changes to optimize the device's operation and increase its efficiency.

J. Zhao's research was focused on inertia studies [22], which presents the technology of measuring the flywheel's inertial masses using the Mass-Spring model as the simulation models of the flywheel before or after attaching counterweights in the SIM-Mechanics application from Matlab.

R. Miyamoto and A. Goedel in [10] proposed a way to connect to an electrical network of an induction generator with a short-circuited rotor connected to a cylindrical flywheel with high inertia to reduce perturbations during a transition in the electrical grid.

The work [17] is devoted to developing a design based on Maxwell's lift forces and Lorentz to stabilize the flywheel using minimal power losses, even with a significant increase in the size of the flywheel.

The hybrid designs of electrical mechanisms using flywheels are equipped with the most advanced technical solutions, in particular W. Yang in [20] proposed an integrated triboelectric nanogenic with a flywheel and a spiral spring to improve energy collection during intermittent excitation/launches.

In [3, 8, 13], the advantages of flywheels made of light and durable materials, such as carbon fiber and nanocomposites, and identified areas of their using by a multi-criteria decision-making method for selecting and verifying the fabric of the flywheel design.

From the review of literary sources, it follows that the development of designs of flywheels and hybrid systems based on the use of regenerated energy sources is an urgent task. But in these studies, issues regarding the prospects for the benefit of flywheels in machine-building enterprises' technological equipment and the analysis of the design parameters of flywheels from composite materials by methods of finite element analysis. The use of kinetic energy drives in technological equipment is also relevant and because the machine's rotating spindle is spent either the energy of the electromagnetic field or the stop occurs with the help of friction brake mechanisms. This carries the additional costs of electricity or the need to use brake mechanisms that are wearing in the work process require repair and replacement.

Thus, the study aims to determine the optimal form and material of the flywheel for the mechanism of energy recovery from the drive of metalworking machines using finite element analysis methods.

Research Methodology

Development of a mechanical energy storage concept for metalworking equipment

Energy accumulation and storage systems using a flywheel can be divided into two main categories; The first is a system with low flywheel rotation speeds (less than 10 000 revolutions per minute); The second is a system with a high speed of the flywheel (up to 60 000 revolutions per minute). In general, the second system consists of:

- electric generator motor, which runs as an engine when charging and as a generator during discharge;
- flywheel of the rotor, which retains kinetic energy;
- magnetic bearings to reduce friction losses;
- bidirectional converter providing electrical power in both directions during charging and discharge;

- vacuum pump to create a vacuum in the rotation chamber.

As already mentioned in the literary review, such systems are actively used in wind power, hybrid installations, in racing cars. Still, references to the use of mechanical energy drives in metalworking equipment failed to find. Therefore, the article proposes an embodiment of an automatic movement based on a stationary installation of kinetic energy accumulation based on a flywheel from a composite material with a high speed of rotation using magnetic bearings.

The rotor design concept with the flywheel, the generator, and bearings is shown in Fig. 1.

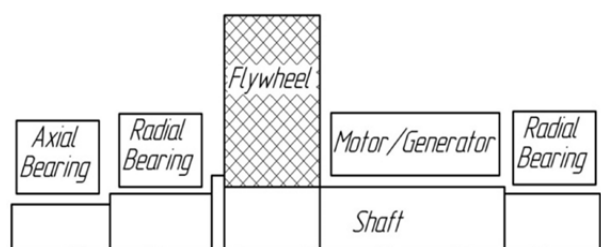


Fig. 1. Principle scheme of mechanical energy storage

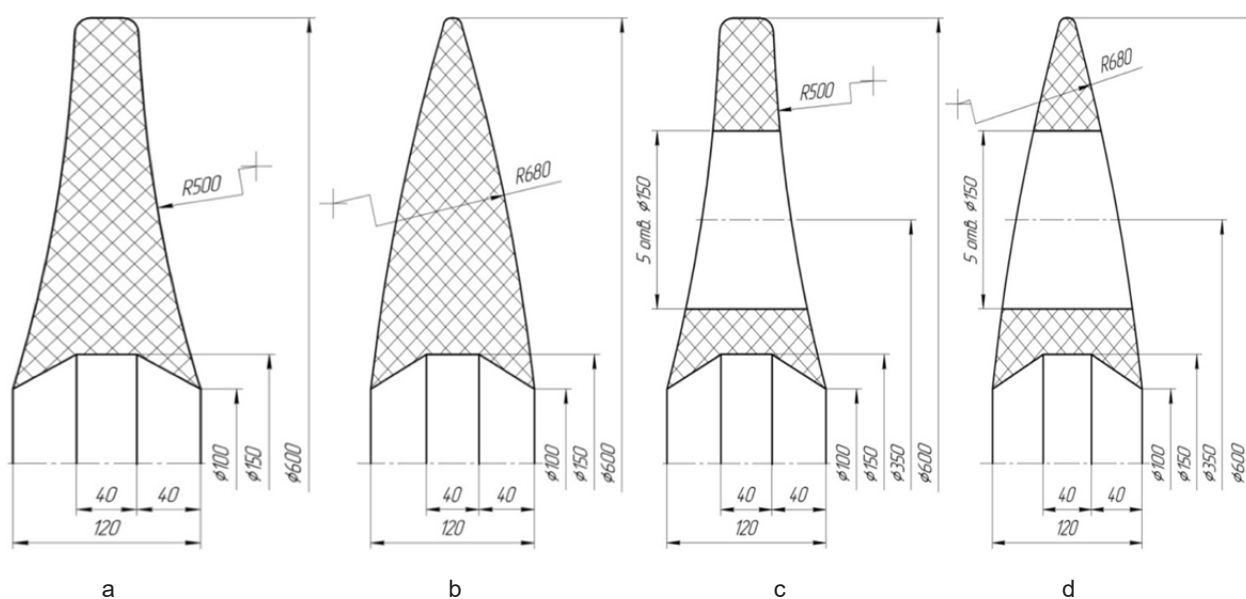


Fig. 2. Flywheel designs for research: a - with concave side surfaces; b - with convex side surfaces; c - with concave side surfaces and radially located holes; d - with convex side surfaces and radially located holes

Development of design and rationale for choosing materials for mechanical energy storage

Based on the concept (Fig. 1), the selected sizes of the flywheel, the parameters of the magnetic bearings, and the rotor's size, a design of a mechanical energy storage device is proposed, placed in a closed case with a lid (Fig. 3). As a material for the body and the cover, cast iron is used, so it is cheap and has a reasonably high weight to preserve the position's stability while working

Flywheels with low speed are made, mechanical or magnetic bearings maintain steel and rotor. High-speed flywheels typically use lighter but durable composite materials and use exclusively magnetic or hydrostatic bearings. The cost of the energy accumulation system with high-speed flywheels can be five times higher than the cost of systems with a low speed of the flywheel. The energy accumulation system's worth depends on the price of all parts and components used, especially from the flywheel's cost that allows a high rotation speed. Therefore, it is necessary to minimize the use of an expensive composite material in the mechanical energy storage system design for metal-cutting equipment but simultaneously achieve a sufficiently high energy density by studying the various configurations of the flywheels (Fig. 2). The flywheel designs with convex and concave radii of side surfaces were chosen based on recommendations [4] at the flywheel design's maximum flatness coefficients (Fig. 2 a, b). At the same time, it is proposed to reduce the volume of composite material, in addition to the above structures (Fig. 2 a, b), explore the flywheels with holes located around the circle (Fig. 2 c, d).

without the use of a large number of fastening elements. To eliminate losses for friction, the flywheel in the chamber of the case will be created by a vacuum. Magnetic bearings also exclude friction in the rotor supports. As a rotor shaft material to reduce its mass, the titanium alloy WT1-0 is adopted to ensure sufficient strength.

To increase the flywheel's strength characteristics as a material, a carbon fiber HEXTOW AS4 is selected. HEXTOW Carbon Fiber AS4 is a continuous,

high-strength, spectacted PAN-based fiber (polyacrylonitrile). The flywheel, entirely made of carbon fiber, fasten directly on the rotor shaft is not possible without additional parts of the design.

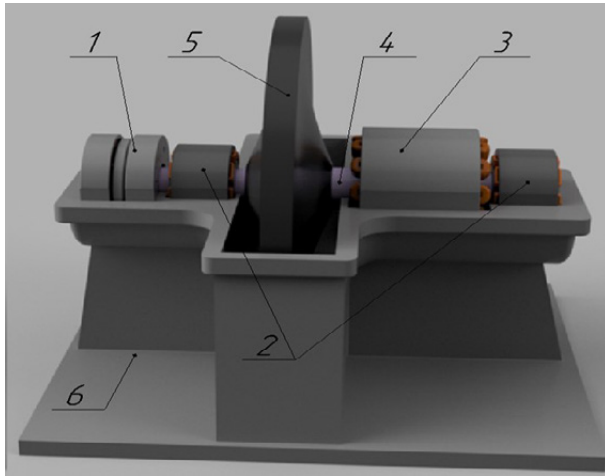


Fig. 3. 3D-model of the proposed design of the mechanical energy storage with flywheel

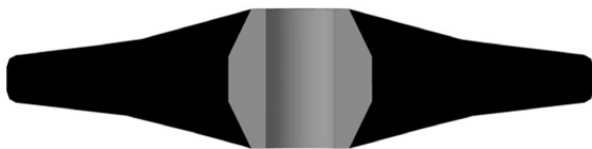


Fig. 4. Connection sleeve-flywheel

Therefore, to possibly molding a carbon fiber, its mechanical processing, and balancing separately from the rotor in the mechanical energy drive's proposed method, the flywheel is composite. It consists of a central sleeve and a direct flywheel from the composite material (Fig. 4). The mid sleeve has a base surface for planting a flywheel on the rotor shaft, the material of which is adopted by titanium alloy W1-0. The physicommechanical properties of the materials of the flywheel, the rotor shaft, and the central sleeve are presented in tab. 1.

According to the built 3D models of the designs of flywheels (Fig. 2 A-d), we define the masses of the flywheels and the inertia moments according to the formula for parts of the type of disc, and the results of the calculations are reduced to the Tab. 2.

$$I = \frac{1}{2} mR^2 \quad (1)$$

m – a mass of the disk, kg;

R – disk radius, m.

To determine the number of stored kinetic energy, the flywheel needs to know its maximum permissible rotation frequency. This implies the definition of its frequencies of the designed structure to eliminate resonance appearance, which is possible using programs for the finite element analysis.

Table 1. Physical and Mechanical Properties of Rotor Materials

Material (DIN standard)	Modulus of elasticity E, GPa	Poisson's ratio μ	Density ρ , kg/m ³	Tensile strength [σ_t], GPa	Ultimate strength of compression, [σ_c], GPa	Yield strength σ_y , GPa
Titanium alloy WT1-0	88	0.33	4820	0.860	0.860	0.585
Carbon fiber HexTow AS4	231	0.15	1790	4.720	4.720	-

Table 2. Results of calculations of the mass-center characteristics of flywheels

Flywheel design	Number figure of the flywheel	Mass flywheel without the basic sleeve, kg	Moment of inertia, kg · m ²
With concave side surfaces	2a	27.8	1.251
With convex side surfaces	2b	28.2	1.269
With concave side surfaces and radially located holes	2c	17.9	0.806
With convex side surfaces and radially located holes	2d	16.7	0.752

Results

Study of eigenfrequencies of oscillations of the rotor mechanical energy storage

To prevent the resonance phenomenon during the mechanical drive of energy due to the coincidence of its oscillations with equipment fluctuations in the working workshop, we define our frequencies using the built-in MODAL ANALYSIS module in the Ansys Workbench estimated complex. Equipment fluctuations arise as a result of its work in the cutting process. The analysis results make it possible to determine the critical frequencies of oscillations and prevent these values' achievements

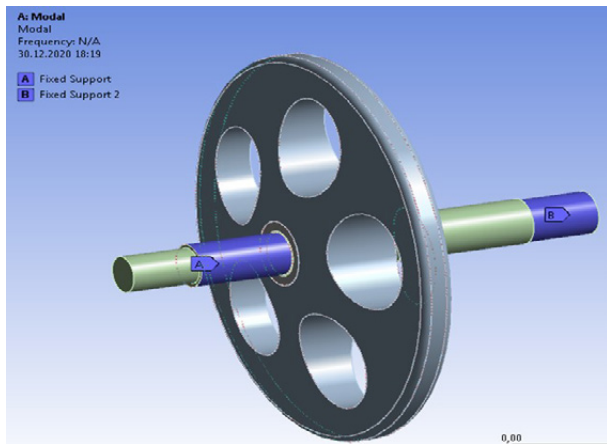


Fig. 5. Boundary conditions with finally element modeling of the rotor

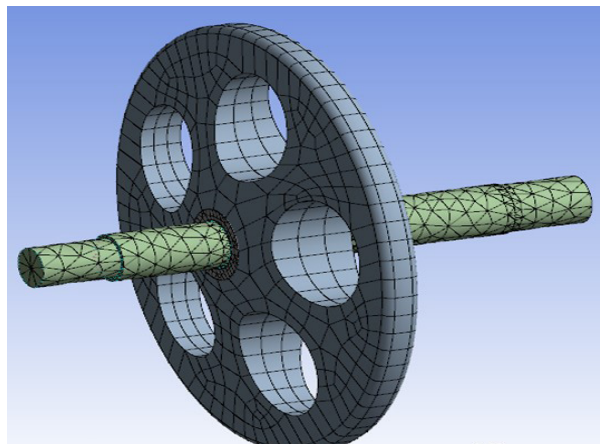


Fig. 6. A finite-element mesh of the rotor

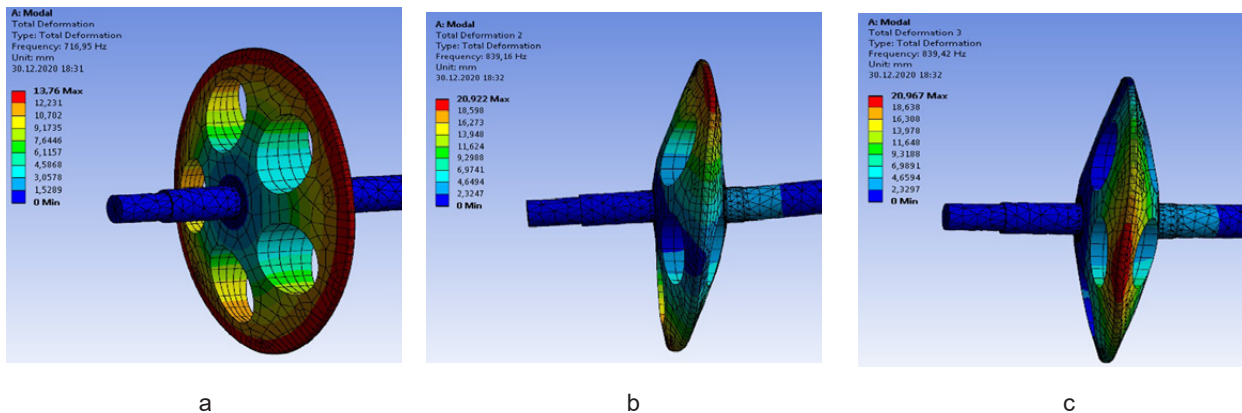


Fig. 7. Illustrations of own oscillation frequencies: a - the first frequency; b - second frequency; c – the third frequency

An example of the first three-eating frequencies of oscillations for a rotor with a flywheel with convex side surfaces and radially located holes is shown in Fig. 7. Also, to control the frequency of rotation of the flywheel and preventing the exit to the resonance region, the frequency of oscillations in turns in one minute by multiplying the calculated frequency by 60 is carried out by multiplying the calculated frequency.

when the flywheel is accelerated (Tab. 3). When calculating the rotor shaft, the central bush and the flywheel bind to each other by combining the nodes with the type "Bonded" contact. This is justified because the landing of the sleeve on the shaft is carried out on triangular slots with tension, and the flywheel is connected to the central sleeve tight bond by laying the fibers into unique grooves and filling fibers with epoxy resin. Fixing in the process of modeling was made according to the raw surfaces of radial bearings, which is shown on the example of the rotor with a flywheel, which is characterized by concave side surfaces and radially located holes (Fig. 5), the finite element mesh of which is presented in Fig. 6.

Tab. 3 shows that the rotor's design with a flywheel characterized by convex side surfaces and radially located holes has the most significant value of the first one's frequency. This means that this design is most resistant to external fluctuations since entering the resonance from external sources is the least likely among the rotors' constructions.

Table 3. Researches of studies of eigenfrequencies of rotor oscillations with various designs of flywheels

Rotor with Flywheel Design	Eigenfrequencies of rotor oscillations, Hz / Rotor rotation frequency, rpm		
	1	2	3
With concave side surfaces	594 / 35640	725 / 43500	726 / 43560
With convex side surfaces	628 / 37680	803 / 48180	804 / 48240
With concave side surfaces and radially located holes	436 / 26160	469 / 28140	499 / 29940
With convex side surfaces and radially located holes	717 / 43020	839 / 50340	840 / 50400

To determine the most significant energy efficiency of the designs under consideration, we define a possible amount of pointed kinetic energy by the formula:

$$E = \frac{1}{2} I \omega^2 \quad (2)$$

I – a moment of the disk inertia;
 ω – the angular speed of the disk, sec^{-1} .

$$\omega = \frac{\pi \cdot n}{30} \quad (3)$$

n – frequency of rotation of the disk, rpm.

It has been established that the rotor with a flywheel with convex side surfaces and radially located openings has the most significant kinetic energy value stored by the flywheel per 1 kg of mass. Simultaneously, the flywheel mass is 16.7 kg, which is less than that of other designs' flywheels under consideration. In absolute terms, the most significant amount of kinetic energy is 9.9 MJ at the speed of 37680 rpm allows you to accumulate a whole flywheel with convex side surfaces. Still, it has the most significant weight of 28.2 kg.

Conclusions

1. With the help of numerical modeling of rotors with various designs of the flywheels, their frequencies are defined, which will control the limit rotation frequency with the flywheel, which will avoid its destruction. It is also established that the rotor resonance caused by the coincidence of its frequency with the frequencies of the equipment in the workshop is unlikely since the smallest first critical frequency of the rotor from all the studied structures is 436 Hz, which corresponds to 26 160 rpm.
2. It has been established that the design of the rotor with a flywheel from the composite material Hextow AS4 with convex side surfaces and radially located holes at a weight of 16.7 kg has the most considerable specific amount of kinetic energy stored by the flywheel per 1 kg of mass – 0.457 MJ/kg. In absolute

ex-pression, the flywheel of this design can accumulate 7.6 MJ energy at 43020 rpm. Thus, the theoretically proved the possibility of using mechanical energy storage with the flywheel in metalworking workshops' technological equipment.

Thus, the flywheel's design with convex side surfaces and radially located holes is most optimal from the point of view of energy intensity and the composite material cost because it has a lot of 11 to 68% less than the designs under consideration.

3. Further research is aimed at a dynamic study of the rotor's accelerating dynamics with a flywheel with convex side surfaces and radially located holes under the action of centrifugal forces with a change in over-clocking time and acceleration during acceleration to modes close to the first one's frequency.

References

- [1] Arabkoohsar A., Sadi M. 2021. Flywheel energy storage. In *Mechanical Energy Storage Technologies*, 101–124. *Mechanical Energy Storage Technologies*.
- [2] Arani A., Karami H., Gharehpetian G., Hejazi M. 2017. "Review of flywheel energy storage systems structures and applications in power systems and microgrids" *Renewable and Sustainable Energy Re-views*69: 9–18.
- [3] Asodariya H., Patel H., Babariya D., Maniya K. 2018. "Application of multi criteria decision making method to select and validate the material of a flywheel design" *Advances in Materials & Processing: Challenges & Opportunities (AMPCO-2017)*, Metallurgical and Materials Engineering Department, IIT Roorkee, India, 30th November to 2nd December 20175(9): 17147–17155.
- [4] Bolund B., Bernhoff H., Leijon M. 2007. "Flywheel energy and power storage systems" *Renewable and Sustainable Energy Reviews* 11(2):235–258.
- [5] Erdemir D., Dincer I. 2020. "Assessment of renewable energy-driven and flywheel integrated fast-charging station for electric buses: a case study" *Journal of Energy Storage* 30(9): 101576.
- [6] Hamzaoui A., Bouchafaa F., Talha A. 2016. "Advanced control for wind energy conversion systems with flywheel storage dedicated to improving the quality of energy" *International Journal of Hydrogen Energy* 41(45):20832–20846.
- [7] Hutchinson A., Gladwin D. 2020. "Optimisation of a wind power site through utilisation of flywheel energy storage technology" *Energy Reports* 6(5): 259–265.
- [8] Kale V., Secanell M. 2018. "A comparative study between optimal metal and composite rotors for fly-wheel energy storage systems" *Energy Reports*4: 576–585.

- [9] Mansour M., Mansouri M., Bendoukha S., Mimouni M. 2020. "A grid-connected variable-speed wind generator driving a fuzzy-controlled PMSG and associated to a flywheel energy storage system" *Electric Power Systems Research* 180: 106137.
- [10] Miyamoto K., Goedel A., Castoldi M. 2020. "A proposal for the improvement of electrical energy quality by energy storage in flywheels applied to synchronized grid generator systems" *International Journal of Electrical Power & Energy Systems* 118:105797.
- [11] Mousavi G., Faraji F., Majazi A., Al-Haddad K. 2017. "A comprehensive review of flywheel energy storage system technology" *Renewable and Sustainable Energy Reviews* 67: 477–490.
- [12] Pullen K. 2019. "The status and future of flywheel energy storage" *Joul* 3(6): 1394–1399.
- [13] Qiang L., Kun W., Yuan R., Xiaocen C., Limei M., Yong Z. 2019. "Optimization design of launch locking protective device (LLPD) based on carbon fiber bracket for magnetically suspended flywheel (MSFW)" *Acta Astronautica* 154: 9–17.
- [14] Rastegarzadeh S., Mahzoon M., Mohammadi H. 2020. "A novel modular designing for multi-ring fly-wheel rotor to optimize energy consumption in light metro trains" *Energy* 206(1): 118092.
- [15] Roy N., Das A. 2017. *Prospects of Renewable Energy Sources*. In *Renewable Energy and the Environment*, 1–39. Springer Link.
- [16] Sebastian R., Pena-Alzola R. 2015. "Control and simulation of a flywheel energy storage for a wind diesel power system" *International Journal of Electrical Power & Energy Systems* 64: 1049–1056.
- [17] Sonsky Y., Tesar V. 2019. "Design of a stabilised flywheel unit for efficient energy storage" *Journal of Energy Storage* 24:100765.
- [18] Spiryagin M., Wolfs P., Szanto F., Sun Y., Cole C., Nielsen D. 2015. "Application of flywheel energy storage for heavy haul locomotives" *Applied Energy* 157(1): 607–618.
- [19] Yang S., Xu T., Li C., Liang M., Baddour N. 2016. "Design, modeling and testing of a two-terminal mass device with a variable inertia flywheel" *Journal of Mechanical Design* 138(9): 095001.
- [20] Yang W., Wang Y., Li Y., Wang J., Tinghai C., Wang Z. 2019. "Integrated flywheel and spiral spring triboelectric nanogenerator for improving energy harvesting of intermittent excitations/triggering" *Nano Energy* 66:104–104.
- [21] Zhang Y., Zhang X., Qian T., Hu R. 2020. "Modeling and simulation of a passive variable inertia flywheel for diesel generator" *Energy Reports* 6(7):58–68.
- [22] Zhao J., Ni B., Jun L., Luo H., Yuan J. 2020. "Research on in-situ measurement simulation test of inertia of flywheel simulator by simmechanics" *Procedia Computer Science* 166:31–36.
- [23] Electronic resource - access mode: <https://www.eia.gov/todayinenergy/detail.php?id=41433>
- [24] Electronic resource - access mode: <https://www.bp.com/en/global/corporate/energy-economics/statistical-review-of-world-energy/renewable-energy.html>
- [25] Electronic resource - access mode: <https://www.irena.org/europe>
- [26] Electronic resource - access mode: <https://www.iea.org/reports/renewables-2020>
- [27] Electronic resource - access mode: <https://www.epa.gov/energy/electricity-storage>
- [28] Electronic resource - access mode: <https://www.azoclean-tech.com/article.aspx?ArticleID=593>
- [29] Electronic resource - access mode: https://en.wikipedia.org/wiki/Flywheel_energy_storage.

Dr. Ivan DEHTIAROV, Ph. D,
Sumy State University, Ukraine,
e-mail: ivan_dehtiarov@tmvi.sumdu.edu.ua

dr hab. inż. Katarzyna ANTOSZ,
Rzeszow University of Technology, Poland
e-mail: kcktmiop@prz.edu.pl

Serhiy AVRAMENKO, MSc.,
Sumy State University, Ukraine
e-mail: sergey.avramenko7@gmail.com

Kostyantyn HERASKO, BSc.,
Sumy State University, Ukraine
e-mail: rocky76nirvana@gmail.com

Prof. Vitalii IVANOV, DSc.,
Sumy State University, Ukraine
e-mail: ivanov@tmvi.sumdu.edu.ua

przemysł chemiczny

www.przemchem.pl

Najstarsze, liczące ponad 100 lat,
polskie czasopismo chemiczne
notowane na liście filadelfijskiej,
adresowane do menadżerów,
inżynierów i technologów w przemyśle



- 12 wydań w roku
- Baza ponad 7300 publikacji naukowych
- Baza ponad 2650 publikacji jako open access z lat 2014–2021 dostępnych na Portalu Informacji Technicznej www.sigma-not.pl

Kontakt: tel.: 22 818 51 71, 22 818 72 86

Redakcja: przemyslchemiczny@sigma-not.pl

Prenumerata: prenumerata@sigma-not.pl

Reklama: reklama@sigma-not.pl

WYDAWNICTWO SIGMA-NOT

TESTS OF THE TIME CONSUMPTION OF THE OPERATIONS PERFORMED AT THE WORKSTATION FOR ASSEMBLING AND DISASSEMBLING ENGINES

Badania czasochłonności czynności wykonywanych na stanowisku pracy do montażu i demontażu silników

Robert CIEŚLAK
Paweł SOBCZAK
Krzysztof MAKOWSKI

ORCID: 0000-0002-1320-0410

DOI: 10.15199/160.2021.2.4

Abstract: The paper includes the description of the tests on the time consumption of the operations performed at the workstation for assembling and disassembling bus engines. The paper presents the method called ChronFoto_RC which was used to analyse the workstation. Then, the authors proposed to improve the workstation with a specially designed mobile scissor lift. The summary presents the assessment of this solution.

Keywords: time consumption, assembling, disassembling

Streszczenie: W artykule zawarto opis badań czasochłonności operacji wykonywanych na stanowisku pracy przy montażu i demontażu silników autobusowych. Przedstawiono metodę ChronFoto_RC, która została wykorzystana do analizy stanowiska pracy. Następnie autorzy zaproponowali usprawnienie stanowiska pracy za pomocą specjalnie zaprojektowanego mobilnego podnośnika nożycowego. W podsumowaniu przedstawiono ocenę tego rozwiązania.

Słowa kluczowe: czasochłonność, montaż, demontaż

Introduction

The assembly technological process is the final stage of the production process during which the elements are joined according to a series of logically planned actions in such a way that the assembly units and the final product can meet specific technical requirements proposed by the construction engineer.

One of the main tasks performed during the design of the assembly technological process is to determine the correct sequence of operations as well as their duration time. Faced with strong market competition, an increasing number of types, variants and an increasing complexity of products, a modern assembly company requires continuous improvement of both the organization and technological flexibility of systems, especially the automated, robotic and hybrid ones [3, 6].

Measuring the working time of humans in assembly processes is used to:

- determine the actual workflow and the manner in which the work is completed,
- identify losses resulting from the method used (determining production reserves),
- establish rational ways and methods of working as well as the necessary time of work completion [7, 8, 10].

Measuring the working time also belongs to the elements of economical business management. In order to plan, manage and control the workflow, which are the

essential activities for implementing a given production programme, it is necessary to precisely calculate the duration time of work completion. This calculation is essential, especially when the duration time is managed consciously. Out of concern for the worker, it is made sure that workers performing their work in assembly departments are able to do it without a significant effort. The usefulness of testing the working time also results from the fact that the economical efficiency of the business (reducing production costs to the minimum) is possible when the workflow at individual workstations is organized in a rational manner.

The aim of testing the working time

One of the key factors for improving the work organization is the technical standardization of work, that is, determining its optimal workload for the performance of a given work task in specific organizational and technical conditions [5].

In modern industry, proper and systematic research into work is an integral part of managing technical, technological, organizational and economic progress and is part of the system of activities aimed at continuous increase in work efficiency [1].

The aim of the test performed at the workstation for assembling and disassembling bus engines in the repair shop of the Municipal Transport Company is to determine the actual duration of the operation at a normal pace of

work and to determine the efficiency of the worker (taking into account working times and breaks). In order to improve the conditions and reduce the duration time of assembling and disassembling bus drive units, a model of a mobile scissor lift was presented.

Methodology of testing the time consumption of operation by means of the ChronFoto_RC method

The tests carried out within industrial practice encouraged the authors to try to develop a method of testing the time consumption of assembling. The method is based on the combination of chronometric analysis modules and working-day activity study (working-day photo). The combination of these two modules resulted in the development of the ChronFoto_RC program, equipped with a simple operation menu, that can be installed on almost any computer.

It was assumed that the suggested method of testing the time consumption of technological assembly processes should:

- accurately record working times and rest periods, i.e. the pace of technological operations,
- assign different types of times to individual elements of the operation (chronometric analysis module),
- take into account the possibility of calculating the coefficient (the so-called percentage surplus of supplementary time) in the working time standard for the assembly operation (working day photo module).

The criteria to assess the effectiveness of this method, allowing to obtain satisfactory results quickly and easily, include:

- accuracy of time consumption measurements,
- short duration time (costs) of taking measurements,
- the ability to analyse measurements of the time consumption of complex activities (operations).

The most important steps in the application of the ChronFoto_RC method are as follows: defining the aim and subject matter of the test, determining the necessary number of measurements; dividing the tested activity into its elements; carrying out measurements; performing a chronometric sequence analysis which involves the rejection of values significantly different from the average by means of the so-called coefficient of chronometric sequence content; assigning types of working time to sections of the operation (process); selecting and adding time consumption categorised by type; compiling the sums of the types of time consumption; evaluation of worker productivity and compiling the sums of the types of time consumption in the form of a graph [2].

Description and characteristics of the workstation for assembling and disassembling bus engines

The assembling and disassembling process in the repair shop of the Municipal Transport Company is performed when:

- the bus is intended for scrapping,

- the engine has broken down and it is impossible to repair the failure without removing the engine,
- the engine had a complete failure, preventing its further operation.

The measurement of the working time during the assembly of the bus engine involved the following activities:

- collecting data on activities performed by workers while assembling selected engines; measuring the working time of assembling the engine included one team of mechanics who performed their work in a closed hall (it had two repair lines) (Fig. 1),
- dividing the analysed activity into elements; the assembly operations performed while the engine was being assembled are presented later in the article,
- determining the testing method and the scope of the activity being tested; it was agreed with the manager of the repair shop that the new method, ChronFoto_RC, would be used for the measurement of the working time,
- establishing boundary points; the boundary points are understood as distinct and easily noticeable moments when individual elements of the procedure start and finish; as a general rule, the same point is both the end of the previous element and the start of the next one,
- setting the time and date of the measurements; the time and date of the measurements were agreed with the manager of the repair shop; the measurements were taken from 06:00 to 14:00,
- carrying out measurements; it was agreed with the manager of the repair shop that the time of individual activities would be measured with stopwatches (with an accuracy of one second); at the same time, the results of the measurements will be transferred to the forms prepared in advance,
- compiling observation results and performing their analysis; after the measurements, the results of the observations were shown to the manager of the repair shop.



Fig. 1. Workstation for assembling and disassembling engines

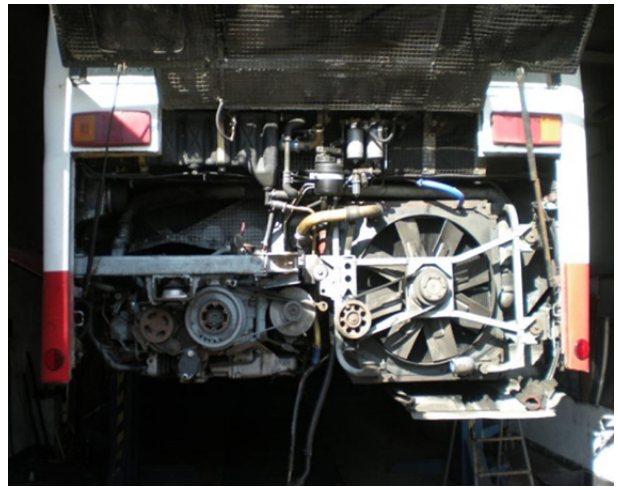


Fig. 2. Mounting the engine to its compartment inside the bus

Detailed assembly operations for the bus engine are presented below (Fig. 2), (the authors' own idea on the basis of the data obtained in the tests):

- assembling the engine, mounting the clutch,
- mounting the gearbox to the engine,
- mounting the engine to the compartment,
- mounting the drive shaft,
- assembling the exhaust system,
- making the electrical connections for the alternator, automatic gearbox, sensors,
- connecting the water pump and cooling system pipes,
- connecting the diesel fuel supply system,
- connecting pneumatic system hoses, air supply turbine,
- replenishing the fluid in cooling system of the engine and gearbox,
- mounting the rear beam (bumper).

The ChronFoto_RC method was used to measure the working time during the assembly of the bus engine and the obtained data was recorded on:

- measurement sheet ZE 2 (Fig. 3) and (Fig. 6),
- the appendix (Fig. 4),
- diagram (Fig.5).

Measurement Sheet ZE2 (Fig.3) contains a list of assembly operations, as well as the results of individual measurements of the technological assembly process. The ChronFoto_RC program was used to calculate the value of unit times t_j , i.e. the production rate L, the

Nr	assembly operations	reference worker count	influencing factors	Zy											\bar{t} [min.]	t [min.]		
					1	2	3	4	5	6	7	8	9	10				
1	assembling the engine, mounting the clutch	1	distance, weight	L	100.00	100.00	100.00	100.00									100.00	241.67
				ti	241.22	241.89	242.02	241.55									241.67	
				F	241.22	866.06	1493.93	2120.13										
2	mounting the gearbox to the engine	1	distance, weight	L	100.00	100.00	100.00	100.00									100.00	24.30
				ti	24.22	24.57	23.89	24.52									24.30	
				F	265.44	890.63	1517.82	2164.65										
3	mounting the engine to the compartment	1	distance, weight	L	100.00	100.00	100.00	100.00									100.00	41.25
				ti	40.89	41.22	41.05	41.82									41.25	
				F	306.33	321.05	358.87	1086.47										
4	mounting the drive shaft	1	distance, weight	L	100.00	100.00	100.00	100.00									100.00	25.34
				ti	25.88	25.38	24.89	25.22									25.34	
				F	332.21	957.23	1583.76	2211.69										
5	assembling the exhaust system	1	distance, weight	L	100.00	100.00	100.00	100.00									100.00	64.59
				ti	64.44	64.84	64.02	65.05									64.59	
				F	396.65	1022.07	1647.78	2276.74										
6	making the electrical connections for the alternator, automatic gearbox, sensors	1	distance, weight	L	100.00	100.00	100.00	100.00									100.00	45.09
				ti	45.02	44.86	45.52	44.95									45.09	
				F	441.67	1066.93	1693.36	2321.63										
7	connecting the water pump and cooling system pipes	1	distance, weight	L	100.00	100.00	100.00	100.00									100.00	35.46
				ti	35.35	35.88	35.62	34.98									35.46	
				F	477.82	1102.91	1728.92	2356.63										
8	connecting the diesel fuel supply system	1	distance, weight	L	100.00	100.00	100.00	100.00									100.00	50.18
				ti	50.33	50.56	49.98	49.85									50.18	
				F	527.35	1153.37	1778.98	2406.52										
9	connecting pneumatic system hoses, air supply turbine	1	distance, weight	L	100.00	100.00	100.00	100.00									100.00	48.78
				ti	48.25	48.88	49.98	48.82									48.78	
				F	575.60	1202.23	1828.88	2454.54										
10	replenishing the fluid in the cooling system of the engine and gearbox	1	distance	L	100.00	100.00	100.00	100.00									100.00	36.78
				ti	36.55	36.88	36.85	36.82									36.78	
				F	612.15	1239.12	1865.73	2491.36										
11	mounting the rear beam	1	distance	L	100.00	100.00	100.00	100.00									100.00	12.55
				ti	12.82	12.78	12.85	12.55									12.55	
				F	624.17	1291.91	1878.58	2509.91										
n = 4				k = 1	sum of times in cycle tz				624.17	627.74	626.67	625.33			2503.91	suma t		
Tz sr = 625.98				Distraction Rz								3.57			suma Rz	625.98		
Rz sr = 3.57				z = (Rz sr / tz sr) 100% = 0.57									e = 1%	e' = 5%				

Fig. 3. View of the measurement sheet ZE2 for assembling the bus engine

Nr	assembly operations	t	types of working time [min.]							AZ
			G	Vsk	Vsv	Vp	Er	N	F	
1	assembling the engine, mounting the clutch	241,67	241,67							
2	mounting the gearbox to the engine	24,30	24,30							
3	mounting the engine to the compartment	41,25	41,25							
4	mounting the drive shaft	25,34	25,34							
5	assembling the exhaust system	64,59	64,59							
6	making the electrical connections for the alternator	45,09	45,09							
7	connecting the water pump	35,46	35,46							
8	connecting the diesel fuel supply system	50,18	50,18							
9	connecting pneumatic system	48,78	48,78							
10	replenishing the fluid in the cooling system	36,78	36,78							
11	mounting the rear beam	12,55	12,55							
12	intervals in the course of work (rest breaks)	15,12		15,12						
13	intervals in the course of work (work-related conversations)	14,24			14,24					
Sum			625,99	15,12	14,24	0	0	0	0	655,35

Fig. 4. View of the Appendix sheet for assembling the bus engine [2]

sum of unit times per cycle t_z , the range R_z and the coefficient of dispersion z . On basis of the data given above, the setpoint value ε' was determined by means of the nomogram. Then, on the sheet "Appendix" (Fig. 4), individual types of time were assigned to the sections of the tested technological assembly process.

In the next stage of the technological assembly process (Fig. 5), the surplus percentage of the time and

worker productivity were calculated and the percentage shares of individual types of time for one shift were presented graphically. The following parameter symbols G , V_{sk} , V_{sv} , V_p , E_r , N and F were adopted on the basis of REFA [8, 9]

The performed measurements show that the productivity of workers in the repair shop is 95.52%. This result should be considered satisfactory.

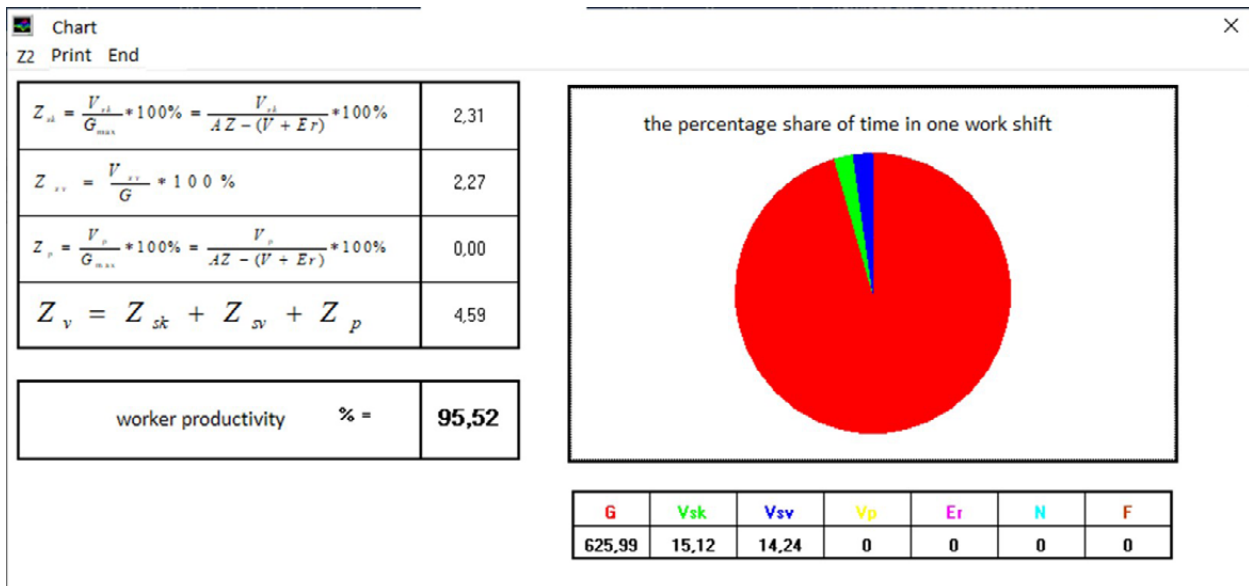


Fig. 5. View of the chart sheet for assembling the bus engine [2] (V_{sk} – material, fixed supplementary time, V_{sv} – material, variable supplementary time, V_p – personal supplementary time, G – main time, Z_{sk} , Z_{sv} and Z_p – percentage surcharges of supplementary time)


Z2		time consumption calculation sheet - ChronFoto_RC method				reference number		
						page		
work task assembly MAN								
Order Number:		Count:		Department:		MPK:		
Date: 08.02.2021 r.		Start time: 6:00 Count: 1		Finish time: 14:00 Count: 1		Duration time: 8h		
		Types of working time						
		main time		625.98				
		rest time		0.00				
		supplementary time		62.60				
		other time additions		0.00				
		unit time		688.58				
		target time		0.00				
		preparation-completion time		0.00				
Technology and methods of work								
Bus engine assembly								
Subject matter of work	Designation	Material	Initial State			Figure Number	Material Number	Dimensions, shape, weight
	engine	GG12	good			1	1	
Worker	Name	Personal Number	m	f	age	Period of performing similar tasks	Period of performing the tested task	
	Swobodny	15	X		52	27 years		
means of production	Designation, type	Count	Number	Year	Technical date, state of means of production			
	Toolbox	1						
	Assembly workbench	1						
Comments:								
Compiled:		Checked:		Date:		Important:		

Fig. 6. View of the sheet Z2 for assembling the bus engine [2]

The proposal for the improvement of the assembly workstation for bus engines

In order to improve the assembling and disassembling of bus engines, a model of a mobile scissor lift was designed (Fig. 7), which replaces the currently used forklift.

The frame to which the scissor lift unit is attached has been designed as a welded structure using c-profiles (C-channels). An electrically controlled hydraulic cylinder that allows the scissor lift to rise as well as the wheels of the trolley bolted to the frame were selected from the catalogues [4].

For the analysis of the lift itself, the engine weight was assumed to be 750 kg, whereas for the calculation of the trolley structure, the weight was assumed to be 1000 kg

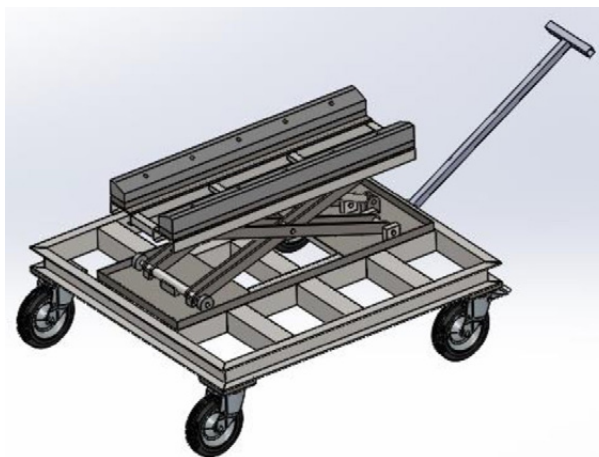


Fig. 7. The model of the scissor lift

(where 250 kg is the weight of the lift and 750 kg is the weight of the bus engine). For the calculations for the output stroke of the hydraulic cylinder, the weight was assumed to be 2000 kg, and for its lowering, 1200 kg. The minimum height of the lift is 360 mm, the maximum – 550 mm; the height of the trolley – 437.8 mm, the trolley with a lift – 797.8 mm (minimum height), 987.8 mm (maximum height).

Below there are the results of the strength analysis performed in the SolidWorks program (Fig. 8 – 13):

The maximum nodal stresses of the lift do not exceed 175 MPa at the connection of the sleeve and the guide (Fig. 8)

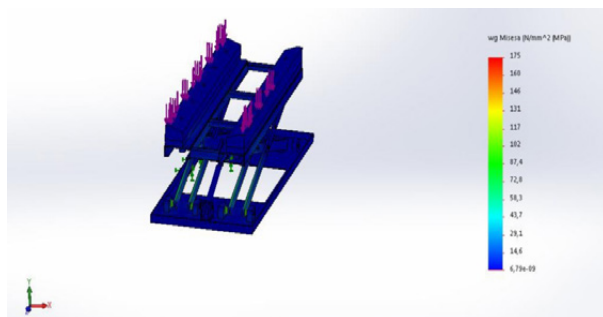


Fig. 8. Nodal stresses of the lift

The maximum value of the static deformation of the lift is 0.000635 (Fig. 9).

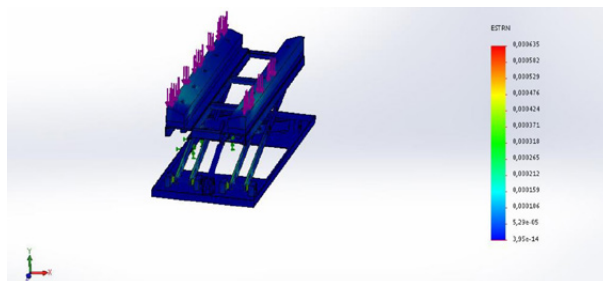


Fig. 9. Static deformations of the lift

The maximum value of the lift structure displacement under the load is 9.78 mm (Fig. 10).

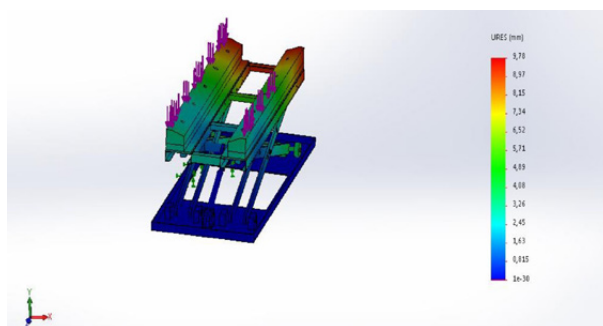


Fig. 10. Static displacement of the lift structure

As for the static analysis of the lift structure frame, the maximum nodal stress is 67 MPa (Fig. 11).

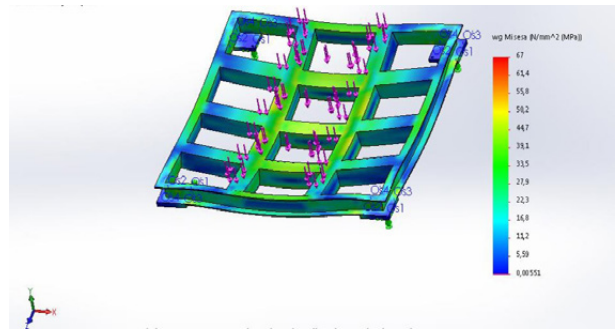


Fig. 11. Nodal stresses of the trolley structure frame

The maximum value of the static deformation of the trolley structure is 0.000225 (Fig. 12).

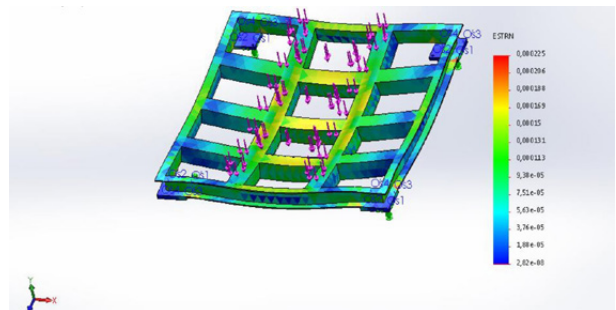


Fig. 12. Static displacement of the trolley structure

The maximum displacement of the frame of the lift frame structure (Fig. 13) under load is 1.11 mm and it is most visible in the centre of the frame.

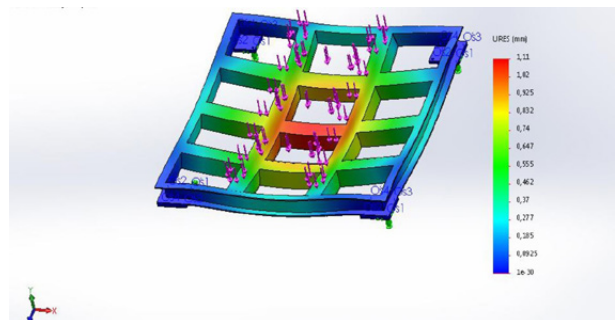


Fig. 13. Static displacement of the trolley structure frame

The main objectives of the designed trolley for assembling and disassembling bus engines primarily include:

- an increase in productivity and, at the same time, a reduction of production costs,
- a more effective use of the available working time,
- stabilization and regularity of the assembling / disassembling process, enabling a more accurate productivity planning,

- an improvement of the organization and working conditions.

Summary

The workstations for disassembling accessory-equipped engines found in city transport buses require precise and safe repair operations. The efficiency of this process and the number of people involved in it are equally important.

In the repair shop of the Municipal Transport Company, the process of replacing the accessory-equipped engine is currently performed by means of a forklift truck. This process lacks sufficient precision and therefore requires a greater number of auxiliary procedures. The ability to precisely position the engine during the replacement is lower.

The presented model of a mobile scissor lift will enable efficient and safe assembling and disassembling of bus drive units. Significant advantages offered by the proposed device include the ability to lift the engine of a considerable weight and of asymmetrically located centre of gravity as well as the ability to adjust the height in a considerably smooth manner.

References

- [1] Błaszczkiewicz M., Tybor I., Woźniakowski M. 1968. Zasady technicznego normowania pracy w przemyśle lekkim. Warszawa: Wydawnictwo Przemysłu Lekkiego i Spożywczego.
- [2] Cieślak R. 2011. Ocena metod badania czasu pracy w procesach technologicznych montażu, praca doktorska. Poznań: Politechnika Poznańska.
- [3] Cizak O., Żurek J. 2008. „Badanie wydajności gniazda montażu wrzeciennika głównego centrum tokarskiego”. Archiwum Technologii Maszyn i Automatykacji 284:99–105.

- [4] Katalog kół: <https://www.blickle.pl/produkt/L-RD-282R-42580>, <https://www.blickle.pl/produkt/L-RD-282R-ST-50658>,

katalog siłownika: <https://www.bipromasz.pl/wp-content/uploads/2014/11/CBL.pdf>

- [5] Kurek S., Lach J., Pronobis L., Grzeszczuk A. 1984. Metodyka Technicznego normowania pracy. Częstochowa: SPPW „UDZIAŁOWA”.
- [6] Prabhu, Girish V., Martin G. Helander and Valerie Shalin. 1995. “Effect of Product Structure on Manual Assembly Performance”. The International journal of Human Factors in Manufacturing 5(2): 151.
- [7] Prasolek Ł. 2019. Dokumentacja czasu pracy. Wyliczenia, obliczenia, przykłady i wzory, Warszawa: Wydawnictwo C.H. Beck,
- [8] REFA. 1984. Metody badania prac cz. 1 i cz. 2. Cieszyn: Cieszyńska Drukarnia Wydawnicza.
- [9] Materiały szkoleniowe REFA.
- [10] Wołk R. 2013. Normowanie pracy – metody. Sulejówek: Wiedza i Praktyka.

dr inż. Robert Cieślak
Państwowa Wyższa Szkoła Zawodowa w Koninie
ul. kard. S. Wyszyńskiego 35
62-510 Konin
e-mail: robert.cieslak@konin.edu.pl

dr Paweł Sobczak
Państwowa Wyższa Szkoła Zawodowa w Koninie
ul. kard. S. Wyszyńskiego 35
62-510 Konin
e-mail: pawel.sobczak@konin.edu.pl

Krzysztof Makowski
Państwowa Wyższa Szkoła Zawodowa w Koninie
ul. kard. S. Wyszyńskiego 35
62-510 Konin



Zapraszamy Autorów do współpracy!
www.sigma-not.pl
tiam@sigma-not.pl



CUT LAYER IN A MACHINING OF THE CYLINDRICAL GEARS BY THE METHOD OF 5-AXIS ROLL AWAY OF THE END MILL CUTTER ON THE OUTLINE OF THE TOOTH

Warstwa skrawana w obróbce walcowych kół zębatych metodą 5-osowego odtaczania frezu palcowego po zarysie zęba

Michał CHLOST

ORCID 0000-0001-9420-4239

DOI: 10.15199/160.2021.2.5

Abstract: Gear trains are a key element in the transmission of torque and rotational speed of rotating parts. Technological progress, and five-axis machining in particular, is an interesting and still little-known alternative in the production of this type of kinematic nodes in relation to traditional methods. This paper presents the issue and describes the kinematics of the tool operation in an innovative method of shaping five-axis gears by means of the peripheral milling method. The influence of geometry and material on the selection of the tool and its technological parameters was taken into account. A simulation analysis of the cut layer cross-sections and surface topography was carried out. It was shown that the machining direction was of great importance in the described method.

Keywords: gears, hardened machining, 5-axis roll away machining

Streszczenie: Przekładnie zębate w dalszym ciągu stanowią kluczowy element w przenoszeniu momentu oraz prędkości obrotowej części wirujących. Postęp technologiczny, a w szczególności proces obróbki pięcioosiowej na obrabiarkach CNC, stanowi ciekawą i wciąż mało poznaną alternatywę w wytwarzaniu tego typu węzłów kinematycznych w odniesieniu do metod tradycyjnych. W niniejszej pracy przedstawiono problematykę zagadnienia oraz opisano kinematykę pracy narzędzia w nowatorskiej metodzie kształtowania wieloosiowego kół zębatych metodą 5-osowego odtaczania frezu palcowego po zarysie zęba. Uwzględniono wpływ geometrii oraz materiału przedmiotu obrabianego, na dobór narzędzia oraz jego parametrów pracy. Przeprowadzono badania symulacyjne i analizę warstwy skrawanej oraz topografii powierzchni obrabianej w środowisku CAD/CAM. Pokazano, iż w opisywanej metodzie duże znaczenie ma kierunek obróbki.

Słowa kluczowe: koła zębate, obróbka w stanie utwardzonym, odtaczanie pięcioosiowe

Introduction

Five-axis milling technologies are gaining some increased recognition in the production of elements with advanced geometry, sometimes replacing the methods used so far. The reason for this is the high flexibility of machines and programming of the manufacturing process. It results, among others, from a possibility of controlling the position of the tool in the working space of the machine through displacements in three linear axes, and additionally in two rotary axes. Free positioning of the tool allows reducing the amount of over-clamping of the object, and enables to reduce the tool overhang. This has a positive effect on the stiffness of the machining system, thus increasing the dimensional and shape accuracy of the workpiece after machining [1, 6].

One of the still developing issues in freeform milling is a possibility of making toothings of gears. The techniques of classic gear machining used so far are based on the use of specialized machine tools and dedicated tools. The kinematics of the manufacturing process in this case consists in rolling away the tool around the envelope in order to shape the involute profile [6, 11, 14]. This process

results in simultaneous processing of both the right and left sides of the tooth, which ensures high efficiency of the process, but does not allow individual shaping of each of the surfaces machined. The detailed analysis of chip formation in hobbing was performed by Bouzakis et al. [4], and Krömer et al. [13] described the process in terms of the obtained roughness R_{th} in the direction of the line and the tooth profile. Additional analyzes in the case of the innovative skiving method described by Davim [7] were carried out by Böß et al. [3, 2] where they analyzed cross-section values of the cutting layer depended on the position of the tool cutting edge.

A completely different approach to the issue of gear manufacturing is the use of five-axis machining methods on multi-axis CNC machine tools. When shaping elements using this process, two basic technological variants of tool guidance are distinguished: machining with a point contact and machining of the cutter's side with a linear contact. In the works [10, 12, 15, 16, 19] the linear contact was obtained by tangential positioning of the tool surface at the point of its corner or transition to a spherical face, to the tooth side contour curve. A different machining kinematics was adopted by Talar et al. [18], who

carried out an analysis of multi-axis cutting using a disc head for machining, where the contact of the tool with the machined tooth side surface was also unchanged, and moreover based on the transition point of the linear cutting edge of the insert into the corner radius.

Depending on the method adopted, the cross-sectional area of the cutting layer changes, which has a significant impact on the values of the cutting force components in the milling process. In the case of the envelope machining, the method of determining the cross-sectional area of the cut layer was shown by Bouzakis et al. [4] and Böß et al. [2, 3]. In the process of five-axis milling in the variant with point contact, the methodology of determining the cross-sectional area of the cut layer was presented by Boz et al. [5], and with the use of a toroidal milling cutter by Gdula et al. [9]. For the linear contact, the problem of the cut layer cross-section was discussed by Talar et al. [18].

The last element influencing the correct collaboration of the tooth active surfaces in the gear is the machined surface texture. The basic types of machining marks obtained in the envelope processes were presented by Sun et al. [17]. In addition, Kromer et al. [13] and Piotrowski et al. [14], performed an analysis of the machined surface after hobbing. The geometry of the tooth side surface after five-axis shaping in the variant of point contact was presented by Klocke et al. [12] and Staudt et al. [16].

This article presents an analysis of the cross-sections of the cut layer in the new proposed method of machining the toothings by the 5-axis roll away of the end mill along the involute contour of the tooth side of a wheel with a cylindrical geometry. The assumption is the continuous and controlled movement of the contact point of the tool and the workpiece along the outline of tool. (Fig. 1.) shows the idea of the process, i.e. inscribing a monolithic tool into the outline of a tool for envelope machining, which in the analyzed case is represented by the MAAG rack cutter.

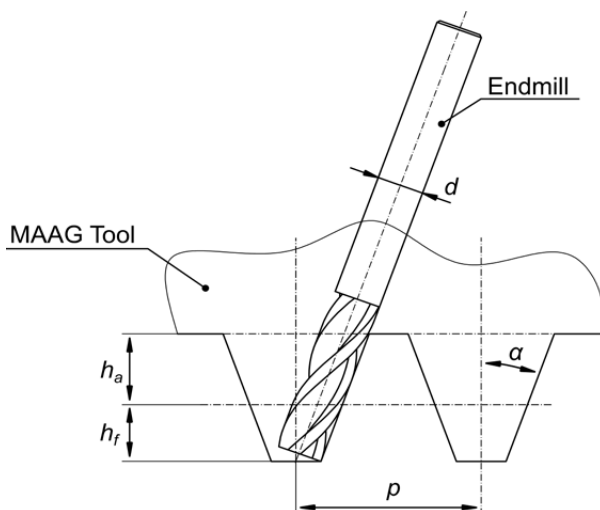


Fig. 1. The idea of a five-axis roll away process

Materials and methods

The simulation of the machining of the gear tooth flank was carried out for an involute contour, delimited by the based circle and the addendum circle. The simulation omits the transition curve at the root of teeth, whose processing due to the geometry, requires the use of a ball end mill end, and in the five-axis milling process it can be performed in a separate operation.

The tool feed rate v_f was adopted along the tooth profile, as a result of which the involute curve was divided into segments whose length corresponds to the adopted tool feed per revolution f . Two machining cases were considered. In the first case, the tool runs from the root to the tooth top (Fig. 2.), while in the second, the direction of the feed rate speed v_f and the rolling movement are changed, so that the machining proceeds from the top to the tooth root.

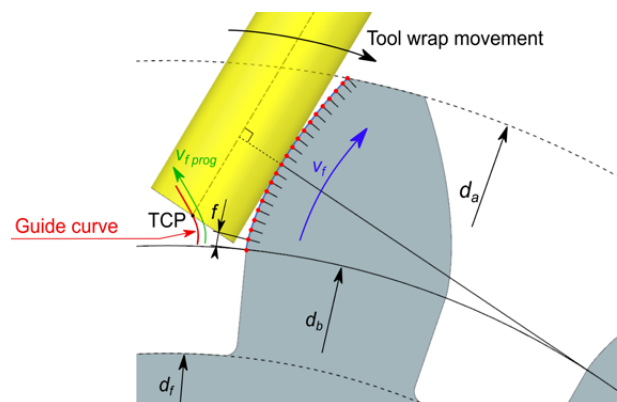


Fig. 2. Tool work kinematics

In the simulation, the tool positions were determined geometrically, as positions tangent to the involute at points determined by the value of the feed per revolution f . In real machining, the tool path represented by the TCP point will be based on the guide curve resulting from rolling away the tool around the contour, and the tool feedrate will be converted from the speed on the involute profile v_f to the speed along the guide curve $v_{f \text{ prog}}$.

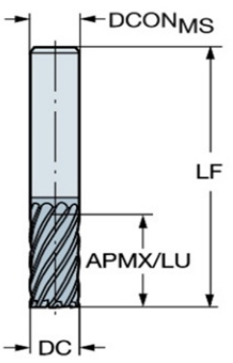
The cross-section analysis of the cut layer in the new five-axis turning method was carried out for the adopted material and technological parameters. The hardened 40HM steel was used as the material, for which the hardness was 60 HRC, and the mechanical properties are presented in Tab. 1. The selection of the steel grade was dictated by its susceptibility to mechanical and heat treatment.

Table 1. 40 HM steel properties [8]

Density ρ g/cm ³	Young's modulus E GPa	Tensile strength R_m MPa	Yield strength $R_{p0.2}$ MPa	Elongation A %	Hardness HRC
7.82	205 - 210	1030	880	10	60

Using material from the H group, i.e. the material with increased strength, it became necessary to choose the right tool for processing this type of material. In this case, a Sandvik tool with the parameters shown in Tab. 2 was selected.

Table 2. Tool geometry

	R215.38-08030-AC19H 1610	
	DC mm	8
	APMX/LU mm	19
	LF mm	63
	DCONMS mm	8

According to catalogue notes, for the selected tool, the technological parameters of machining proposed by the manufacturer and described in Tab. 3 were adopted.

Table 3. Technological parameters

Cutting speed v_c m/min	Feed per revolution f mm/rev	Cutting width $a_{e\max}$ mm	Cutting depth $a_{p\max}$ mm
80	0.8	0.05 DC	1.5 DC

The quantities having a significant impact on the selection of the tool geometry, in addition to the material used, were the geometrical parameters of the workpiece, which is the gear wheel. First of all, the width of the space s , which influences the maximum diameter DC of the tool, as well as the length of the involute profile L_{inv} of the tooth, which is important when selecting the maximum useful depth of cut $APMAX/LU$ of the tool, were taken into account. The main parameters of the machined gear are presented in Tab. 4.

Table 4. Gear parameters

Pressure angle α °	Modulus m_n mm	Teeth number z -	Helix angle β °	Involute length L_{inv} mm	Space width s mm
20	10	14	0	15.7589	15.707

The values in the above table were determined as follows. The length of the involute curve is described by the equation (1),

$$L_{inv} = \int_0^t \sqrt{\left(\frac{dx}{dt}\right)^2 + \left(\frac{dy}{dt}\right)^2} dt \quad (1)$$

where the derivatives after the variable t refer to the functions expressed by equation (2). In this case, the variable t represents the involute angle.

$$\begin{cases} x(t) = \frac{d_b}{2} (\sin(t) - t \cos(t)) \\ y(t) = \frac{d_b}{2} (\cos(t) + t \sin(t)) \end{cases} \quad (2)$$

In equations (2) there is a variable d_b , which is the diameter of the base circle and is expressed by equation (3).

$$d_b = d_p \cos(\alpha) = m_n z \cos(\alpha) \quad (3)$$

The value of the width of the space s was determined using the equation (4).

$$s = \frac{\pi m_n}{2} \quad (4)$$

The study of the cross-sections of the cut layers was carried out in 4 separate cutting zones towards the tooth line. The zones were determined on the basis of the tool wrap angle analysis. One can distinguish: entrance zone I, stable cutting zone II, output zone N-1, and the last cut of the tool N (Fig. 3.). The analysis was carried out in representative zones, while the total number of cutting zones is determined by the parameter N, which is calculated from the formula (5)

$$N = \frac{b}{b_r} + 1 \quad (5)$$

where: b - gear width, b_r - distance between next passes of the tool. For the purposes of the study, the b_r parameter was assumed to be 1 mm.

Each zone is characterized by a different value of the wrap angle of the tool. The determination of the wrap angle in individual zones was important for the correct division of the cutting zone in order to analyze the cross-section area of the cut layer A.

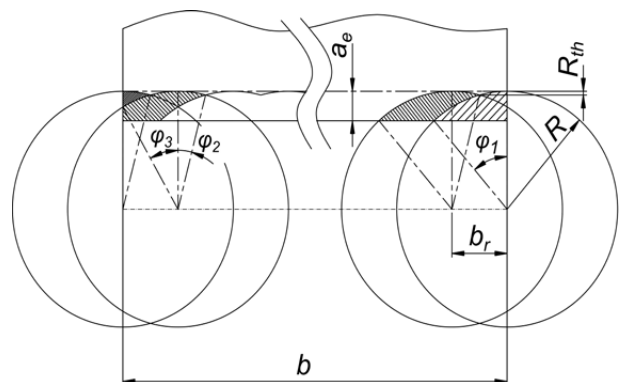


Fig. 3. Tool wrap angles in designated zones

The values of the wrap angles, determined by equations (5-8), in the separate zones are described as sums of partial angles.

$$\varphi_I = \varphi_1 \quad (5)$$

$$\varphi_{II} = \varphi_1 + \varphi_2 \quad (6)$$

$$\varphi_{N-1} = \varphi_2 + \varphi_3 \quad (7)$$

$$\varphi_N = \varphi_2 \quad (8)$$

The partial angles that make up the wrap angles of tool are described by equations (9-11)

$$\varphi_1 = \tan^{-1} \left(\frac{R^2 - (R - a_e)^2 - br}{R - a_e} \right) \quad (9)$$

$$\varphi_2 = \tan^{-1} \left(\frac{\frac{b_r}{2}}{R - R_{th}} \right) \quad (10)$$

$$\varphi_3 = \sin^{-1} \left(\frac{b_r}{R} \right) \quad (11)$$

where: R - tool radius, a_e - cutting width (machining allowance), b_r - width between next passes of the tool, R_{th} - theoretical roughness in the direction of the tooth line expressed by the formula (12).

$$R_{th} = R - \sqrt{R^2 - \left(\frac{b_r}{2} \right)^2} \quad (12)$$

In order to thoroughly analyze the cutting layers A , as well as to determine the total cross-sectional area of the cutting layers A_z , the wrap angles were discretized with a step $\Delta\varphi$ equal to 2° from the 0° position, i.e. the plane normal to the machined surface, passing through the tool axis. Due to the irrationality of the wrap angles value, the last step was taken as the remainder from the division $\pm\varphi$ as shown in (Fig. 4.).

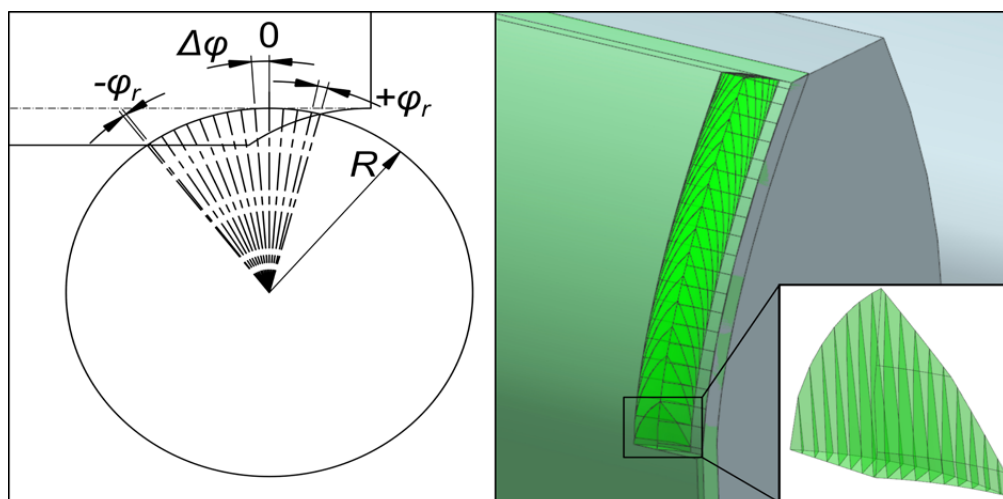


Fig. 4. Cutting zone discretization

Results

Due to the complex geometry of the cutting layer, the measurement of individual sections A was carried out using the Measure Face tool, which is part of the NX11 software. The accuracy of the measurement was $\pm 0.0001 \text{ mm}^2$.

Figures 5-8 show the change in the value of the cross-sectional area of the cutting layer A depending on the wrap angle φ for the strategy in which the tool works from the top to the tooth root. The analysis of the graphs shows that the highest value of the cross-sectional area was obtained in zone I, as shown in (Fig. 5.). In this case, it can be clearly observed that the largest cross-sectional area of the cutting layer $A = 1.5148 \text{ mm}^2$ occurs at the first position of the tool, i.e. at the tooth top for the angular position of 0° .

The smallest values of the cross-sectional area A were observed for the zone N-1 (Fig. 8.), where the maximum value was $A = 0.2807 \text{ mm}^2$. The waveforms for the zones II and N-1 are characterized by the same maximum values of $A = 1.0613 \text{ mm}^2$, but with a variable slope of the left side of the plot (Figures 6-7). Three areas can be noticed on all the waveforms showing the change in the cross-section of the cut layer depending on the considered tool position on the involute curve. The area of the tool entry into the material in the range 1-2, where there is the largest cross-sectional area A , the stable cutting zone, which for zone I is within the limits of 2-16, for zone II and zone N-1 within the border 2-17, and for zone N within the limits 2-18. In addition, the cutting area with the face cutting of the tool was separated, where the value of the cross-sectional area of the cut layer decreases.

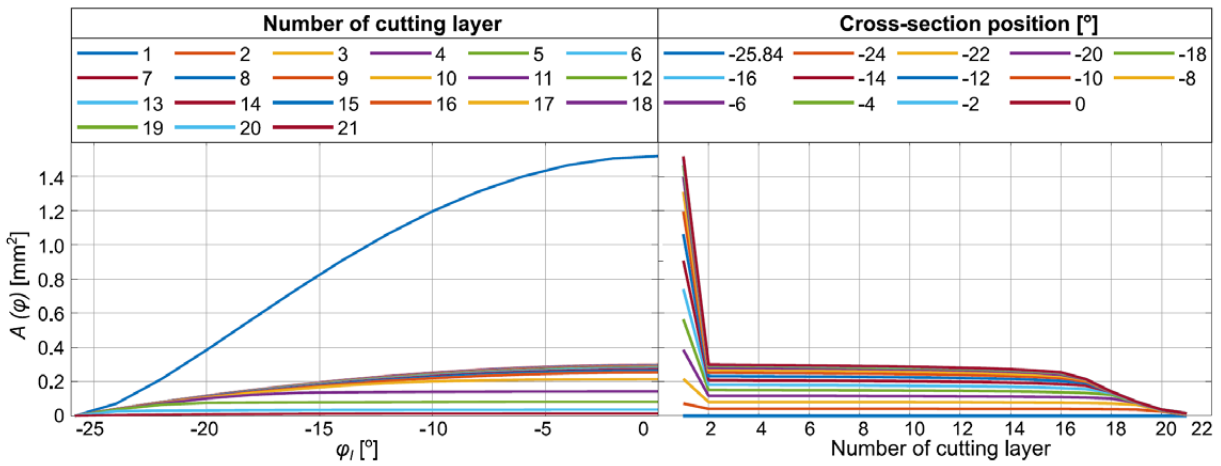


Fig. 5. The cross-sectional areas of the cut layer in zone I

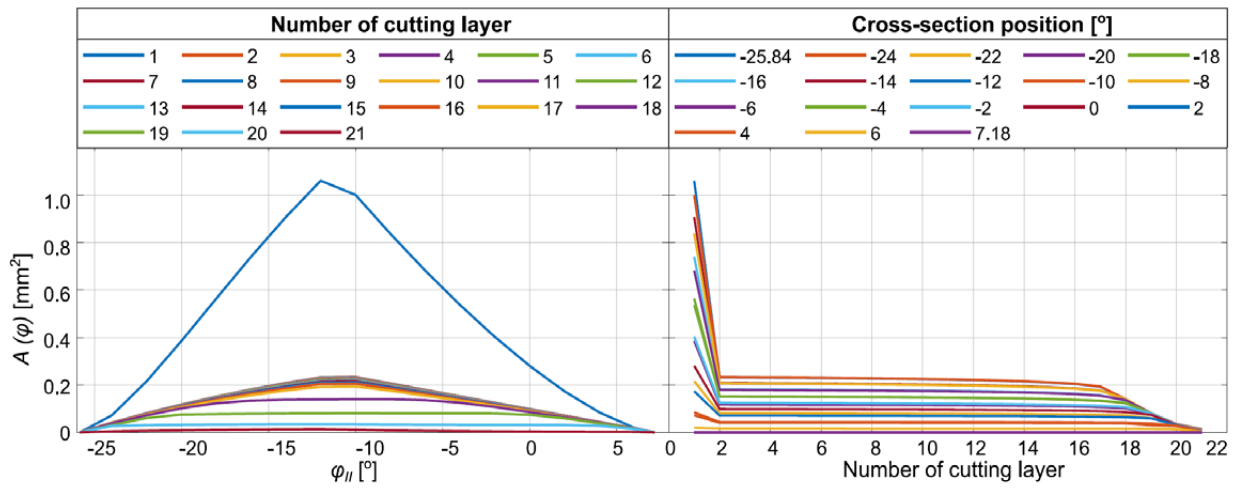


Fig. 6. The cross-sectional areas of the cut layer in zone II

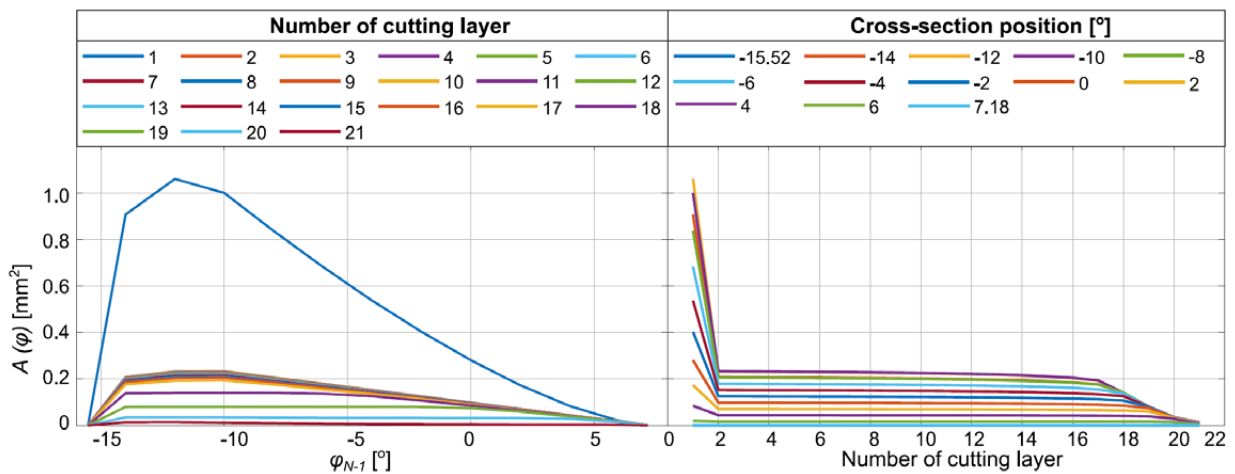


Fig. 7. The cross-sectional areas of the cut layer in zone N-1

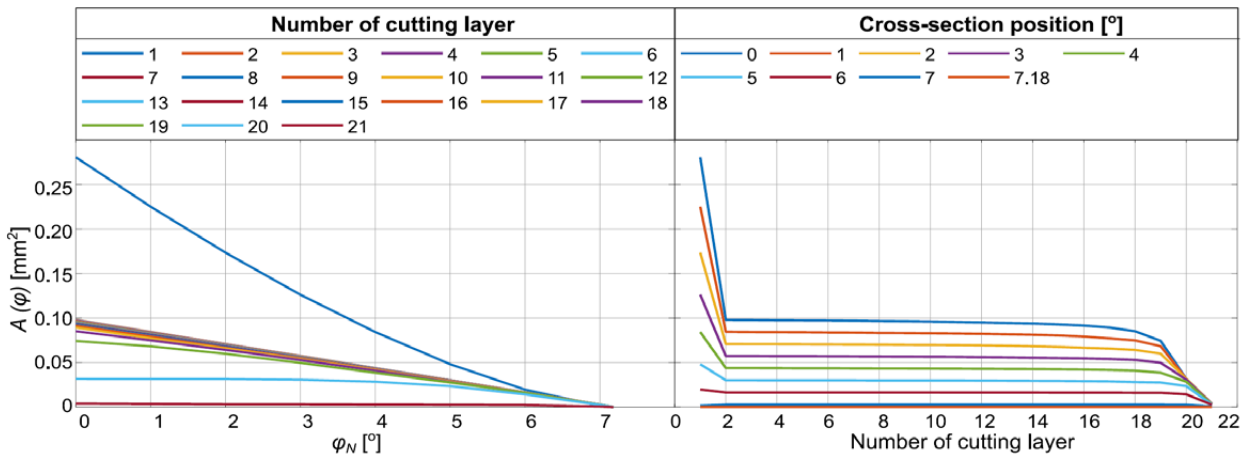


Fig. 8. The cross-sectional areas of the cut layer in zone N

The analysis of the milling strategy from the root to the top of the tooth showed some differences as seen in (Figures 9.-11.). A similar distribution of maximum values for individual zones was observed, as in the previous strategy. In this case, for zone I, the highest maximum

value of the cross-sectional area $A = 0.6652 \text{ mm}^2$ (Fig. 9.) was recorded, and the smallest for zone N, which was $A = 0.174 \text{ mm}^2$ Fig 12. In the case of zones II and N-1 of (Figures 10.-11.), the same maximum values of $A =$

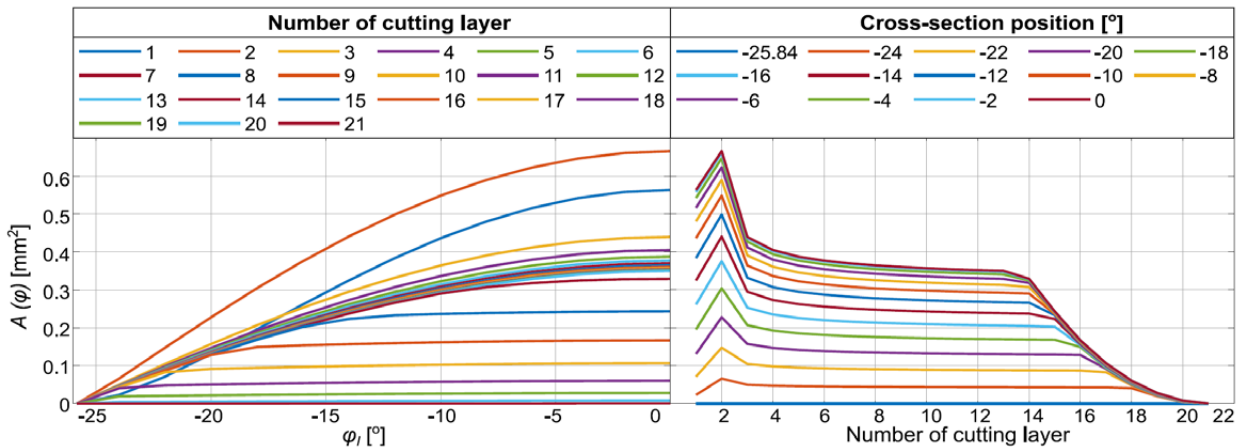


Fig. 9. The cross-sectional areas of the cut layer in zone I

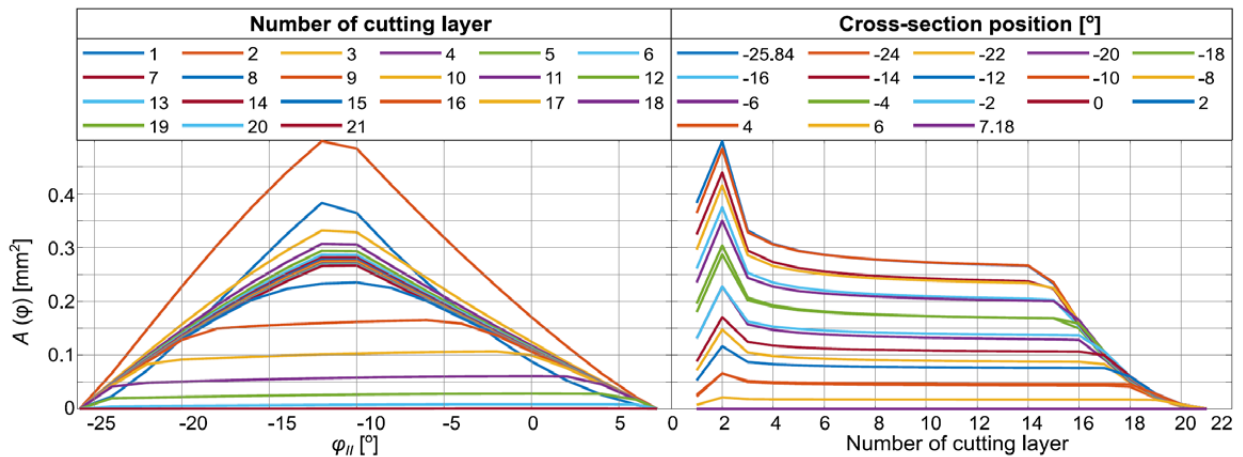


Fig. 10. The cross-sectional areas of the cut layer in zone II

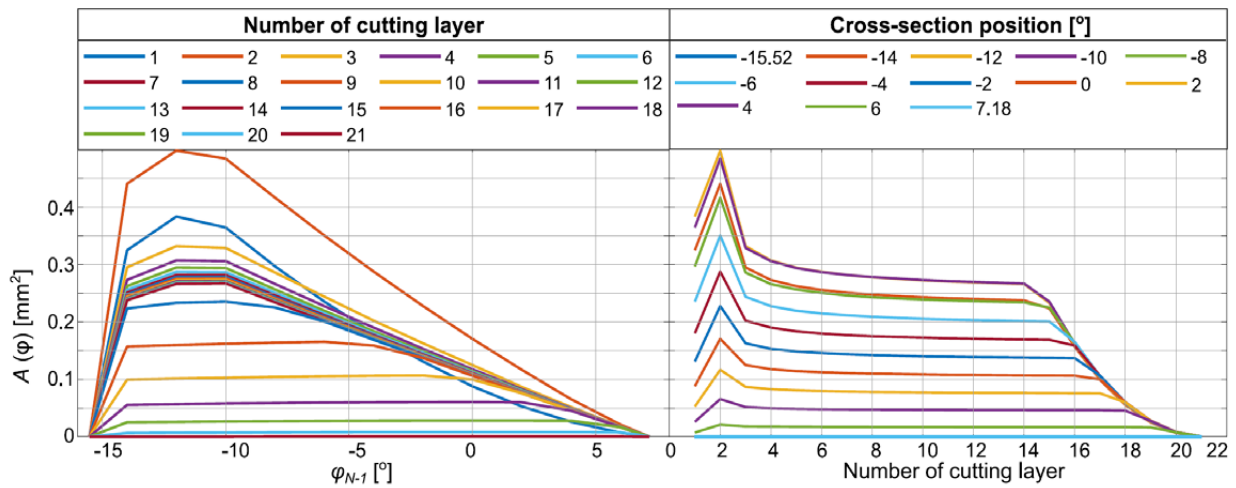


Fig. 11. The cross-sectional areas of the cut layer in zone N-1

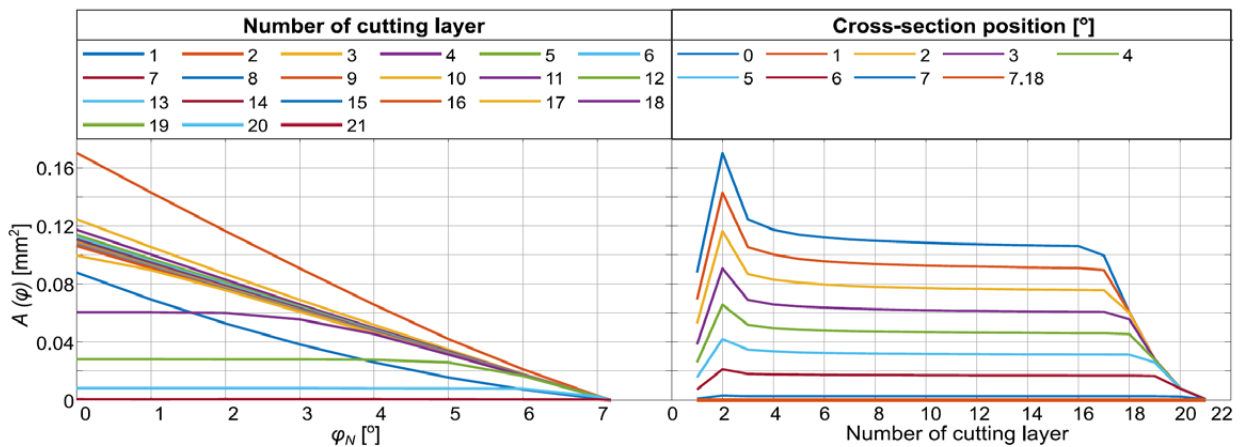


Fig. 12. The cross-sectional areas of the cut layer in zone N

0.4981 mm^2 and a similar change in the slope of the left side of the plot were observed.

The main difference was observed in the changes of the cross-sectional area depending on the position of the tool. The area of the tool entry into the material covers the positions 1-3, where the maximum value was noted for the position 2. The stable cutting area for zone I ranges from 2-13, for zones II and N-1 it ranges from 2-14, and for N zone in the boundary 2-10. The area of the tool contact

from the material, in which the cross-section of the cutting layer decreases in the case under consideration, has a wider range than in the previous strategy.

Based on the above data, graphs of the total cross-sectional area of the cutting layers A_z in individual zones were prepared for the milling strategy from the top to the root of the tooth (Fig. 13.), and from the root to the top of the tooth (Fig. 14.).

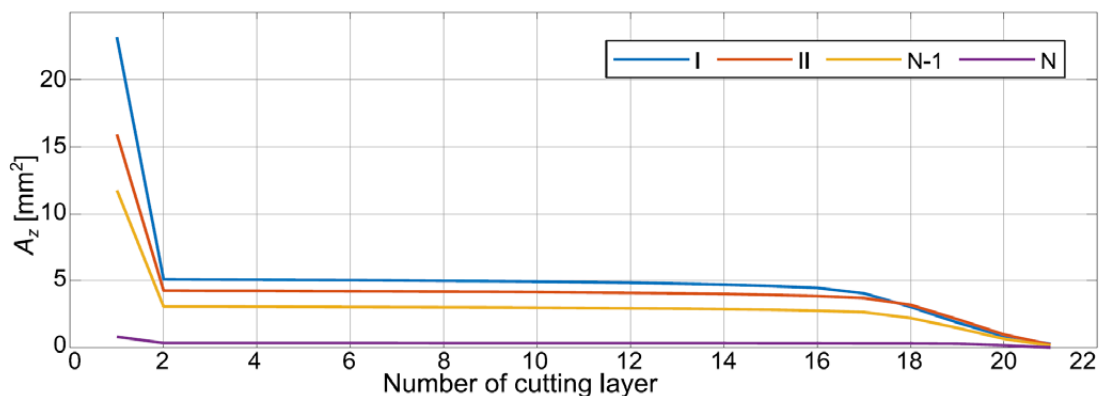


Fig. 13. The total cross-sectional area of the cutting layers for the direction from top to tooth root

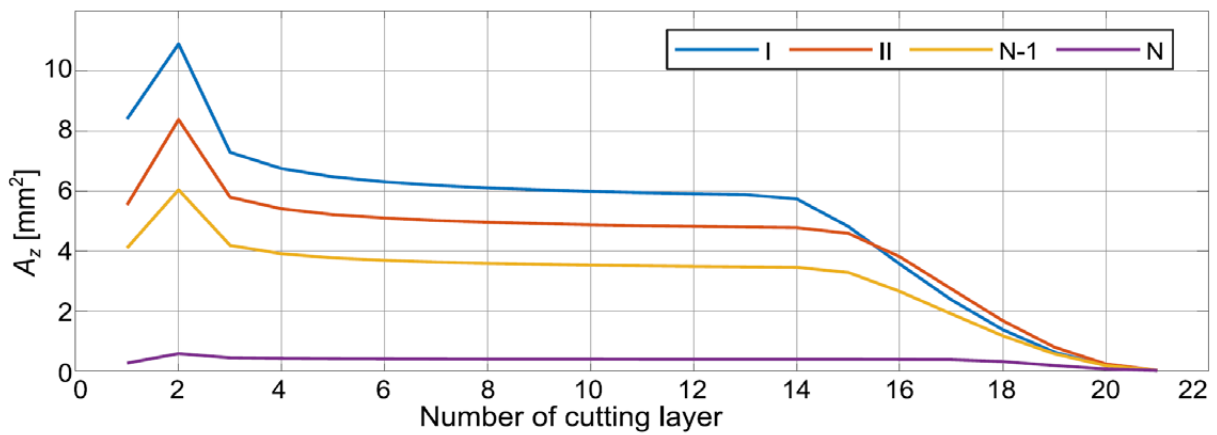


Fig. 14. The total cross-sectional area of the cutting layers for the direction from root to tooth top

For all four zones (I, II, N-1, N), the total cross-sectional area A_z was calculated as the sum of the cross-sections $A(\varphi)$ at individual positions of the tool, which is expressed by the general formula (13)

$$A_z = \sum_{i=1}^n A(\varphi)_i \quad (13)$$

where: n – number of cross-section position.

It was observed, that in the case of the root to tooth top strategy, the obtained values of the total A_z cross-sectional areas were about half lower than those obtained in the top to tooth root strategy. Moreover, the highest

values occurred for the zone I, and the lowest for the zone N. The nature of the change in the total values of the cross-section areas A_z for individual zones and strategies coincides with the previously discussed results for the cross-section areas A .

The last element of the analysis was the presentation of a map of surface deviations depending on the adopted machining direction (Figures 15a, b.) The maximum deviation in both cases coincided with the theoretical roughness towards the tooth line expressed by the formula (12) and amounted to 0.0314 mm. It was observed that the machining marks arranged up along the tooth profile, while the deviation for individual marks took the saddle, biconcave character (Fig. 15c.).

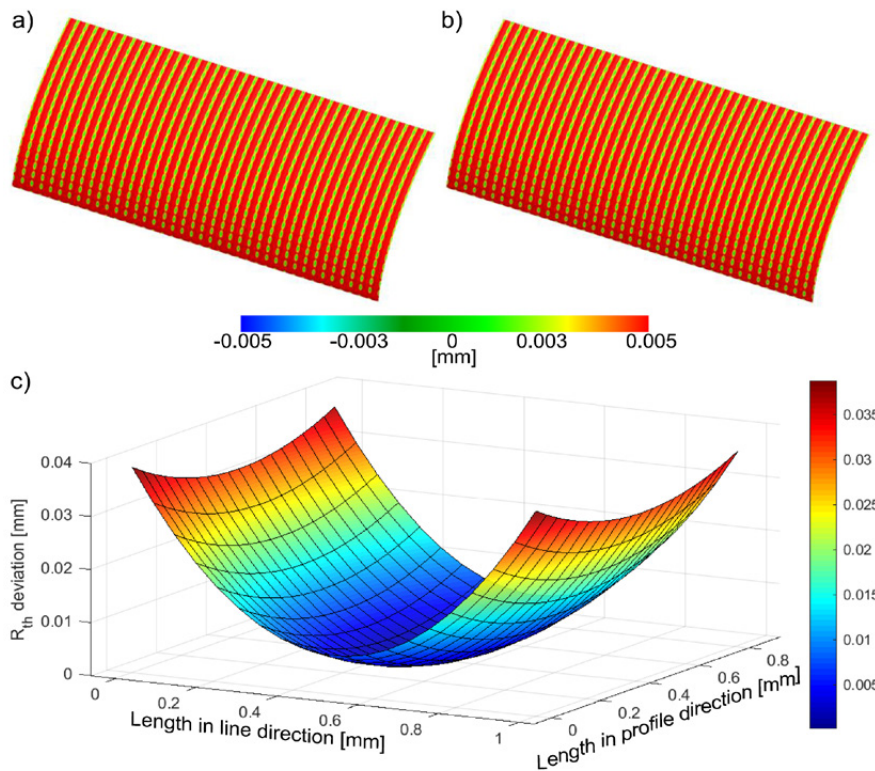


Fig. 15. Map of surface deviations for: a) root-top strategy, b) top-root strategy, c) deviation distribution for one cut layer

Summary

The analyzed milling method in the technological variant of 5-axis roll away of the end mill cutter is a completely new look at the issue of five-axis gear machining. Simulation tests and the analysis of the cross-sections of the cut layers showed a different distribution of values along the tooth profile depending on the adopted machining direction.

The values of the cross-sectional areas of the cut layers have a particular impact on the values of the components of the cutting forces generated during machining, and thus on the deformation of the machining system.

On the basis of the results obtained, it should be concluded that:

- The machining from the root to the tooth's top will be a more advantageous strategy due to the smaller values of the cross-sections of the cut layers. In this case, the greatest value of the cross-sectional area is noted at the root of the tooth.
- In the case of the top to tooth root strategy, the cross-sectional area values are more than twice as high. Moreover, in this case, the largest cross-sectional area is recorded in the first position, i.e. at the top of the tooth. Such a distribution of values can result in the application of the greatest resultant cutting force to the area of the tooth top, thus deforming both the tool and the workpiece.

The results and conclusions obtained from the conducted analyzes provide the basis for further research on the five-axis roll away process. In the next steps, one should focus on:

- Developing the control program by replacing the feed along the involute curve v_f with the feed along the guide curve v_f prog.
- The values of the cross-sectional areas A should be made dependent on the parameters: feed per revolution f , cutting width a_e and the distance between tool paths b_r .
- In the case of the adopted method of finishing the material in the hardened state, it will be necessary to precisely determine the maximum cross-sections for individual cut layers A_{max} and to analyze the components of the cutting force.

References

- [1] Álvarez, Á., A. Calleja, M. Arizmendi, H. González, and L. de Lacalle. 2018. "Spiral Bevel Gears Face Roughness Prediction Produced by CNC End Milling Centers." *Materials* 11 (8).
- [2] Böß, V., B. Denkena, M. Dittrich, and S. Henning. 2016. "Geometrical Contact Zone Analysis of the Skive Hobbing Process." *Advanced Materials Research* 1140: 157–64.
- [3] Böß, V., B. Denkena, and S. Henning. 2015. "Investigation of the Skive Hobbing Process by Applying a Dexcel-Based Cutting Simulation." *Procedia CIRP* 37: 182–87.
- [4] Bouzakis, K. D., E. Lili, N. Michailidis, and O. Friderikos. 2008. "Manufacturing of Cylindrical Gears by Generating Cutting Processes: A Critical Synthesis of Analysis Methods." *CIRP Annals - Manufacturing Technology* 57 (2): 676–96.
- [5] Boz, Y., H. Erdim, and I. Lazoglu. 2011. "Modeling Cutting Forces for Five Axis Milling of Sculptured Surfaces." *Advanced Materials Research* 223 (April): 701–12.
- [6] Burek, J., M. Gdula, M. Płodzień, and J. Buk. 2015. "Gear's Tooth Profile Shaping in Dialog and Parametric Programming." *Mechanik*, no. February (February): 142/7.
- [7] Davim, J. 2011. *Machining of Hard Materials. Machining of Hard Materials*.
- [8] Dobrzański, L. A. 2006. "Stale i Inne Stopy Żelaza." In *Podstawy Nauki o Materiałach i Metaloznawstwo*, 591–92. Warszawa: Wydawnictwo Naukowo-Techniczne.
- [9] Gdula, M., and J. Burek. 2017. "Cutting Layer and Cutting Forces in a 5-Axis Milling of Sculptured Surfaces Using the Toroidal Cutter." *Journal of Machine Engineering* 17 (4): 98–122.
- [10] Guo, E., N. Ren, Z. Liu, X. Zheng, and C. Zhou. 2019. "Study on Tooth Profile Error of Cylindrical Gears Manufactured by Flexible Free-Form Milling." *The International Journal of Advanced Manufacturing Technology* 103: 4443–51.
- [11] Karpuschewski, B., H. J. Knoche, and M. Hipke. 2008. "Gear Finishing by Abrasive Processes." *CIRP Annals - Manufacturing Technology* 57 (2): 621–40.
- [12] Klocke, F., M. Brumm, and J. Staudt. 2015. "Quality and Surface of Gears Manufactured by Free-Form Milling with Standard Tools." *Gear Technology*, no. January/February: 64–69.
- [13] Krömer, M., D. Sari, C. Löpenhaus, and C. Brecher. 2017. "Surface Characteristics of Hobbed Gears." *Gear Technology*, no. July: 68–75.
- [14] Piotrowski, A., and T. Nieszporek. 2012. "GRANIA-STOŚĆ POWIERZCHNI ZĘBA KOŁA WALCOWEGO PRZY FREZOWANIU OBWIĘDNIOWYM THE LOBBING OF THE TOOTH OF THE SPOOR GEAR AT HOBGING." *Mechanik* 85 (7CD): 795–806.
- [15] Solf, M., R. Bieker, C. Löpenhaus, F. Klocke, and T. Bergs. 2019. "Influence of the Machining Strategy on the Resulting Properties of Five-Axis Hard-Milled Bevel Gears." *Proceedings of the Institution of Mechanical Engineers, Part C: Journal of Mechanical Engineering Science* 233 (21–22): 7358–67.
- [16] Staudt, J., C. Löpenhaus, and F. Klocke. 2017. "Performance of Gears Manufactured by 5-Axis Milling," no. April: 58–65.
- [17] Sun, W., and A. Lancaster. 2017. *Surface Texture Measurements of Gear Surfaces Using Stylus Instruments*. National Physical Laboratory. Vol. 147.
- [18] Talar, R., P. Jablonski, and W. Ptaszynski. 2018. "New Method of Machining Teeth on Unspecialised Machine Tools." *Tehnicki Vjesnik* 25 (1): 80–87.
- [19] Xiang, T., J. Yi, and W. Li. 2018. "Five-Axis Numerical Control Machining of the Tooth Flank of a Logarithmic Spiral Bevel Gear Pinion." *Transactions of Famenia* 42 (1): 73–84.

Mgr inż. Michał Chlost
Rzeszów University of Technology,
Faculty of Mechanical Engineering and Aeronautics,
Department of Manufacturing Techniques and
Automation
ul. Wincentego Pola 2, 35-959 Rzeszów, Poland
e-mail: m.chlost@prz.edu.pl

THE INFLUENCE OF THE DIRECTIVITY OF THE GEOMETRIC STRUCTURE ON THE LOAD CAPACITY OF SINGLE-LAP ADHESIVE JOINTS

Wpływ kierunkowości struktury geometrycznej powierzchni na nośność połączeń klejowych

Władysław ZIELECKI
Łukasz BĄK
Ewelina GUŻLA

ORCID 0000-0002-7864-5525

ORCID 0000-0002-7359-6007

DOI: 10.15199/160.2021.2.6

Abstract: The aim of the work was to investigate the influence of the directivity of the geometric structure obtained in the grinding process on the load capacity of single-lap adhesive joints made of steel S235JR and aluminum alloy 2024-T3. The research was carried out for five different variants of joints differing in the direction of grinding and the arrangement of the ground surfaces to each other. The test results show that in the case of steel joints, the most advantageous solution in terms of joint load capacity is grinding the adhesive surfaces at an angle of 45° to the direction of the force loading the joint and connecting them in such a way that the created texture crosses (joint load capacity $P_t = 4667.36$ N). However, in the case of joints made of aluminum alloy, the best solution is to grind the adhesive surfaces perpendicular to the direction of the force loading the joint (joint load capacity $P_t = 3210.46$ N). The results of the significant difference test (test-t) show that in the assumed range of variability of the input parameters, the directionality of the geometric structure has a significant impact on the load capacity of the adhesive joints.

Keywords: surface roughness, directivity of the geometric structure, texture, adhesive joint

Streszczenie: Celem pracy było zbadanie wpływu kierunkowości struktury geometrycznej, uzyskanej w procesie szlifowania, na nośność jednozakładkowych połączeń klejowych wykonanych ze stali S235JR oraz ze stopu aluminium 2024-T3. Badania przeprowadzono dla pięciu różnych wariantów połączeń różniących się kierunkiem szlifowania i ułożeniem szlifowanych powierzchni klejonych względem siebie. Wyniki badań wskazują, że w przypadku połączeń ze stali, najkorzystniejszym rozwiązaniem pod względem nośności złącza jest szlifowanie powierzchni klejonych pod kątem 45° względem kierunku działania siły obciążającej złącze i sklejanie ich w taki sposób, aby utworzona tekstura się krzyżowała (nośność połączeń $P_t = 4667,36$ N). Natomiast w przypadku połączeń ze stopu aluminium, najkorzystniejszym rozwiązaniem jest szlifowanie powierzchni klejonych prostopadle względem kierunku działania siły obciążającej złącze (nośność połączeń $P_t = 3210,46$ N). Wyniki testu znaczących różnic (test-t) wskazują, że w przyjętym zakresie zmienności parametrów wejściowych, kierunkowość struktury geometrycznej ma istotny wpływ na nośność połączeń klejowych.

Słowa kluczowe: chropowatość powierzchni, kierunkowość struktury geometrycznej, tekstura, połączenie klejowe

Introduction

Adhesive technology has many advantages. One of them is the ability to combine almost all materials. Adhesives makes it possible to connect even materials that differ significantly in thermal expansion coefficient or electric potential. As a result, adhesive technology is successfully used, among others, in the automotive industry to combine various materials into so-called hybrid structures with reduced weight. Examples of materials that are used in such automotive construction are aluminum alloys and steels [2].

The strength of adhesive joints depends on many factors. One of them is the condition of the surface layer of the joined elements. An integral part of the surface layer is the geometric structure of the surface, which is composed of surface roughness, among others. Surface roughness is a set of irregularities repeating periodically or

non-periodically, for which the ratio of the average width of the elements to the average height of these elements is less than 40 [1, 22].

The relationship between the surface roughness and the strength of the adhesive joints results from the mechanical theory of adhesion. According to this theory, the adhesive penetrates the microporosity occurring on the surface of the joined elements and creates mechanical anchors that enable the transfer of loads [7, 9, 18].

The influence of surface roughness on the strength of adhesive joints has been analyzed in numerous studies [5, 6, 10, 24, 25, 26, 27]. In the work [5] the influence of the surface roughness on the shear strength of adhesive bonds joined with the Araldite epoxy resin was analyzed. Some of the joints were made of AA6063 aluminum alloy and some of the mild steel AISI1045. As a result of the research, it was found that with the increase of the R_a (arithmetical mean height) parameter the strength of

joints made of both aluminum alloy and steel initially increased. The initial increase in the strength of the joints with the increase in roughness resulted from enhancing the contact surface between the adhesive and the bonded material and formation mechanical anchors. After exceeding the optimum roughness value, the strength of the joints began to decrease due to the reduction of the surface wettability. The maximum strength values were obtained for $Ra = 2.05 \pm 0.19$ for aluminum alloy and $Ra = 1.98 \pm 0.10$ for steel.

In paper [24], a relationship between the load capacity of adhesive joints and surface roughness parameters measured in the two-dimensional (2D) system was analyzed. Adhesive joints made of S235JR steel were used for the tests. The adherents (substrates) surfaces were milled or milled with the following abrasive treatment with corundum. The joints were made using two different compositions which resulted in flexible and rigid joints. It has been shown that the parameters Ir (roughness profile length coefficient), Rda (arithmetic mean slope of the roughness profile), Rdq (mean square roughness profile inclination) are strongly related to the strength of elastic joints and can be used to predict the shear strength of lap joints.

The authors of the work [25] examined the relationship between the strength of adhesive joints and the roughness parameters measured in the three-dimensional (3D) system. The tests were carried out for joints made of S235JR steel using the Epidian 5 composition with the PAC curing agent. According to the results of the analysis, the parameters $SqSpd$ (root-mean square density of peaks), Spc (arithmetic mean peak curvature), Sdr (developed interfacial ratio) and Sdq (root-mean square gradient) had the strongest influence on the shear strength of the adhesive joints.

In [10] the substrates surfaces of joints made of 5054 aluminum alloy were milled. It was shown that the highest shear strength was obtained when the roughness parameters of the adherents' surfaces were $Ra = 1.226 \mu\text{m}$, $Sa = 3.242 \mu\text{m}$.

The object of work [27] was the finite element analysis of the influence of the surface geometric structure on the stress state in the adhesive joint. The authors of the study pointed out that the surface irregularities such as indentations may become stress concentrators in the adhesive joint. They showed that the degree of stress concentration increases with an increase in the mean spacing of profile elements RSm and an increase in the maximum height of the profile Rz .

The subject of many studies was also the assessment of the influence of various methods of substrates surface treatment (resulting in different values of surface roughness) on the strength of adhesive joints [8, 14, 19, 23]. In the study [14] the effect of five types of surface treatment on the strength of single-lap joints made of AA 6082-T6 aluminum alloy made with the use of epoxy resin was investigated. The following types of treatments were used in the research: sodium dichromate–sulphuric acid

etch, abrasive polishing, caustic etch, Tucker's reagent etch and acetone cleaning. It was found that the highest strength was obtained in the case of etching with sodium dichromate and sulfuric acid and in the case of abrasive polishing. Moreover, under the assumed conditions, increasing the roughness of the substrates surface resulted in a decrease in the strength of the joints.

In the work [19], adhesive joints made of the titanium alloy Ti6Al4V were tested. The applied methods of treating the substrates surface were: anodizing, alkaline degreasing, anodizing with vibrational shot peening and vibratory shot peening. As a result of the research, it was found that higher strength is obtained in the case of anodizing combined with vibration peening than in the case of using each of these techniques separately. The study also pointed out that the properties of the adhesive (mainly viscosity) and the geometric structure of the substrates surface have a significant impact on the strength of the joints, which results from the mechanical theory of bonding. Higher bond strengths were observed with the more flexible adhesive.

Some methods of treating the substrates surface may, under certain conditions, reduce the strength of the adhesive joints. According to the results of the research presented in [23], polishing the substrates surface resulted in a decrease in the strength of adhesive joints made of Mg AZ31B with the use of epoxy adhesive (Lord Versilok 253/254). The authors of the study suggested that changes in the surface morphology and surface chemistry of Mg AZ31B could be the reasons for the reduction in joint strength.

The applied method of preparing the substrates surface can also largely affect the impact strength of the adhesive joints. In [8], the impact strength of connections made of 2017A aluminum alloy was examined. Two types of adhesives were used in the research. The substrates surfaces were subjected to roughening with sandpaper or abrasive blasting. The conducted research showed that the applied methods of surface machining allowed to increase the impact strength of the joints. It has also been shown that the impact strength of the joints was also influenced by the properties of adhesive (in particular, the adhesive longitudinal modulus of elasticity).

In addition to the surface roughness, another feature of the surface layer that can also affect the strength of the adhesive bonds is texture. Texturing is a well-known method of improving the tribological properties of mechanical components. One of the most obvious examples of the use of surface texturing is cylinder liner honing [3].

Currently, more and more studies are conducted on the influence of the texture on the strength of adhesive joints [4, 12, 13, 20, 21]. The authors of the work [4] investigated the effect of laser texturing on the strength of adhesive joints made of 30CrMnSiA steel. Three different patterns: dimple, groove and grid were performed on the substrates surfaces. It was shown that in the case of pits, the strength of the joints was not significantly improved. The samples with the groove and the grid increased the

strength by 219% and 348%, respectively, compared to the samples whose surfaces were not texturized. Moreover, in the case of the grid pattern, the Ra value increased by 400% and the contact angle decreased from 65 degree to 24 degree.

The impact of the laser texturing on the mechanical behavior of the aluminium alloy 2024 adhesive joints was investigated in [21]. The authors of the study claim that the laser treatment of the adherents leads to comparable or even higher fracture energy values than a long sequence of mechanical, electrochemical and chemical treatment. What is more, the study also suggested that changes in the chemical composition occur on the treated surface as a result of laser treatment, may translate into the strengthening of interfacial bonds between the adhesive and the material.

In the work [12] a statistical optimization of the laser treatment process with a green fiber laser was carried out in order to improve the mechanical properties of adhesive joints of the aluminum alloy 2024.

The paper [20] showed an 80% increase in the strength of adhesive joints made of CFRP and epoxy adhesive as a result of CO₂ laser texturing. The positive effect of laser surface texturing on the load capacity of adhesive joints was also proven in the case of joining polymeric materials [13].

Summarizing, the surface roughness and texture may affect the strength of the adhesive bonds. Most of the research currently being conducted focuses on the analysis of the effect of laser texturing on the strength of adhesive joints. However, in addition to beam methods, mechanical

methods, for example grinding, lapping or polishing, can also be used for texturing the surface layer. The aim of the research presented in this article was to assess the influence of the directivity of the geometric structure obtained in the grinding process on the load capacity of adhesive joints made of steel S235JR and aluminum alloy 2024-T3.


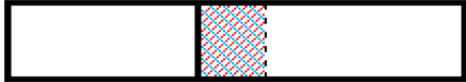
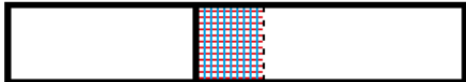


Methodology

The analysis was carried out for single-lap adhesive joints. The first group of connections was made of S235JR non-alloy structural steel. The chemical composition and properties of this steel can be found in the PN-EN 10025-1:2007 standard [15]. The second group of connections is made of the aluminum alloy 2024-T3. The chemical composition of this alloy and its basic properties are presented in the PN-EN 3997:2016-02 standard [17]. Steel plates and aluminum alloy plates were cut from a 2 mm thick rolled sheet.

The adhesive surfaces of the plates were ground in order to obtain the appropriate surface roughness and directivity. The grinding process was carried out with the use of a tool grinder EUROMET SN-200 (manufacturer - Eurometal Sp. z o.o, Poland) with a 80x30x6 mm P40 flap disc (manufacturer – Klingspor, Poland). The treatment was carried out at a rotational speed of 3000 rpm. The adopted grinding directions for individual pairs of the plates are presented in Table 1.

Residues left after the grinding process were removed with compressed air. Then, the plates were cleaned with

Table 1. Grinding directions and variants of the adhesive joints

Adhesive connection variant - steel S235JR	Adhesive connection variant - aluminum alloy 2024-T3	Grinding directions	Scheme
ST45	AL45	Post-machining marks at an angle of 45° to the direction of the force loading the joint on both joined surfaces	
ST45K	AL45K	Cross direction - post-machining marks at an angle of 45° to the direction of the force loading the joint on both joined surfaces	
STK	ALK	Cross direction – post-machining marks perpendicular on one joined surface, and parallel on the other	
STP	ALP	Perpendicular arrangement of the post-processing marks in relation to the direction of the force loading the joint	
STR	ALR	Parallel arrangement of the post-machining marks in relation to the direction of the force loading the joint	

acetone. The next stage of the research was to measure the surface roughness of the plates subjected to grinding. The parameters Rz (maximum peak to valley height of the profile within a sampling length), Ra (arithmetic mean of the absolute departures of the roughness profile from the mean line), RSm (mean spacing between profile peaks at the mean line) and Rda (arithmetic mean slope of the profile) were measured. The surface roughness was measured using a Taylor Hobson SURTRONIC 25 contact profilometer (manufacturer - Taylor Hobson, England) and TalyProfile Lite software.

Then, the surfaces of the plates were degreased with acetone. After the adhesive surface has dried, single-lap adhesive joints were made. The length of the overlap was 12.5 mm. The joining variants are shown in Table 1. The joints were created using the Loctite 3430 two-component epoxy adhesive (manufacturer – Henkel, Germany), which fills the gaps well, therefore it can be used on rough and poorly adhering surfaces [11]. The samples were placed in a mechanical clamping device and loaded with a one-kilogram weight. The cross-linking time was

48 hours. The cross-linking temperature ranged from $23\pm 2^{\circ}\text{C}$ and the humidity was 35%.

The adhesive joints have been subjected to a static tensile test in accordance with PN-EN 1465:2009 (Adhesives - Determination of the shear strength of lap joints) [16]. The tests were carried out on the Zwick / Roell Z030 testing machine (manufacturer - Zwick Roell, Germany). The connections were loaded until they were broken. The breaking force was taken as the load capacity Pt [N] of the adhesive joint.

Results and discussion

Table 2 and Table 3 contain the mean values of the measured roughness parameters as well as selected surface profilograms and the corresponding photos of microstructures made with a microscope with 10x magnification.

As a result of machining with a 80x30x6 mm P40 flap disc, the geometric structure of the surface with uni-directional directivity was constituted. Based on Table

Table 2. Selected microstructures and profilograms of ground surfaces for S235JR steel

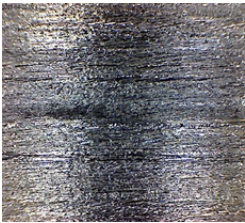
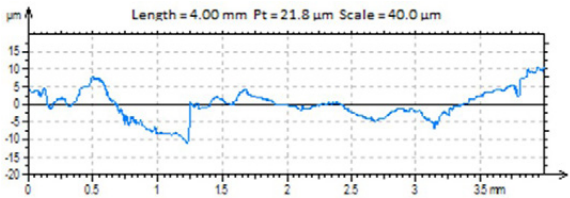
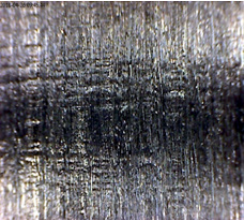
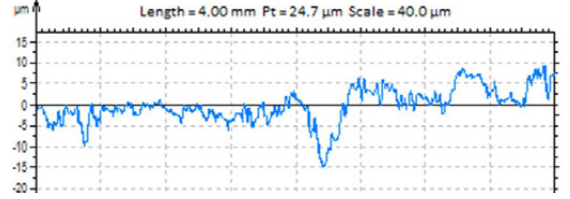

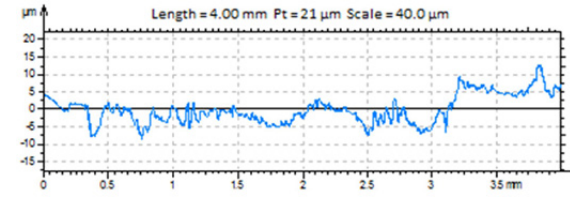

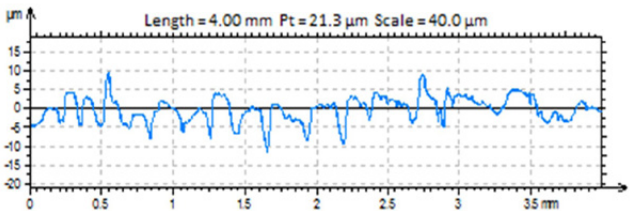
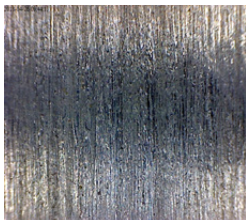
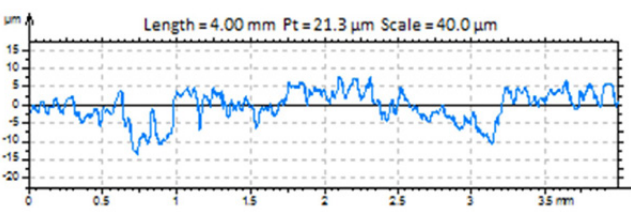
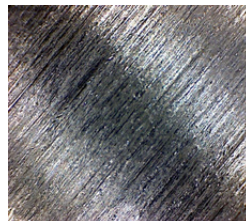
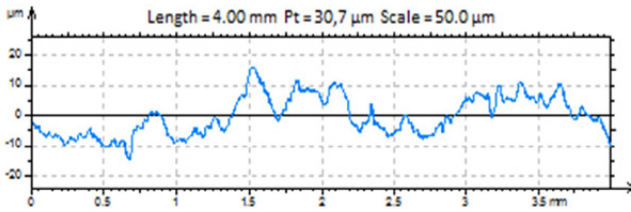
Parallel direction (S235JR steel)							
Rz [μm]	7.41	Ra [μm]	1.16	RSm [mm]	0.278	Rda [$^{\circ}$]	2.88
							
Perpendicular direction (S235JR steel)							
Rz [μm]	10.10	Ra [μm]	1.74	RSm [mm]	0.140	Rda [$^{\circ}$]	6.96
							
Post-machining marks at an angle of 45° (steel S235JR)							
Rz [μm]	9.60	Ra [μm]	1.52	RSm [mm]	0.137	Rda [$^{\circ}$]	6.13
							

Table 3. Selected microstructures and profilograms of ground surfaces for aluminum alloy 2024-T3

Parallel direction (aluminum alloy 2024-T3)							
Rz [μm]	14.4	Ra [μm]	2.32	RSm [mm]	0.193	Rda [$^\circ$]	6.39
							
Perpendicular direction (aluminum alloy 2024-T3)							
Rz [μm]	12.8	Ra [μm]	2.27	RSm [mm]	0.114	Rda [$^\circ$]	8.08
							
Post-machining marks at an angle of 45° (aluminum alloy 2024-T3)							
Rz [μm]	13.9	Ra [μm]	2.60	RSm [mm]	0.233	Rda [$^\circ$]	6.03
							

2, it can be concluded that in the case of steel S235JR the highest values of the Rz, Ra and Rda parameters were obtained for the surface that was ground perpendicular to the plate length (Rz = 10.1 μm , Ra = 1.74 μm , Rda = 6, 96°). In turn, the highest value of the RSm parameter was obtained for the parallel direction (RSm = 0.278 mm). By analyzing the roughness parameters obtained for the samples from the aluminum alloy 2024-T3, it can be concluded that the highest value of the Rz parameter was obtained in the case of the parallel direction (Rz = 14.4 μm), the highest value of the Ra and RSm parameters was obtained for grinding at an angle of 45° (Ra = 2.60 μm , RSm = 0.233 mm), and the highest values of the Rda parameter were obtained for the perpendicular grinding direction (Rda = 8.08°). Moreover, the aluminum alloy surfaces are characterized by much higher values of Rz and Ra parameters. The reason for the greater surface roughness of the aluminum alloy plates may be greater softness and better machinability of this alloy compared to the steel used in the tests.

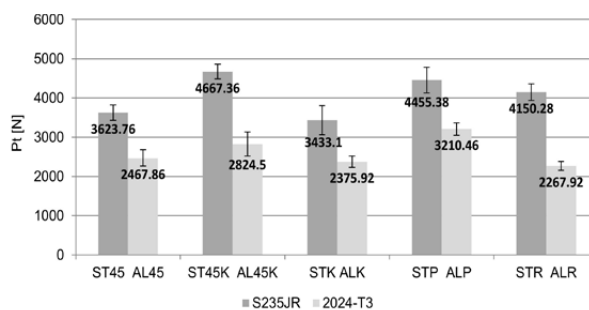


Fig. 1. Comparison of the load capacity of adhesive joints

The average values of the load capacity of adhesive joints and the standard deviations are presented in Figure 1.

The average values of the load capacity were calculated from the measurement results for five samples made for each material and joint variant. Based on the results of the load capacity of the adhesive joints, it can be concluded that the joints made of S235JR steel are

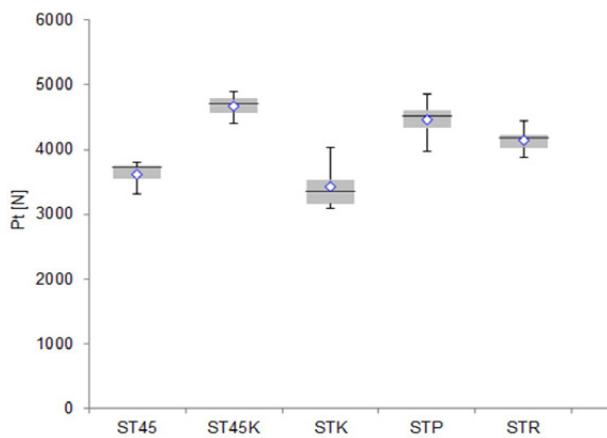


Fig. 2. Box plot - connections made of S235JR steel

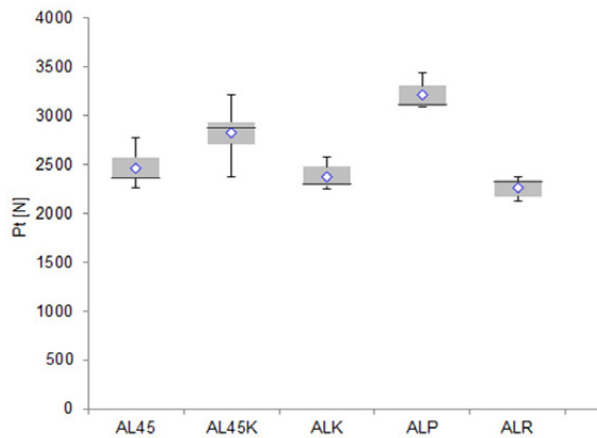


Fig. 3. Box plot - connections made of aluminum alloy 2024-T3

characterized by a much higher load capacity than the joints made of the aluminum alloy 2024-T3. Therefore, higher values of the roughness parameters Ra and Rz in the case of the aluminum alloy did not translate into a higher load capacity of the adhesive joint. In the case of steel connections, the STK45 variant has the highest load capacity ($P_t = 4667.36 \text{ N}$) and, at the same time, the lowest value of the standard deviation. On the other hand, the STK variant had the lowest load capacity. In the case of aluminum alloy, the highest load capacity was observed for the ALP variant ($P_t = 3210.46 \text{ N}$). The lowest load capacity and, at the same time, the lowest value of the standard deviation in the case of aluminum alloy connections were found for the ALR variant.

The normality of distribution of the data obtained from measurements of the load capacity was checked using the Shapiro–Wilk test. According to the test results, the data has a normal distribution.

Figures 2 and 3 show the box plots that were used to present the position and dispersion, as well as the shape of the distribution of the load capacity results.

Based on the box plots (Fig. 2 and Fig. 3), it can be concluded that in the case of steel adhesive joints, the STK variant is characterized by the greatest dispersion of the load capacity results. In the case of an aluminum alloy, the variant with the highest scattering of results is AL45K. Moreover, based on the diagrams, it can be assumed that the distribution of measurement results in the case of most variants is asymmetrical (for both steel and aluminum alloy adhesive joints). An example may be the STK variant, the graph of which may indicate right-hand asymmetry.

The next stage of the analyzes was performing the test-t, which made it possible analysis of significant differences between the load capacity of adhesive joints made of the 2024-T3 aluminum alloy and S235JR steel differing in the variants of the mutual arrangement of post-machining marks. Statistical significance $\alpha = 0.05$ was assumed for the analyzes. The results of the significant difference test for steel connections are presented in Table 4, and for aluminum alloy connections in Table 5.

Based on Table 4 and Table 5, it can be concluded that the probability values p_v are less than 5% in most

Table 4. Student's t-test results (S235JR steel)

Pv [%]	ST45	ST45K	STK	STP	STR
ST45	X				
ST45K	0.001	X			
STK	17.534	0.031	X		
STP	0.108	12.599	0.091	X	
STR	0.181	0.179	0.437	6.214	X

Table 5. Student's t-test results (aluminum alloy 2024)

Pv [%]	AL45	AL45K	ALK	ALP	ALR
AL45	X				
AL45K	3.469	X			
ALK	22.236	1.371	X		
ALP	0.015	2.359	0.001	X	
ALR	5.402	0.625	11.123	0.000	X

cases (probability values less than 5% are marked in red). This means that in most cases the results of the test-t show a statistically significant difference between the load capacity of the adhesive joints belonging to the compared variants (in the case of steel joints, the exceptions are the pairs STK and ST45, STP and ST45K, STR and STP, in the case of joints with of aluminum alloy, the pairs of ALK and AL45, ALR and AL45, ALR and ALK are an exception). Therefore, it can be concluded that in the adopted range of variability of the input factors, the influence of the directivity of the geometric structure of the adhesive surface on the load capacity of the joints is statistically significant.

Conclusions

1. Machining with a 80x30x6 mm P40 flap disc constituted the geometrical structure of the surface with unidirectional directivity. The height parameters of the surface roughness of the samples made of the 2024-T3 aluminum alloy had the value of $R_a = 2.27 \div 2.60 \mu\text{m}$ and $R_z = 12.4 \div 14.4 \mu\text{m}$, while the samples made of S235JR steel, due to the greater hardness of the steel, had lower values $R_a = 1.16 \div 1.74 \mu\text{m}$ and $R_z = 7.4 \div 10.1 \mu\text{m}$.
2. The highest load capacity of the adhesive joints made of 2024-T3 aluminum alloy, amounting to 3210.46 N, had the samples with perpendicular arrangement of the post-machining marks in relation to the direction of the force loading the joint. The lowest load capacity, amounting to 2267.92 N, had the samples with parallel arrangement of the post-machining marks in relation to the direction of the force loading the joint. The difference between the values of the load capacity is 41.5%.
3. The highest load capacity of adhesive joints made of S235JR steel, amounting to 4667.36 N, had the samples with the arrangement of post-machining marks at an angle of 45° to the direction of the force loading the joint. The lowest load capacity, amounting to 3433.10 N, had the joints whose marks on one of the plates was perpendicular, and on the other, parallel to the direction of the force loading the adhesive joint. The difference between the values of the load capacity is 35.9%.
4. The analysis of significant differences between the load capacity of adhesive joints made of the 2024-T3 aluminum alloy and S235JR steel differing in the variants of the mutual arrangement of post-machining marks, performed with the t-test, showed statistically significant differences between the majority of variants, which proves a significant influence of the directivity of the geometric structure of the surface on load capacity of adhesive joints.

References

- [1] Adamczak S. 2008. Pomiary geometryczne powierzchni. Zarysy kształtu, falistość i chropowatość. Warszawa: Wydawnictwo Naukowo-Techniczne.
- [2] Dilger K., Burchardt B., Frauenhofer M. 2018. "Automotive Industry". In da Silva L. F. M., Öchsner A., Adams R. D. (ed.) Handbook of Adhesion Technology, 1332-1366. Springer International Publishing AG.
- [3] Etsion I. 2005. "State of Art in Laser Surface Texturing". Journal of Tribology 127: 248-253.
- [4] Feng Z., Zhao H., Tan C., Zhu B., Xia F., Wang Q., Chen B., Song X. 2019. "Effect of laser texturing on the surface characteristics and bonding property of 30CrMnSiA steel adhesive joints". Journal of Manufacturing Processes 47: 219-228.
- [5] Ghumatkar A., Budhe S., Sekhar R., Banea M. D., de Barros S. 2016. "Influence of Adherend Surface Roughness on the Adhesive Bond Strength". Latin American Journal of Solids and Structures 13: 2356-2370.
- [6] Grzesik W. 2016. "Prediction of the Functional Performance of Machined Components Based on Surface Topography: State of Art". Journal of Materials Engineering and Performance 25: 4460-4468.
- [7] Kłonica M., Kuczmaszewski J. 2018. Badania stanu energetycznego warstwy wierzchniej wybranych materiałów konstrukcyjnych po ozonowaniu. Lublin: Wydawnictwo Politechniki Lubelskiej.
- [8] Komorek A., Godzimirski J. 2018. "The influence of selected adhesive properties and the manner of surface preparation upon impact strength of block adhesive joints". Journal of KONES Powertrain and Transport 25: 463-469.
- [9] Kuczmaszewski J. 2006. Fundamentals of metal-metal adhesive joint design. Lublin: Lublin University of Technology Polish Academy of Sciences, Lublin Branch.
- [10] Liu S., Jin S., Zhang X., Chen K., Wang L., Zhao H. 2018. "Optimization of 3D surface roughness induced by milling operation for adhesive-sealing". Procedia CIRP 71: 279-284.
- [11] Loctite 3430 technical data, <http://elektronika.mcc.pl/system/files/1545/loctite-ea-3430.pdf> [access: April 2021].
- [12] Loutas T. H., Kliafa P. M., Sotiriadis G., Kostopoulos V. 2019. "Investigation of the effect of green laser pre-treatment of aluminum alloys through a design-of-experiments approach". Surface & Coatings Technology 375: 370-382.
- [13] Mandolino C., Pizzorni M., Lertora E., Gambaro C. 2018. "Laser surface texturing of polypropylene to increase adhesive bonding". AIP Conference Proceedings 1960: 060004.
- [14] Pereira A.M., Ferreira J.M., Antunes F.V., Bártolo P.J. 2010. "Analysis of manufacturing parameters on the shear strength of aluminium adhesive single-lap joints". Journal of Materials Processing Technology 210: 610-617.
- [15] PN-EN 10025-1:2007. Wyroby walcowane na gorąco ze stali konstrukcyjnych - Część 1: Ogólne warunki techniczne dostawy. Warszawa: Polski Komitet Normalizacyjny.

- [16] PN-EN 1465:2009. Kleje - Oznaczenie wytrzymałości na ścinanie przy rozciąganiu połączeń na zakładkę. Warszawa: Polski Komitet Normalizacyjny.
- [17] PN-EN 3997:2016-02. Lotnictwo i kosmonautyka - Stop aluminium AL-P2024- AlCu4Mg1 - T3 - Blachy i taśmy - 0,4 mm ≤ a ≤ 6 mm. Warszawa: Polski Komitet Normalizacyjny.
- [18] Rudawska A. 2013. Wybrane zagadnienia konstytuowania połączeń adhezyjnych jednorodnych i hybrydowych. Lublin: Wydawnictwo Politechniki Lubelskiej.
- [19] Rudawska A., Zaleski K., Miturska I., Skoczylas A. 2019. "Effect of the Application of Different Surface Treatment Methods on the Strength of Titanium Alloy Sheet Adhesive Lap Joints". *Materials* 12: 4173.
- [20] Sorrentino L., Marfia S., Parodo G., Sacco E. 2020. "Laser treatment surface: An innovative method to increase the adhesive bonding of ENF joints in CFRP". *Composite Structures* 233: 111638.
- [21] Spadro C., Sunseri C., Dispenza C. 2007. "Laser surface treatments for adhesion improvement of aluminium alloys structural joints". *Radiation Physics and Chemistry* 76: 1441–1446.
- [22] Zaleski K., Matuszak J., Zaleski R. 2018. *Metrologia warstwy wierzchniej*. Lublin: Wydawnictwo Politechniki Lubelskiej.
- [23] Zheng R., Lin J., Wang PC, Wu Y. 2016. "Correlation between surface characteristics and static strength of adhesive-bonded magnesium AZ31B". *The International Journal of Advanced Manufacturing Technology* 84: 1661–1670.
- [24] Zielecki W. 2007. „Wpływ rozwinięcia struktury powierzchni na wytrzymałość zakładkowych połączeń klejowych”. *Technologia i Automatykacja Montażu* 2 i 3: 108: 111.
- [25] Zielecki W., Pawlus P., Pełowski R., Dzierwa A. 2011. „Analiza wpływu struktury geometrycznej powierzchni w układzie 3D na wytrzymałość połączeń klejowych”. *Technologia i Automatykacja Montażu* 1: 33-37.
- [26] Zielecki W., Pawlus P., Pełowski R., Dzierwa A. 2013. „Surface topography effect on strength of lap adhesive joints after mechanical pre-treatment”. *Archives of Civil and Mechanical Engineering* 13: 175-185.
- [27] Zielecki W., Zielecki K. 2010. „Analiza MES wpływu struktury geometrycznej powierzchni na stan naprężeń w spoinie klejowej”. *Technologia i Automatykacja Montażu* 4: 49-51.

dr hab. inż. Władysław Zielecki, prof. PRZ
Wydział Budowy Maszyn i Lotnictwa Politechniki Rzeszowskiej, Katedra Technologii Maszyn i Inżynierii Produkcji al. Powstańców Warszawy 8, 35-959 Rzeszów, Polska
e-mail: wzktmiop@prz.edu.pl

dr inż. Łukasz Bąk
Wydział Budowy Maszyn i Lotnictwa Politechniki Rzeszowskiej, Katedra Przeróbki Plastycznej al. Powstańców Warszawy 8, 35-959 Rzeszów, Polska
e-mail: lbak@prz.edu.pl

mgr inż. Ewelina Guźła
Wydział Budowy Maszyn i Lotnictwa Politechniki Rzeszowskiej, Katedra Technologii Maszyn i Inżynierii Produkcji al. Powstańców Warszawy 8, 35-959 Rzeszów, Polska
e-mail: e.guzla@prz.edu.pl

maszyny • technologie • materiały •
projektowanie • konstrukcje • eksploatacja •
automatykacja • montaż • dozór techniczny •

Czasopisma dla Fachowców

- » TECHNOLOGIA I AUTOMATYZACJA MONTAŻU
- » INŻYNIERIA MATERIAŁOWA
- » PRZEGLĄD MECHANICZNY
- » DOZÓR TECHNICZNY

- Artykuły specjalistyczne pisane przez ekspertów
- Przegląd nowości z rynku, relacje z wydarzeń branżowych
- Wersja drukowana i on-line

ZAPRASZAMY DO WSPÓŁPRACY
prenumerata@sigma-not.pl, 22 840 30 86
reklama@sigma-not.pl, 22 827 43 65

WYDAWNICTWO SIGMA-NOT

INFLUENCE OF TEMPERATURE BASED PROCESS PARAMETER COMPENSATION ON PROCESS EFFICIENCY AND PRODUCTIVITY

Wpływ kompensacji parametrów procesu w oparciu o temperaturę na wydajność i produktywność procesu

Jerzy PATER ORCID 0000-0001-7571-0603

Damian BASARA ORCID 0000-0001-9342-4790

Dorota STADNICKA ORCID 0000-0002-4516-7926

DOI: 10.15199/160.2021.2.7

Abstract: Conditions in the working environment related e.g. to dust, vibration or temperature may have a negative impact on both, the production process and the manufactured product. Inappropriate and unstable conditions can cause instability of the production process and deteriorate the quality of manufactured products. Moreover, this can induce time waste and decrease the efficiency and productivity. In this paper the problem of temperature influence on a manufacturing process is analyzed. Monitoring of the temperature is not enough to ensure the achievement of manufacturing goals. It is necessary to adapt the parameters of the production process accordingly so that no nonconformities arise due to changes in temperature values and no delays appear. This paper deals with the efficiency and productivity of a manufacturing system which work under unstable working environment. The authors prove that application of the manufacturing process parameters compensation can significantly improve both, efficiency and productivity. The values of efficiency and productivity were monitored within a fixed period of time for a manufacturing system, on where the manufacturing process is realized. Then, a procedure of process parameters compensation was introduced. Next, within a fixed period of time the data were collected and the efficiency and productivity values were compared with the values obtained before. Additionally, the authors propose to introduce the Overall Equipment Effectiveness (OEE) indicator and present information about ways of data collecting.

Keywords: Overall Equipment Effectiveness (OEE), Utilization, Efficiency, Productivity, Quality, Flexible Manufacturing System (FMS), CNC machine, Control of accuracy, Test of machines, Repeatability, Capability

Streszczenie: Warunki w środowisku pracy związane np. zapyleniem, wibracjami lub temperaturą mogą mieć negatywny wpływ zarówno na proces produkcyjny, jak i na wytwarzany produkt. Nieodpowiednie i niestabilne warunki mogą powodować niestabilność procesu produkcyjnego i pogarszać jakość wytwarzanych wyrobów. Co więcej, może to spowodować stratę czasu i zmniejszyć wydajność i produktywność. W artykule przeanalizowano problem wpływu temperatury na proces produkcyjny. Monitorowanie temperatury nie wystarczy, aby zapewnić osiągnięcie celów produkcyjnych. Konieczne jest odpowiednie dostosowanie parametrów procesu produkcyjnego, aby nie powstawały niezgodności wynikające ze zmian wartości temperatury i aby nie pojawiały się opóźnienia. Artykuł dotyczy wydajności i produktywności systemu produkcyjnego, który pracuje w niestabilnym środowisku pracy. Autorzy udowadniają, że zastosowanie kompensacji parametrów procesu produkcyjnego może znacząco poprawić zarówno wydajność, jak i produktywność. Wartości wydajności i produktywności były monitorowane w ustalonym okresie czasu dla systemu produkcyjnego, na którym realizowany jest proces produkcyjny. Następnie wprowadzono procedurę kompensacji parametrów procesu. Po czym, w określonym przedziale czasu zebrano dane i porównano wartości wydajności i produktywności z wartościami uzyskanymi wcześniej. Dodatkowo autorzy proponują wprowadzenie wskaźnika całkowitej efektywności wyposażenia (OEE) i w artykule przedstawiono informacje o sposobach zbierania danych dla obliczenia OEE.

Słowa kluczowe: Całkowita efektywność wyposażenia (OEE), wykorzystanie, wydajność, produktywność, jakość, elastyczny system produkcji (FMS), obrabiarki CNC, kontrola dokładności, test maszyn, powtarzalność, zdolność

Introduction

The efficiency and the productivity are important indicators to assess a manufacturing system. For the Flexible Manufacturing Systems (FMS) it is expected that the indicators will have high values. The main advantage of FMS is the fixed unit cost for the flow of both a multi-piece batch and a single batch. The most common disadvantages is the high cost of starting the line and high failure rate resulting from many components. However, when the work on FMS is well organized, prepared and planned the manufacturing process should go on without significant problems. Usually, FMS are monitored

since the production is launched to identify technical and quality problems. They are then analyzed to find and eliminate the source causes.

In this work a FMS operating in a company in which aviation parts, i.e. housings, are manufactured is analyzed. The FMS is monitored, first of all to avoid quality problems, which generate high costs. The material for the products is expensive and the manufacturing process is continued for approximately 20 hours for a part. Moreover, the skilled personnel taking care about the FMS and involved in technical preparation process is costly. When creating the technological process of the product processing, the technologist, fixture designer and

CNC programmer had to take into account all possible scenarios that will affect the quality and compliance with the requirements of the client.

Despite the implementation of various available methods to increase the quality of the process the problems kept coming up again. Implementation of measuring probes and automatic unclamping and clamping of parts during machining to eliminate stresses did not give the expected results. Nonconforming products appeared what causes downtimes, while the problems were solving. Machine geometry measurements and corrections performed by maintenance services as well as nonconformity analyzes significantly worsened productivity. This, in turn, affects the production flow and inventory levels (WIP - Work In Process).

Analyzes and tests have shown that there are many variable parameters that affect part quality. Two of them that have the greatest influence on the process are temperature fluctuations and machine repeatability.

In this paper the first factor is analyzed - temperature fluctuations and its influence on the efficiency and productivity. The article presents the results of efficiency and productivity improvement that were achieved after the introduction of innovative, fully automatic methods of compensation to minimize temperature fluctuations and machine repeatability.

Other indicator, used to assess a manufacturing system is Overall Equipment Effectiveness (OEE) indicator. This indicator combines information about quality of the products manufactured on a manufacturing line with time spent on the process. In the analyzed company the OEE is currently not calculated. Therefore, in this work it is also analyzed how OEE can be introduced in the FMS assessment process.

The next section presents the work methodology. Section 3 describes the analyzed flexible manufacturing system. Section 4 indicates data, which are collected in the system. In the section 5 efficiency and productivity are defined and their calculation procedure is presented. Next section describes a methodology of process parameters compensation. In section 7 the values of efficiency and productivity indexes calculated before and after

compensation procedure implementation are compared. Section 8 presents a proposal of OEE implementation. The last section summarizes the work

The research goal and work methodology

The goal of the research presented in this paper was to prove that minimization of the temperature fluctuations by implementation on an automatic compensation of the manufacturing process parameters can significantly improve the efficiency and productivity of the FMS.

The work methodology was as follows:

- Step 1 – Collecting a manufacturing process data to calculate efficiency and productivity – the current state.
- Step 2 – Designing and implementation of the manufacturing process parameters compensation.
- Step 3 – Collecting process data to calculate efficiency and productivity after implementation of the process parameters compensation.
- Step 4 – Comparative analysis of the results – efficiency and productivity before and after implementation of the process parameters compensation.
- Step 5 – Proposal of a system that will allow to calculate Overall Equipment Effectiveness (OEE).

Presentation of the flexible manufacturing system

The Flexible Manufacturing System (FMS) analyzed in this paper consists of:

- Machines (5-axis milling centers) (M1-M4) in a linear or circular system connected with each other by a system of controllers and computers controlled by a central machine management system,
- robot (R1) for transporting pallets with semi-finished and finished products,
- loading and unloading stations (L1-L2),
- pallet warehouse (W1) with equipment for temporary storage of semi-finished and finished products,
- tool magazines (T1-T4) integrated with the machines.

The scheme of FMS components arrangement is presented in Figure 1.

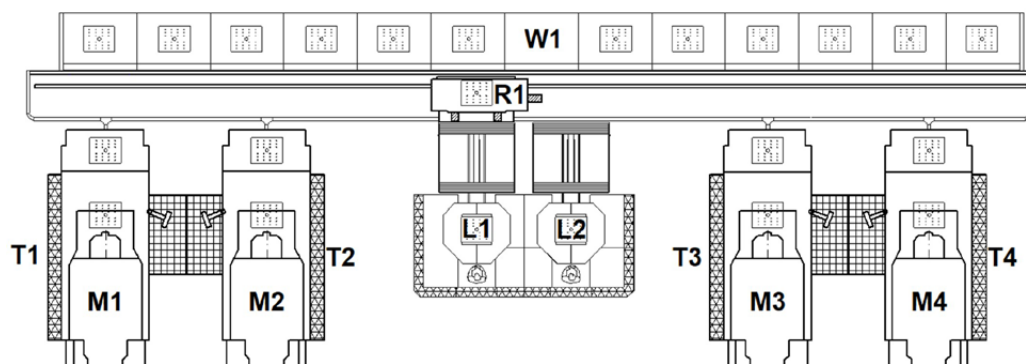


Fig. 1. A scheme of the analyzed FMS; M1 – machine 1, M2 – machine 2, M3 - machine 3, M4 – machine 4, R1 - robot, L1-L2 – loading & unloading stations 1&2, W1 - pallet warehouse, T1-T4 – tool magazines 1-4

The full flexibility of the line is achieved only when the parts implemented for production can be performed on each machine with the same efficiency. This is extremely difficult to achieve when machining large complex parts. The most common limitation is the capacity of the tool magazines. Then the only solution is to indicate specific machines for selected operations. In this case, it is possible to keep the benefits of the setup time reduced to zero. Unfortunately, any problem that appears disrupts flow. Line flexibility always limits the item with the lowest capacity. Most often it is a tool magazine, therefore, to ensure greater flexibility, central warehouses are used that support several or all machines.

Data collected from the analyzed FMS

On the analyzed FMS the following data are registered:

- production order number,
- product name,
- number of operation,
- work type (manual, automatic) – manual work is realized to attach the product to a fixture; automatic work is realized by CNC machines,
- product production start date – production of one product can continue for two days,
- number of products manufactured in a batch,
- standard time for operations, decided by a technologist,
- start and end time of the operations,
- real time of the operations – is calculated automatically taking into account start and end time,
- available time (so called Global Open Time – GOT) – it is usually 8 hours – this is time when employees supporting and working on FMS are available.

The presented data are used to calculate efficiency and productivity.

Efficiency and productivity calculation procedure

The **productivity** is one of the most commonly used Key Performance Indicators (KPIs) to monitor a plant's manufacturing excellence in the analyzed company. The productivity refers to the number of products that were produced in the available working time. In the analyzed company, to calculate the productivity, time units referring to the number of products are used. The productivity consists of two indicators – **efficiency** and **utilization**. In order to correctly calculate the indicators, reliable data should be recorded.

The **productivity** index is calculated by multiplying **utilization** and **efficiency** (equations 1).

$$\text{Productivity} = \text{Utilization} \cdot \text{Efficiency} \quad (1)$$

The **utilization** index is the quotient of the sum of the **real time** and the sum of the *Global Open Time* (equation 2).

$$\text{Utilization} = \frac{\sum \text{Real Time}}{\sum \text{Global Open Time}} \quad (2)$$

Real Time is the sum of time "consumed" for the execution of production tasks included in production orders. *Global Open Time* (GOT) is an available time, and it is calculated as the sum of time available to perform production tasks for a position or group of positions (production line, production department). It is often used to define the time available for an operator or group of operators who work on a specific production line.

The **efficiency** is an indicator that evaluates whether a production process is as efficient as expected. The efficiency index is calculated as the quotient of the sum of the *Standard Time* and the sum of the *Real Time* (equation 3). The indicator gives an information about the efficiency of a process and/or an operator. In the case of technological operations performed manually by a human, the quality of the indicator is determined by the so-called the discipline of *Real Time* registering and the accuracy of standardizing *Standard Time* activities. For technological operations performed in automatic mode, the real-time automatic registration is of key importance. In order to eliminate human error, automatic real-time measurement is increasingly being used. In cases such as the analyzed FMS line, automatic timing gives the ability to track the efficiency index in real time.

$$\text{Efficiency} = \frac{\sum \text{Standard Time}}{\sum \text{Real Time}} \quad (3)$$

Standard Time (STD time) is defined for each operation. The sum of operations standard times for all manufactured parts in a given period of time (day, week, month ...) is used to calculate the **efficiency**. All non-standard downtimes, such as breakdowns, quality stops, and missing production orders, reduce utilization and they are monitored with the productivity indicator. The non-standard downtimes cause that the lower number of products are manufactured.

The productivity can be also calculated as a product of the sum of *Standard Times* and the *Global Open Time*, as it is presented in (equations 4).

$$\text{Productivity} = \frac{\sum \text{Standard Time}}{\sum \text{Global Open Time}} \quad (4)$$

The quality of *Standard Time* determination has direct influence on the **efficiency** as well as the **productivity**. The accuracy of recording *Real Time* is of great importance in correctly calculating **utilization** and **efficiency**.

A common mistake companies make when calculating *Standard Time* is underestimating or overestimating *Standard Time*. In both cases, the **efficiency** calculated

on its basis gives extremely different results, leading to decision errors. In the case of automated production processes, where work is performed by machines in conjunction with robots, determining the *Standard Time* is quite easy and often it is *Real Time* for the undisturbed performance of a set of procedures that make up a technological operation.

The FMS line, which is the subject of the research, is used for machining the housings of aircraft gears. Technical parameters (length, diameter, error of shape, position and surface roughness) made on machines are the final (drawing) dimensions. The basic material used (forging), high accuracy and complicated shape as well as large dimensions mean that even a slight disturbance of the process due to external factors causes the production of a non-compliant part. When a nonconformity is detected, the machine is always stopped in the FMS line in order to determine the cause. Any such stoppage results in lower **productivity**. The role of the **productivity** index is not only to indicate the state of the current situation, but also it gives the possibility of continuous and conscious control of production losses at the organization level through accurate tracking of partial indicators.

Methodology of process parameters compensation

As part of the research and implementation work carried out on the FMS line described in section 3 of this article, a system was developed and implemented whose task is control and calibration of geometric and kinematic parameters of the machine tool.

Due to the variety of manufactured elements, changes in ambient temperature, machine tool failures, it was necessary to periodic monitoring and calibrating machining centers for process suitability. Before the implementation of automatic process suitability control, measurements were performed manually with the use of dial indicator and artifacts. Qualified personnel were required to interpret the measurement results and correct the machine tool. To shorten the measurement time and reduce the involvement of production personnel, measurement procedures were developed using the part probe, temperature probe, master object in the form of a cuboid with

the characteristic dimensions of 750x750 mm, and two reference spheres placed on the machining pallet (Fig. 2).

The individual stages of measurements were designed to reflect, as far as possible, the acceptance instructions contained in the standards (ISO 10791-1) [4] and the acceptance documentation of the machine manufacturer. The measurement procedure was divided into six steps:

- **Step 1** – Cuboid temperature is measured to compensate for the nominal geometrical values of the artifact. The temperature is measured by probe TP44.10 [3].
- **Step 2** – The analysis of the geometrical properties of the machining center using the RMP600 object probe [9] and measuring cycles [11]. Straightness measurements of individual linear axes are made in the YZ, ZX, XY planes. The angular relationships between the YX, YZ and XZ axes are also checked (See Fig. 2.a)
- **Step 3** – The assessment the correctness of the machine zero position (See Fig. 2.b), and verification of the error of parallelism of the rotation axis of the table B in relation to the Y axis in the ZY and XY planes. The assessment of these parameters is made by measuring the position of two artifacts in the form of reference balls whose position in space is changed by means of the rotation axis B in three characteristic positions (B0, B-90, B-180).
- **Step 4** – Correctness of kinematic vectors is tested (See Fig. 2. c), which are used to define 5-axis transformations (TRAORI, TCARR) [10]. The measurement takes place in such a way that with the help of the object probe three positions of the measuring ball are read for each of the two rotary axes (A, B) [11]. The results obtained in this way are compared with the current settings, and corrected if necessary.
- **Step 5** – If the tests are passed (measurements in specified tolerances), the machine zero position and kinematic vectors are automatically corrected by making change to the machine data.
- **Step 6** – Re-inspection of the machine tool is done in order to verify the correctness of the entered new machine data (step 3, step 4).

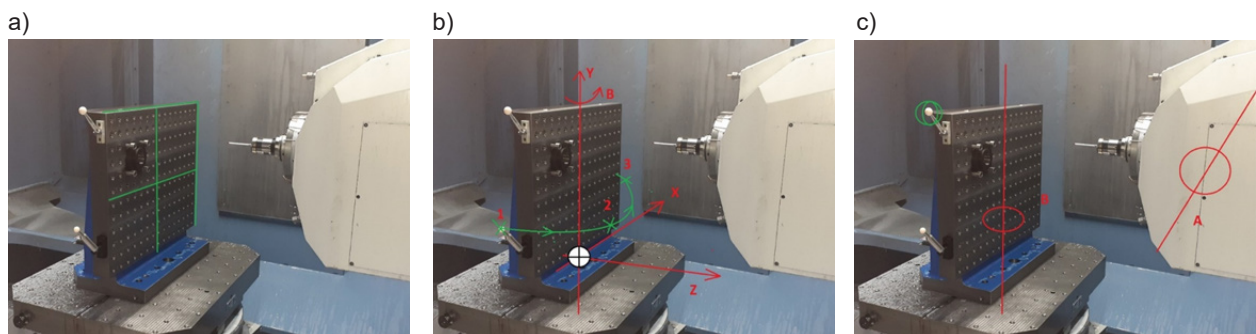


Fig. 2. View of the calibration master (two reference sphere's, calibration column), together with the RMP600 probe, inside 5-axis machine center: a) geometry measurement, b) machine zero measurement, c) kinematic vectors test

The acceptable deviations were adopted in accordance with the acceptance requirements contained in the purchase contract of the analyzed machining center and the requirements of the standard ISO 10791-1 [4]. In case of any of the measured parameters exceeds the assumed tolerances, the machine tool activates a sound and a light signal to call the operator to assess the situation.

All data obtained during the calibration procedure are recorded in the form of a text file. This allows data to be analyzed at any time in the event of problems during auto-calibration.

Assessment of efficiency and productivity

The data used in this analysis was collected in the period from 03-08-2020 to 29-04-2021 and consists of 809 records.

The data necessary to calculate efficiency and productivity are obtained from two sources – the ERP system and production. In order to correctly calculate the efficiency, a detailed analysis of the duration of the operations performed on the FMS line was performed. *Standard Time (STD)* has been entered into the ERP system and is used in calculations. *Standard Time* is defined by a process engineer in the stage of a new product implementation.

The second element for calculating the process efficiency is the *Real Time* of the operation. There are two methods of getting this time – automatic and manual. Both of them are used in the plant, however, for the presented case, the results of manual work time recording are presented. An FMS line employee sends a signal to the ERP system when an operation from a production order is started and ended. Based on the data the system calculates *Real Time*. This way has disadvantages as the reliability of the *Real Time* recorded depends on the discipline of the employees. The productivity index is calculated fully automatically, and the employee has no influence on it. Both, *Standard Time* and *Global Open Time* come from the ERP system.

The nine months of operation of the FMS line, for which the analysis was done, can be divided into three periods (Table 1):

- Period 1 – from August to December 2020 – the data come from the manufacturing line operations before the introduction of parameter compensation.
- Period 2 – January 2021 – the data come from the month when the innovative solution of process parameters compensation was implemented.
- Period 3 – from February to April 2021 – the data come from a operational system with fully automated parameter compensation.

Table 1. Data collected for the purpose of efficiency and productivity calculation for FMS

Year	Month	STD time [h]	REAL time [h]	GOT [h]	Efficiency [%]	Productivity [%]
2020	Aug	160.4	279.6	671	57.4	23.9
	Sep	309.1	527.0	693	58.6	44.6
	Oct	319.7	344.5	609	92.8	52.5
	Nov	81.4	108.4	548	75.1	14.9
	Dec	264.7	283.7	458	93.3	57.8
2021	Jan	416.2	419.9	544	99.1	76.5
	Feb	477.9	485.2	528	98.5	90.5
	Mar	641.1	648.4	737	98.9	87.0
	Apr	530.1	531.0	596	99.8	88.9

Figure 3 presents visual representation of efficiency and productivity in the mentioned periods of time. The warm summer months and the first cold autumn month are connected with large temperature fluctuations. The large volume of the production hall does not help to quickly stabilize the temperature with the existing air conditioning system. Maintenance service employees intervened many times during these periods. This

influenced the quality of the manufacturing process, the stability of machines work and the products quality. This in turn caused production downtime what had a very big influence on the efficiency and productivity.

In the months, before the machines parameters compensation due to temperature fluctuations was introduced, the efficiency equaled from 57.4% to 93,3%. The productivity equaled from 14.9% to 57,8%. This

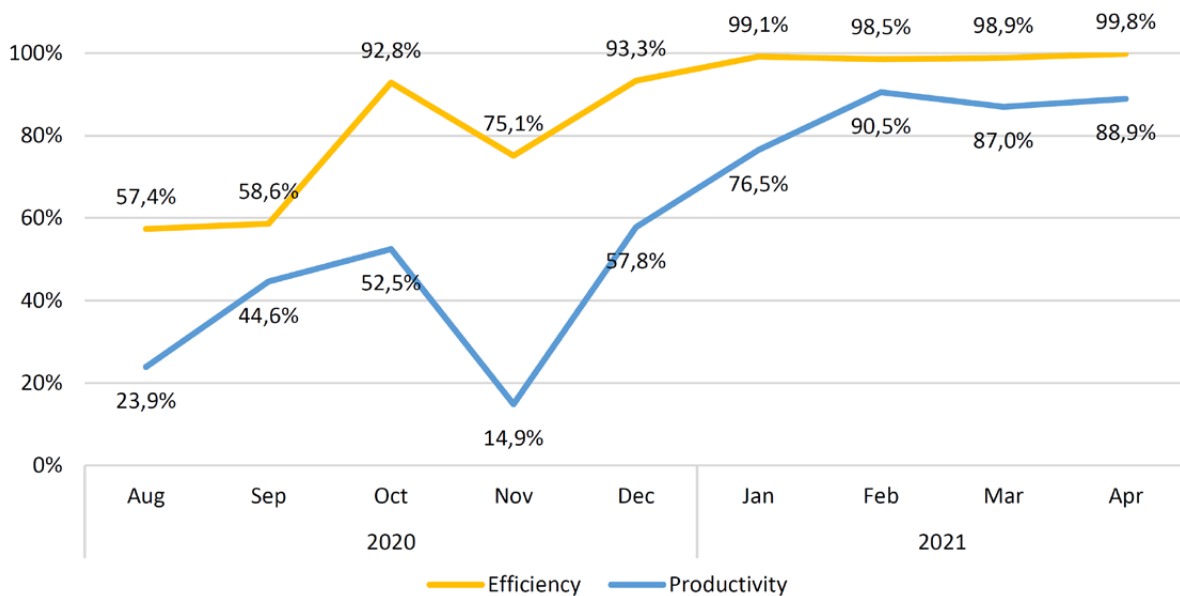


Fig.3. Efficiency and Productivity in the period before and after the introduction of process compensation

means that about half or more of the GOT was devoted to manual measurements of machine geometry and kinematics and analysis of the causes of non-compliance needed to be performed before production could be continued. Only after making sure that all parameters were correct, the machining process could be continued.

In these months, research was carried out on the impact of temperature fluctuations on the geometry and kinematics of machines in relation to the quality of parts. The result of these works was the implemented system of automatic compensation of machines parameters needed to be adjusted due to by temperature fluctuations, without the participation of maintenance services. Before the innovation was introduced, it was necessary to stop the work of the machine after each detection of nonconformity. Machine geometry measurements and corrections performed by maintenance services as well as nonconformity analyzes significantly reduced productivity. This was directly related to the reduction of the standard time (time really used for processing), which is the sum of all standard times of the parts produced. Automatic compensation of machine parameters minimizes the possibility of making a nonconforming part and thus machine downtime.

After introduced of innovation the efficiency was never lower than 98% and the productivity was equal or higher than 87%. The generated downtime has been reduced to a minimum and the quality of parts has improved significantly.

Currently, it is not calculated how much the number of nonconforming products influence on the manufacturing line effectiveness. The information of the nonconformities is registered, however they are not directly connected with operational time. Therefore, the implementation

of the Overall Equipment Effectiveness (OEE) index is planned in the future

Proposal of Overall Equipment Effectiveness indicator implementation

Thanks to the implementation of OEE, it the indicator combining Quality, Performance and Availability in real time can be monitored. This will allow to react quickly if OEE will be below the assumed target.

OEE will help follow the process over a longer period of time by observing the trend. In the event that the currently used method of parameter compensation ceases to be effective, maintenance can start in advance. This can happen with different products, different materials, different technology, different times of the year or in case of problems with cutting tools. Always after achieving the maximum possibilities of machine parameters compensation, the service of specialists is inevitable if the introduced automatic parameter compensation did not solve a problem. Analyzing of partial OEE indicators, such as Quality, Performance or Availability, the root cause of OEE reduction can precisely determine.

Overall equipment effectiveness (OEE) is introduced by Nakajima [7] as a Key Performance Indicators (KPI) to measure the equipment productivity of a manufacturing system. The indicator is widely used in industry [8]. The published works present OEE application in the beverage industry [13], weaving industry [14], pharmaceutical industry [5], on the beerfilling lines [2], for a semiconductor manufacturing [1] and many others. All downtimes and even micro downtimes have significant influence of on OEE [15].

The OEE indicator is planned to be introduced into the FMS monitoring process. The way of OEE calculation will be adopted from [12] (equation 5).

$$\text{OEE} = \text{Quality} \cdot \text{Performance} \cdot \text{Availability} \quad (5)$$

$$\text{Quality} = \frac{\text{Time to manufacture all products} - \text{Time to manufacture all nonconforming products}}{\text{Time to manufacture all products}} \quad (6)$$

$$\text{Performance} = \frac{\sum \text{Real Time}}{\sum \text{Global Open Time}} \quad (7)$$

$$\text{Availability} = \frac{\text{Global Open Time} - \text{Unplanned downtimes}}{\text{Global Open Time}} \quad (8)$$

The performance component of OEE will be calculated in the way which is used currently to calculate productivity. The availability component of OEE will be calculated in the way which is used currently to calculate utilization. To calculate OEE the presented data need to be collected. It looks that not much additional work will have to be done to calculate OEE. The only problem is connected with currently used data bases and connections between them what have to be improved.

Conclusions

The presented paper explains how the manufacturing process parameters compensation can significantly improve both, efficiency and productivity. In the analyzed company it was discovered that temperature fluctuations influence the process and products quality through their impact on repeatability of the machines. The quality problems influenced the efficiency and productivity. Implementation of an automatic method for the process parameters compensations decrease the number of problems and interventions and improve efficiency and productivity indicators. Efficiency increased on average by 31.3% and productivity by as much as 129.3%. It was possible thanks to the maximum reduction of losses related to machine downtime. The process has stabilized at a satisfactory level. Efficiency and productivity remained at 99.1% and 88.8% respectively.

Although, the nonconformities influence the mentioned indicators it is not directly calculated what is the influence. The implementation of OEE indicator can more precisely indicate what influence the most of the manufacturing line effectiveness. This can be for example wrong planning process (availability component), technological problems (performance component) or quality problems (quality component). In the future work the connections between the problems existing on the analyzed FMS and OEE will be studied.

The quality will be calculated from (equation 6). The utilization will be calculated from (equation 7). The availability will be calculated from (equation 8).

References

- [1] Cheah C.K., Prakash J., Ong K.S. 2020. "An integrated OEE framework for structured productivity improvement in a semiconductor manufacturing facility". *Int. J. Product. Perform. Manag.* 69: 1081–1105.
- [2] He F., Shen K., Lu L., Tong Y. 2018. "Model for improvement of overall equipment effectiveness of beerfilling lines". *Adv. Mech. Eng.* 10(8):168781401878924.
- [3] Hexagon Manufacturing Intelligence. Part of Hexagon - m&h Radio-Wave Touch Probe V01.00-REV01.00. Release date: 2016-01-15.
- [4] ISO 10791-1: 2015 - Test conditions for machining centres - Part 1 - Geometric tests for machines with horizontal spindle and with accessory heads (horizontal Z-axis).
- [5] Kuiper A., Van Raalte M., Does R.J.M.M. 2014. "Quality quandaries: Improving the overall equipment effectiveness at a pharmaceutical company". *Qual. Eng.* (26): 478–483.
- [6] Mutilba U., Gomez-Acedo E., Kortaberria G., Olarra A., Yagüe-Fabra J.A. 2017. "Traceability of On-Machine Tool Measurement: A Review". *Sensors* 17(7): 1605.
- [7] Nakajima S. 1988. *Introduction to TPM*. Portland, OR, USA: Productivity Press.
- [8] Ng Corrales L.D.C., Lambán M. P., Hernandez Kerner M.E., Royo, J. 2020. "Overall equipment effectiveness: Systematic literature review and overview of different approaches". *Applied Sciences* 10(18): 6469.
- [9] Renishaw. RMP600 radio transmission probe. Available on-line: resources.renishaw.com [access: 12.05.2019].
- [10] Siemens. 2011. SINUMERIK 840d SI/828d – Przygotowanie do pracy. Podręcznik programowania.
- [11] Siemens. 2015. SINUMERIK 840d SI/828d - Cykle pomiarowe. Podręcznik programowania.
- [12] Stadnicka D., Antosz K. 2018. Overall Equipment Effectiveness: Analysis of Different Ways of Calculations and Improvements. In Hamrol A., Ciszak O., Legutko S., Jurczyk M. (eds) *Advances in Manufacturing. Lecture Notes in Mechanical Engineering*, 45-55. DOI: 10.1007/978-3-319-68619-6_5.

- [13] Tsarouhas P.H. 2019. "Overall equipment effectiveness (OEE) evaluation for an automated ice cream production line: A case study". *Int. J. Product. Perform. Manag.*
- [14] Yilmaz Eroglu D. 2019. "Systematization, implementation and analysis of overall throughput effectiveness calculation in finishing process of weaving industry". *Tekstil Konfeksiyon* 29(2): 121-132.
- [15] Zennaro I., Battini D., Sgarbossa F., Persona A., De Marchi R. 2018. "Micro downtime: Data collection, analysis and impact on OEE in bottling lines the San Benedetto case study". *Int. J. Qual. Reliab. Manag.* (35): 965-995.

mgr Jerzy Pater
Rzeszow University of Technology,
Al. Powst. Warszawy 12, 35-213 Rzeszow, Poland
e-mail: d468@stud.prz.edu.pl

mgr inż. Damian Basara
Rzeszow University of Technology,
Al. Powst. Warszawy 12, 35-213 Rzeszow, Poland
e-mail: d453@stud.prz.edu.pl

dr hab. inż. Dorota Stadnicka, prof. PRZ
Rzeszow University of Technology,
Al. Powst. Warszawy 12, 35-213 Rzeszow, Poland
e-mail: dorota.stadnicka@prz.edu.pl



EKOTECH

XXII Targi Ochrony Środowiska i Gospodarki Odpadami

23-24.02.2022



Pokazy Maszyn Komunalnych
na żywo



Spotkania
B2B



Międzynarodowe Forum
Gospodarki Odpadami



Konferencje
i warsztaty

Tu zaczyna się
biznes!

ekotech.targikielce.pl

Sborka nr 4, 2020

1. The assembly of hermetically sealed contacts

Authors: Ivanov A.A., Kreinin O.V.

It is shown that the structure of the assembly line of sealed contacts largely determined by the position of the assembled product (horizontal or vertical). In their production, automatic equipment of the line is used, both for horizontal and vertical assembly. The technical characteristics of both types of lines are approximately the same. The original technical solutions for orientation and supply of contacts for assembly are given.

2. Ensuring the quality of assembly of high-precision products based on the method of individual selection of parts

Authors: Zadorina N.A., Nepomiluev V.V.

The results of a study of the method of individual selection of parts when assembling machines containing multilink dimensional chains are presented. It is shown that the use of the proposed algorithm for the selection of parts can significantly increase the accuracy of such machines at low cost, which makes it possible to provide the required quality of their assembly at a lower cost.

3. Technological friction machines for the synthesis of lubricants used in mechanical and combined processing

Authors: Schedrin A.V., Aleshin V.F., Ignatkin I.YU., Bugaev A.M., Chikhacheva N.Yu.

The design and capabilities of technological friction machines for the systemic synthesis of innovative lubricants in the methods of mechanical and combined processing by turning, drawing, reduction and cutting are presented.

4. The task of actively influencing forced oscillations machines and mechanisms taking into account nonlinearities of passive forces

Authors: Erlich B.M.

The actual problem of actively influencing forced vibrations of machines and mechanisms with an array passive nonlinearities of elastic and dissipative forces is considered. This problem is described by a differential equation in which the passive nonlinearity function is used, allowing it possible to use both certain known nonlinearities and approximate other possible variants thereof. As an active damping or excitation of oscillations a force impact

is used. The study of the parameters of the passive nonlinearity function carried out allows us to simplify the stage of approximation of this function in solving real problems.

5. Modeling of dynamics of vibration movements of the indenter during the smoothing operation taking into account the influence of the thermodynamic subsystem

Author: Lapshin V.P., Hristoforova V.V., Halina E.V.

Issues related to the mathematical description and numerical modeling of indenter vibrations in the performance of smoothing operations in metal working are considered. Attention is paid to assessment the influence of the temperature released during processing on the dynamics of deformation movements of the tool. It was revealed that due to the thermodynamics of the processing, the deformation movements of the tool are stabilized, although they are complex in terms of the state space.

6. Technical solutions of vibration safety cold riveting performed ship repair

Authors: Rozinov A.Ya.

The parameters of heating and cooling of rivets made of steel and aluminum alloy, as well as data of filling holes with these rivets during hot and cold riveting are compared. The features of the process of performing cold impact riveting by direct and reverse methods, as well as the possibility of reducing the force of this riveting by improving the closing heads and constructive transformation of the rivets themselves are considered. Features of physiological influence of cold shock riveting on hands, elbows and shoulders of workers are determined. Describes the construction of riveting hammers and supports with spring shock absorbers that prevent the disease of workers vibration disease, portable riveting presses of pneumatic and hydraulic action. A description of the press equipment and technology of bolt-riveting connections, allowing mechanizing the process of cold riveting is given.

7. Features of multi-user work with large assemblies on the example of system Onshape

Authors: Samarkina E.I., Samarkin A.I., Dmitriev S.I.

The possibilities and features of the use of cloud systems in modeling large assemblies in mechanical engineering and instrumentation are considered.

8. Training in metrology sphere for machine building

Authors: Boriskin O.I., Anisimova M.A., Nuzhdin G.A.

In order to meet the requirements for quality management of machine-building products and metrological support, the company analyzed the existing standards for confirming the consistency of requirements. Federal state educational standards of higher education of two levels (bachelor's degree and specialty) of the mechanical engineering profile

(ensuring the unity of measurements (GSEEI) and the professional standard of a metro specialist) were selected for the analysis. The obtained results are used in the implementation of term papers. It is recommended to cover issues related to measuring devices and automatic control devices in related disciplines, and to include the topic "Main areas of activity in the field of metrological support of the enterprise".

Link: http://www.mashin.ru/eshop/journals/sborka_v_mashinostroenii_priborostroenii/2026/19/

Sborka nr 5, 2020

1. Assembly of the electronic start-up control device

Authors: Borovik T.N., Mikaeva S.A.

The article describes the assembly of an electronic controlled start-up control device for powering amalgam germicidal lamps of various series. The electrical characteristics are introduced and single and group designs of electronic starting-up devices are described.

2. Assembly of MLT type permanent resistors

Authors: Ivanov A.A., Kretinin O.V.

Considered technological processes of the assemblage of the constant resistors of MLT type for unattended installations, circular layout in two types: with the operation of welding the contact pins without welding (with pressure caps with leads); cutting helical grooves on the metallic base resistor on a special machine; varnishing and painting the raised resistors on the automated line. The equipment for straightening of axial contact terminals and laying of resistors from bulk in the pencil cassette is presented.

3. Analysis of the features of the technology of assembly and welding of mounting joints ship hull structures and changes in their stress state and strength

Authors: Rozinov A.Ya., Logunov V.V.

The classification of mounting connections of ship hull structures is presented. The technological features of their assembly and welding are considered, taking into account the conditions of the spatial position and the complexity of access, various poses of the executors of assembly and welding operations with an assessment of labor productivity. The reasons for the need to change the sequence of assembly and welding of connections of ship's hull structures are specified. Stress state and strength of joints made based on change of assembly

and welding sequence were evaluated. Procedure and results of evaluation of residual welding stresses at traditional and changed sequence of assembly and welding operations are described. Data on strength and operability of connections of ship hull structures under action of stretching and bending cyclic load are given.

4. Non-monoton deformation porous materials

Authors: Vaytsehovich S.M., Afanasev N.YU., Ovechkin L.M.

Based on studies of non-monotonic deformation by a simple shear deformation on the structuring of the volume of porous materials and shown. The designs of molds that realize multi-stage deformation of practical implementation of technological processes, are presented.

5. Features of manufacture of wedge valves for RITM-200 RP

Author: Mironov I.E., Chudaev N.N., Golubev S.V.

The article describes the experience of manufacturing valves with a wedge gate, which is part of the RITM-200 reactor installation of new icebreakers.

6. Stress concentration in frictional polymeric composites reinforced by oriented fibers

Author: Bardushkin V.V., Syichev A.P., Sychev A.A.

Multicomponent frictional polymer composites based on an epoxyphenol binder reinforced with E-glass fibers and dispersed inclusions of rubber, alumina, graphite, and barite are considered. It is believed that glass fibers are oriented along the X and Y axes of a rectangular coordinate system and have the same volume contents in these directions, which corresponds to the reinforcement of the material with fabric. Numerical calculations of the values of the components of the stress concentration

operator (a fourth-rank tensor connecting the local stress values at an arbitrary point in an inhomogeneous medium with external stresses applied to the composite) were carried out for the considered frictional polymer composites, taking into account changes in the volume contents of their fillers.

7. Technology ability of assembly process analysis of important types of connections

Author: Vodolazskaya N.V.

The kinematic calculation of technological design of the stand of technical diagnostics of braking qualities on the example of the truck car KamAZ-5320.

Link: http://www.mashin.ru/eshop/journals/sborka_v_mashinostroenii_priborostroenii/2026/20/

Sborka nr 6, 2020

1. Improvement of technology and means mounting assembly of outer skin joints

Authors: Rozinov A.Ya., Beskrovniy A.Yu.

The technologies and means of assembly the joints of outer skin, as well as the distribution of labor between the operations of the assembly process are analyzed. There are presented analytical dependencies of change of total labor intensity of assembly, standard duration of force operations of this assembly, based on which reasonable reduction of labor costs of force connection of connected edges of outer skin is determined. Disadvantages of existing technology of assembly of outer skin are considered, and design and technological solutions of assembly of outer skin are proposed, which provide improvement of its technology and used means of assembly on the basis of exclusion of elements of temporary fixation of connected edges and traditional grinding of surface of skin in places of installation of these fasteners.

2. Insulation monitoring study electrical apparatus and machines

Authors: Gubarev P.V., Talahadze T.Z., Zinchenko N.N.

The processes in the isolation of traction electric apparatuses and electric rolling stock machines are analyzed. Studies have shown that aging and the state of isolation cannot be judged only by the magnitude of its resistance. The most promising is the measurement of the magnitude and shape of the return voltage.

3. Improving quality control of manufacturing of threads on pipes of from oil industry

Authors: Dubovik E.A.

It is proposed to improve the quality control of production of threads for various grades of pipes used in the oil industry.

4. The use of laser measuring complex of "ULIKA" to control the geometric parameters of column-type apparatus

Author: Kachanov A.V., Kachanov V.V., Ivanov V.V., Golovanchikov A.B.

The problems of ensuring the quality of production and assembly of column-type apparatuses and internal contact devices are considered. A methodical approach to development of a measuring complex for the operational control of surface deviations from flatness during the assembly and mounting of large columns described. The method provides decrease of work volume, reduction of manufacturing cost. Developed software for automated calculation of geometrical parameters of columns.

5. Extension of technological capabilities of the through cutter due to application of the cutting replaceable multiface plate with a cycloidal profile front surface

Author: Kudryashov E. A., Smirnov I. M., Grishin D.V.

The device of a through cutter designed to sharpen the surface of a complex profile in the conditions of intermittent cutting is presented. In this case, a cutting replaceable multifaceted insert with a cycloidal profile of the front surface formed by rolling a circle with a radius equal to the cutting depth from the top along a horizontally producing straight line is used. An increase in the durability period of the material of the cutting interchangeable multifaceted plate is achieved by redistributing the shock loads of intermittent cutting on the front surface of the cutting element having the shape of a cycloidal profile from a brittle top and cutting edges to a more durable, remote area of the front surface of the cutting interchangeable multifaceted plate. The use of a new design of the cutting insert expands the technological capabilities of the through cutter by increasing the stability of intermittent turning.

6. Ways to control reinforced composites

Author: Smelkov S.L.

The main types of reinforced composites, their properties in comparison with metals and alloys are considered, as well as methods of defect control for such materials are given. To diagnose defects, two types of control were compared to each other by accuracy of determination: ultrasonic and electric spark. Methods are proposed for determination of location of defects in thickness of material and research is carried out to determine the most accurate method. Ultrasonic control is characterized by higher accuracy of determining the location of the defect through the thickness of the material.

7. Predicting the operational elastic characteristics of foam-polymer materials

Authors: Bardushkin V.V., Lavrov I.V., Bardushkin A.V., Yakovlev V.B., Sychev A.P., Sychev A.A.

A model for predicting the operational (effective) elastic characteristics of foam materials with spherical pores filled with air is presented. The model is based on a generalized singular approximation of random field theory (in a variant of the self-consistency method) and allows considering the composition of the components of the foams and the volumetric content of pores. For foam epoxides based on binders ED-16 and ED-20, numerical model calculations of the components of the tensor of effective elastic moduli, Young's modulus, and Poisson's ratio with a change in the porosity of inhomogeneous materials were performed.

8. Technique of technological support of operational indicators at assembly of connections with a tightness

Author: Bezyazychny V.F., Fedulov V.M.

The algorithm and technique of determination of technological conditions of processing of surfaces of the details intended for assembly with tension are offered. The algorithm provides for determination of initial data for calculation, of contact pressure and coefficient of friction on the contacting surfaces, of the calculated tension in the connection, as well as the method of assembly.

9. Passive intensifiers in heat exchange devices

Author: Vaytsehovich S.M., Vlasov Y.V., Juravlev A.Yu.

The problems of heat transfer intensification in the tube and annular space of shell-and-tube apparatuses due to the use of spiral-profile tubes, which are an alternation of protrusions and depressions made along a helical line, are considered. A method for calculating the increment of the heat transfer surface is given taking into account all the parameters of the multi-groove groove spiral with an increase in the number of corrugations and the pitch of the spiral for heat transfer pipes. The issues of heat removal intensity in laminar and turbulent fluid flows in the annulus and tube spaces with a change in the shape of the pipe cross section are considered.

10. Setting up a feeding device with a two-component vibratory drive

Author: Kristal M.G., Surikov A.A.

An original technique is proposed for determining the phase angle of the displacement of the vertical and horizontal components of the oscillations of the working body of the loading device with a vibrodrive that implements the elliptic law of oscillations. The problem of planning an extreme experiment with three factors has been solved: the amplitudes of vertical and horizontal vibrations and the angle of shear between them, to obtain the maximum speed of transportation of production items.

Link: http://www.mashin.ru/eshop/journals/sborka_v_mashinostroenii_priborostroenii/2026/21/

korożja kosztuje! *

***) straty korozyjne szacuje się na 3-6% PKB**



Czasopismo
„Ochrona przed Korozją”
– forum wymiany wiedzy
i doświadczeń na temat
ochrony materiałów
przed skutkami korożji

na życzenie wysyłamy bezpłatny
egzemplarz okazowy:
redakcja@ochronapzedkorożja.pl

www.ochronapzedkorożja.pl
www.sigma-not.pl

1. Cabin posture adjustment method based on redundant constrained parallel mechanism

Authors: Wenmin Chu, Xiang Huang, Shuanggao Li

In this paper, a dynamic model of PAS without internal force is constructed. The trajectory planning of posture adjustment based on this model can improve the quality of cabin assembly.

Posture adjustment plays an important role in spacecraft manufacturing. The traditional posture adjustment method, which has a large workload and is difficult to guarantee the quality of posture adjustment, cannot meet the requirements of modern spacecraft manufacturing. This paper aims to optimize the trajectory of posture adjustment, reduce the internal force of the posture adjustment mechanism and improve the accuracy of the system.

First, the measuring point is measured by a laser tracker and the position and posture of the cabin is solved. Then, Newton–Euler method is used to construct the dynamic model of the posture adjustment system (PAS) without internal force. Finally, the adjustment time is optimized based on Fibonacci search method and the trajectory of the cabin is fitted by the fifth order polynomial.

The simulation results show that, compared with the other trajectory planning methods, this method can effectively avoid the internal force of posture adjustment caused by redundant driving, and the trajectory of velocity and acceleration obtained are continuous, meeting the engineering constraints.

2. Wheel design and motion analysis of a new heavy-duty AGV in aircraft assembly lines

Authors: Junxia Jiang, Shenglin Zhang, Yuxiao He

The flexible automatic transportation and manual assembly jobs for large aircraft components demand an automated guided vehicle (AGV) system with heavy-duty capacity and omnidirectional movability. This paper aims to propose a four driving-steering wheels-four supporting-steering wheels (4DSW-4SSW) layout plan to enhance the controllability and moving stability of AGV.

The anti-vibration structure of DS wheels and high-torque steering mechanism of SS wheels with tapered rolling bearings are rigorously designed to meet the

functional requirements. Based on the specific wheel layout and vehicle dynamics, the rotational kinematic model as well as the straight and rotational dynamic models of AGV are established by the authors. To well verify the motion characteristics of wheels under heavy load in three motion states including straight motion, self-rotation and rotation around a certain point, the simulations in ADAMS and factory experiments have all been conducted.

Simulation results indicate that normal and friction forces of DS wheels and SS wheels are very stable except for some small oscillations, which are caused by non-center load distribution on AGV. Experimental results on driving speed of AGV have directly demonstrated that its positioning accuracy is enough for use in real aircraft assembly lines.

The designed AGV system has been applied to the final assembly line of a certain aircraft in Aviation Industry Corporation of China, Ltd, whose assembly efficiency and flexibility have been significantly improved.

3. Estimation for normal contact stiffness of joint surfaces by considering the variation of critical deformation

Authors: Qingchao Sun, Xin Liu, Xiaokai Mu, Yichao Gao

This paper aims to study the relationship between normal contact stiffness and contact load. Its purpose is a new calculation model of the normal contact stiffness of joint surfaces by considering the elastic–plastic critical deformation change of asperities contact.

The paper described the surface topography of joint surfaces based on fractal geometry, and fractal parameters and of fractal function derived from measurement data. According to the plastic–elastic contact theory, the contact deformation characteristic of asperities was analyzed; the critical deformation estimation model was presented, which expressed critical deformation as the function of fractal parameters and contact deformation; the contact stiffness calculation model of single asperity was brought forward by considering critical deformation change.

The paper combined the surface topography description function, analyzed the asperity contact states by

considering the critical deformation change, and calculated normal contact stiffness based on fractal theory and contact deformation analysis. The comparison between theoretical contact stiffness and experimental data indicated that the theoretical normal contact stiffness agreed with the experimental data, and the estimation model for normal contact stiffness was appropriate.

Owing to the possibility of plastic deformation during the loading process, the experimental curve between the contact stiffness and the contact load is nonlinear, resulting in an error between the experimental results and the theoretical calculation results.

4. Enhanced static modeling of commercial pneumatic artificial muscles

Authors: XueAi Li, Kui Sun, Chuangqiang Guo, Teng Liu, Hong Liu

This paper aims to propose an enhanced static model of commercial braided pneumatic artificial muscles (PAMs), which is fully analytical without the need for experimentally determined parameters.

To address the highly nonlinear issues of PAMs, the enhanced model is derived considering the irregular shapes close to their end-fittings, as well as the elastic energy stored in both their braids and rubber bladders. The hysteresis characteristics of PAMs are also explored by analyzing the friction in the crossovers of the interlacing braided strands, together with that between the strands and their surrounding bladders. The isobaric and isometric experiments of a commercial PAM are conducted to demonstrate the enhancement, and the model accuracy is evaluated and compared with some existing models in terms of root mean square errors (RMSEs). Additionally, the proposed model is simplified to facilitate the applications that entail high computational efficiency.

The proposed model agrees well with the experimental results, which indicates its viability to accurately predict the static behaviors. An overall RMSE of 5.24 N shows that the enhanced model is capable of providing higher accuracy than the existing analytical models, while keeping the modeling cost at a minimum.

The proposed model, taking account of non-cylindrical shapes, elastic energy and friction, succeeds in enhancing the static predictions of commercial PAMs. The fully analytical model may accelerate the development of novel PAM-based robots for high-precision control, while giving a deeper understanding of commercial PAMs.

5. A new hybrid particle swarm optimization and parallel variable neighborhood search algorithm for flexible job shop scheduling with assembly process

Authors: Parviz Fattahi, Naeeme Bagheri Rad, Fatemeh Daneshamooz, Samad Ahmadi

The purpose of this paper is to present a mathematical model and a new hybrid algorithm for flexible job shop

scheduling problem with assembly operations. In this problem, each product is produced by assembling a set of several different parts. At first, the parts are processed in a flexible job shop system, and then at the second stage, the parts are assembled and products are produced.

As the problem is non-deterministic polynomial-time-hard, a new hybrid particle swarm optimization and parallel variable neighborhood search (HPSOPVNS) algorithm is proposed. In this hybrid algorithm, particle swarm optimization (PSO) algorithm is used for global exploration of search space and parallel variable neighborhood search (PVNS) algorithm for local search at vicinity of solutions obtained in each iteration. For parameter tuning of the metaheuristic algorithms, Taguchi approach is used. Also, a statistical test is proposed to compare the ability of metaheuristics at finding the best solution in the medium and large sizes.

Numerical experiments are used to evaluate and validate the performance and effectiveness of HPSOPVNS algorithm with hybrid particle swarm optimization with a variable neighborhood search (HPSOVNS) algorithm, PSO algorithm and hybrid genetic algorithm and Tabu search (HGATS). The computational results show that the HPSOPVNS algorithm achieves better performance than competing algorithms.

Scheduling of manufacturing parts and planning of assembly operations are two steps in production systems that have been studied independently. However, with regard to many manufacturing industries having assembly lines after manufacturing stage, it is necessary to deal with a combination of these problems that is considered in this paper.

6. A lean production system design for semiconductor crystal-ingot pulling manufacturing using hybrid Taguchi method and simulation optimization

Authors: Taho Yang, Yuan-Feng Wen, Zong-Rui Hsieh, Jianxia Zhang

The purpose of this study is to propose an innovative methodology in solving the lean production design from semiconductor crystal-ingot pulling manufacturing which is an important industry. Due to the complexity of the system, it is computationally prohibited by an analytical approach; thus, simulation optimization is adopted for this study.

Four control factors that affect the system's performance, including the pulling strategy, machine limitations, dispatching rules and batch-size control, are identified to generate the future-state value stream mapping. Taguchi two-step procedure and simulation optimization are used to determine the optimal parameter values for a robust system. The proposed methodology improved the system performances by 6.42 and 12.02 per cent for service level and throughput, respectively.

This study does not investigate operations management issues such as setup reduction, demand forecasting and layout design. A real-world crystal-ingot pulling

manufacturing factory was used for the case study. The results are promising and are readily applied to other industrial applications.

The improved performances, service level and throughput rate, can result in an improved customer satisfaction level and a reduced resources consumption, respectively.

The proposed methodology innovatively solved a practical application and the results are promising.

7. A precision analysis method for the kinematic assembly of complex products based on equivalence of deviation source

Authors: Dongping Zhao, Gangfeng Wang, Jizhuang Hui, Wei Hou, Richard David Evans

The assembly quality of complex products is pivotal to their lifecycle performance. Assembly precision analysis (APA) is an effective method used to check the feasibility and quality of assembly. However, there is still a need for a systematic approach to be developed for APA of kinematic mechanisms. To achieve more accurate analysis of kinematic assembly, this paper aims to propose a precision analysis method based on equivalence of the deviation source.

A unified deviation vector representation model is adopted by considering dimension deviation, geometric deviation, joint clearance and assembly deformation. Then, vector loops and vector equations are constructed, according to joint type and deviation propagation path. A combined method, using deviation accumulation and sensitivity modeling, is applied to solve the kinematic APA of complex products. When using the presented method, geometric form deviation, joint clearance and assembly deformation are considered selectively during tolerance modeling. In particular, the proposed virtual link model and its orientation angle are developed to determine joint deviation. Finally, vector loops and vector equations are modeled to express deviation accumulation.

The proposed method provides a new means for the APA of complex products, considering joint clearance and assembly deformation while improving the accuracy of APA, as much as possible.

8. Job rotation scheduling in the Seru system: shake enforced invasive weed optimization approach

Authors: Ashkan Ayough, Mohammad Hosseinzadeh, Alireza Motameni

In this research, integration of job rotation scheduling and line–cell conversion problems was introduced, considering lack of an integrated look at these two practices in the literature. In addition, a new improved invasive weed optimization (IWO) equipped with shake enforcement was introduced.

Line–cell conversion and rotation of operators between cells are common in lean production systems.

Thus, the purpose of this study is to provide an integrated look at these two practices through integrating job rotation scheduling and line–cell conversion problems, as well as investigating the effect of rotation frequency on flow time of a Seru system. First, a nonlinear integer programming model of job rotation scheduling problem and line–cell conversion problem (Seru-JRSP) was presented. Then, because Seru-JRSP is NP-hard, an efficient and effective IWO algorithm was developed. Exploration process of IWO was enhanced by enforcing two shake mechanisms.

Computations of various sample problems showed shorter flow time and less number of assigned operators in a Seru system scheduled through job rotation. Also, nonlinear behavior of flow time versus number of rotation periods was shown. It was demonstrated that, setting number of rotation frequency to one in line with the literature leads to inferior flow time. In addition, ability of developed algorithm to generate clusters of equivalent solutions in terms of flow time was shown.

9. Human-computer interaction based on machine vision of a smart assembly workbench

Authors: Shiqing Wu, Zhonghou Wang, Bin Shen, Jia-Hai Wang, Li Dongdong

The purpose of this study is to achieve multi-variety and small-batch assembly through direct cooperation between equipment and people and to improve assembly efficiency as well as flexibility.

Firstly, the concept of the human–computer interaction is designed. Secondly, the machine vision technology is studied theoretically. Skin color filter based on hue, saturation and value color model is put forward to screen out images that meet the skin color characteristics of the worker, and a multi-Gaussian weighted model is built to separate moving objects from its background. Both of them are combined to obtain the final images of the target objects. Then, the key technology is applied to the smart assembly workbench. Finally, experiments are conducted to evaluate the role of the human–computer interaction features in improving productivity for the smart assembly workbench.

The result shows that multi-variety and small-batch considerable increases assembly time and the developed human–computer interaction features, including prompting and introduction, effectively decrease assembly time.

This study proves that the machine vision technology studied in this paper can effectively eliminate the interferences of the environment to obtain the target image. By adopting the human–computer interaction features, including prompting and introduction, the efficiency of manual operation is improved greatly, especially for multi-variety and small-batch assembly.

10. A novel optimization approach for segmented rabbit chase oriented U-type assembly line design: an application from lighting industry

Authors: Emre Cevikcan, Mehmet Bulent Durmusoglu

This study provides convenience for capacity management (assessing capacity and adjusting capacity by changing the number of workers) for industrial SRCUAL applications. Meanwhile, SRCUAL applications give the opportunity to increase the capacity for a product or transfer the saved capacity to the assembly of other products. As it is possible to provide one-piece flow with equal workloads via walking workers, SRCUAL has the potential for quick realization of defects and better lead time performance.

Rabbit chase (RC) is used as one of the most effective techniques in manufacturing systems, as such systems have high level of adaptability and increased productivity in addition to providing uniform workload balancing and skill improving environment. In assembly systems, RC inspires the development of walking worker assembly line (WWAL). On the other hand, U-type assembly lines (UALs) may provide higher worker utilization, lower space requirement and more convenient internal logistics when compared to straight assembly lines. In this context, this study aims to improve assembly line performance by generating RC cycles on WWAL with respect to task assignment characteristics of UAL within reasonable walking distance and space requirement. Therefore, a novel line configuration, namely, segmented rabbit chase-oriented U-type assembly line (SRCUAL), emerges.

The proposed mathematical programming approach is applied to the light-emitting diode (LED) luminaire assembly section of a manufacturing company. The adaptation of SRCUAL decreased the number of workers by 15.4% and the space requirement by 17.7% for LED luminaire assembly system when compared to UAL. Moreover, the results indicate that the integration of RC not only decreased the number of workers in 40.28% (29 instances) of test problems in U-lines, but also yielded less number of buffer points (48.48%) with lower workload deviation (75%) among workers in terms of coefficient of variation.

11. Optimally scheduling and loading tow trains of in-plant milk-run delivery for mixed-model assembly lines

Authors: Binghai Zhou, Zhixin Zhu

This paper aims to investigate the scheduling and loading problems of tow trains for mixed-model assembly lines (MMALs). An in-plant milk-run delivery model has been formulated to minimize total line-side inventory for all stations over the planning horizon by specifying the departure time, parts quantity of each delivery and the destination station.

An immune clonal selection algorithm (ICSA) combined with neighborhood search (NS) and simulated

annealing (SA) operators, which is called the NSICSA algorithm, is developed, possessing the global search ability of ICSA, the ability of SA for escaping local optimum and the deep search ability of NS to get better solutions.

The modifications have overcome the deficiency of insufficient local search and deepened the search depth of the original metaheuristic. Meanwhile, good approximate solutions are obtained in small-, medium- and large-scale instances. Furthermore, inventory peaks are in control according to computational results, proving the effectiveness of the mathematical model. This study works out only if there is no breakdown of tow trains. The current work contributes to the in-plant milk-run delivery scheduling for MMALs, and it can be modified to deal with similar part feeding problems. The capacity limit of line-side inventory for workstations as well as no stock-outs rules are taken into account, and the scheduling and loading problems are solved satisfactorily for the part distribution of MMALs.

12. Design, engineering and testing of an innovative adaptive automation assembly system

Authors: Marco Bortolini, Maurizio Faccio, Francesco Gabriele Galizia, Mauro Gamberi, Francesco Pilati

Industry 4.0 emerged as the Fourth Industrial Revolution aiming at achieving higher levels of operational efficiency, productivity and automation. In this context, manual assembly systems are still characterized by high flexibility and low productivity, if compared to fully automated systems. Therefore, the purpose of this paper is to propose the design, engineering and testing of a prototypical adaptive automation assembly system, including greater levels of automation to complement the skills and capabilities of human workers.

A lab experimental field-test is presented comparing the assembly process of a full-scale industrial chiller with traditional and adaptive assembly system. The analysis shows relevant benefits coming from the adoption of the adaptive automation assembly system. In particular, the main findings highlight improvements in the assembly cycle time and productivity, as well as reduction of the operator's body movements. The prototype is applied in an Italian mid-size industrial company, confirming its impact in terms of upgrades of the assembly system flexibility and productivity. Thus, the research study proposed in this paper provides valuable knowledge to support companies and industrial practitioners in the shift from traditional to advanced assembly systems matching current industrial and market features.

This paper expands the lacking research on adaptive automation assembly systems design proposing an innovative prototype able to real-time reconfigure its structure according to the product to work, e.g. work cycle, and the operator features.

ASSEMBLY TECHNIQUES AND TECHNOLOGIES

INFORMATION FOR AUTHORS

Please submit to the editorial office author's application form with contact details, a title of the proposed article, number of pages, illustrations and tables and a brief abstract. After receiving information about the acceptance of the proposed paper submit the entire text prepared according to the editorial instructions as well as a complete declaration form.

Submitted articles are subjected to editorial assessment and receive a formal editorial identification number used in further stages of the editorial process. Every submitted article is reviewed. Publication is possible after receiving positive reviews (see review procedure).

The editorial office does not pay royalties.

GUIDELINES FOR PREPARING PAPERS

- Articles for publication in Assembly Techniques and Technologies should have scientific and research character and deal with current issues of the industry.
- Articles must be original, not previously published (if the article is a part of another work i.e. PhD thesis, Habilitation etc. the information about that should be placed in the reference section).
- The article should involve a narrow topic but treated thoroughly without repeating general knowledge information included in the widely known literature.
- If the problem is extensive break it into articles for separate publications.
- Articles should be of a clear and logical structure: the material should be divided into parts with titles reflecting its content. The conclusions should be clearly stated at the end of the paper.
- The article should be adequately supplemented with illustrations, photographs, tables etc. however, their number should be limited to absolute necessity.
- The title of the article should be given in Polish and English as well as the abstract and key words.
- The article should not exceed 8 pages (1 page – 1 800 characters).
- The article should include mailing and e-mail addresses of the author(s).
- The article should be electronically submitted in * doc or * docx format. Equations should be written in the editors, with a clear distinction between 0 and O. If the equations exceed the width of column (8 cm) they must be moved, otherwise use double width column (16 cm).
- The editorial staff does not rewrite the texts or prepare illustrations. Apart from doc, * docx formats it is recommended to submit the source files of illustrations (in *.eps, *.jpg or *.tif format).
- Drawings and graphs must be clear, taking into account the fact that the width of the columns in the magazine is 8 cm, width of the single column - 17 cm, height of the column - 24.5 cm.
- The text on the drawings cut to the size must be legible and not less than 2 mm.
- The authors are required to give at the end of the article a full list of sources used for the paper. The text must include citation references to the position of cited work in the bibliography. The bibliography prepared according to the references in the text must include: books – surname and first letter of the author's name, title, publisher, year and a place of publication (optionally page numbers), magazines – author's name and surname, title of the article, title of the magazine, number, year and optionally page numbers. The bibliography should present the current state of knowledge and take into account publications of world literature.
- The authors guarantee that the contents of the paper and the drawings are originally their property (if not, the source should be indicated). The authors who submit the paper, will receive the following documents from the Publisher SIGMA-NOT to be signed by them:
 - The declaration on granting a licence
 - The licence agreement
 - The Authors' agreement
 on the right of the Publisher to:
 - a) Preservation and reproduction of the article, via production of its copies by paper and electronic way,
 - b) Turnover of the copies on which the article has been preserved – by introduction to market, lending or lease of the copies,
 - c) Making available to the public, including the Internet pages,
 - d) Dissemination as a whole or of its parts for advertisement and/or promotional purposes.
- The editorial staff will document all forms of scientific misconduct, especially violations of the rules of ethics applicable in science.



Zapraszamy Autorów do współpracy!

www.tiam.pl

tiam@sigma-not.pl

tel. 22 853 81 13

Warszawski Dom Technika

Klimatyczne wnętrza w samym sercu Warszawy

WYNAJEM SAL – tel. 729 052 512

WYNAJEM POWIERZCHNI BIUROWEJ – tel. 729 052 516

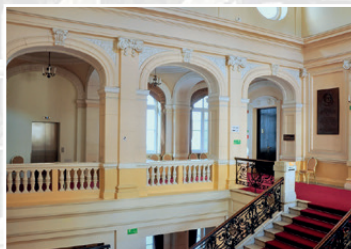
6 klimatyzowanych, w pełni wyposażonych sal mogących pomieścić od 15 do 400 osób.

Doświadczony zespół pomoże, doradzi, zorganizuje, każde wydarzenie w reżimie sanitarnym.

www.wdtnot.pl



*Nie ma na co czekać,
rezerwuj już teraz!*



W PRENUMERACIE

2021

TANIEJ

Sprawdź to!

www.sigma-not.pl



WARIANTY PRENUMERATY

- **PAPIEROWA** – czasopismo tylko w wersji papierowej (z opłatą za dostarczenie przesyłki),
- **CYFROWA** – czasopismo wyłącznie w wersji cyfrowej dostępne na Portalu Informacji Technicznej www.sigma-not.pl, prenumerator otrzyma indywidualny kod dostępu do zaprenumerowanego tytułu,
- **PLUS** – czasopismo w wersji **papierowej** (bez opłaty za dostarczanie prasy) oraz **cyfrowej**, a także dostęp do **archiwum** zaprenumerowanego tytułu na Portalu Informacji Technicznej www.sigma-not.pl wraz z indywidualnym kodem dostępu.



więcej informacji: 22 840 30 86, prenumerata@sigma-not.pl